Aus dem Institut für Physiologie

der Universität Würzburg

Vorstand: Professor Dr. med. M. Kuhn

Characterisation of Mena Promoter Activity and Protein Expression in Wild-type and Gene-trapped Mice

Inaugural - Dissertation

zur Erlangung der Doktorwürde der

Medizinischen Fakultät

der

Julius-Maximilians-Universität Würzburg

vorgelegt von

Carla Jennifer Merkel

aus Hofheim am Taunus

Würzburg, Juni 2011

Referent : Univ.- Prof. Dr. rer.nat. Kai Schuh

Koreferent : Priv.- Doz. Dr. Oliver Ritter

Dekan : Prof. Dr. med. Matthias Frosch

Tag der mündlichen Prüfung: 19.03.2012

Die Promovendin ist Ärztin

TO MY FAMILY

Table of contents

1. Introduction _____ *1*

1.1 Actin _____ **1**

1.1.1 Actins are Abundant Proteins in Eukaryotic Cells _____ 1

1.1.2 Organization of Actin Filaments _____ 1

1.1.3 Actins Ensure Cell Stability _____ 2

1.1.4 Role of Actin Filaments in Muscle Contraction _____ 3

1.1.4.1 Skeletal Muscle _____ 3

1.1.4.2 Smooth Muscle _____ 4

1.1.5 Actin Filaments at Adherens and Tight Junctions and at Focal Adhesions _____ 5

1.1.6 Actin Dynamics are Important for Cell Motility _____ 5

1.2 The Cardiovascular System _____ **6**

1.2.1 Histology of Blood Vessels _____ 6

1.2.2 Histology of Heart Muscle Tissue _____ 6

1.2.3 Histology of Lungs _____ 7

1.3 Ena/VASP Protein Family _____ **10**

1.3.1 Structural Organization of Ena/VASP Family Proteins _____ 10

1.3.2 Functions of Ena/VASP Proteins _____ 12

1.3.2.1 Ena/VASP Proteins are involved in Bacterial and Cell-Movement _____ 12

1.3.2.2 Ena/VASP Proteins at Cell-Contacts _____ 14

1.3.2.3 Aspects about the Regulation of Ena/VASP Proteins _____ 15

1.3.2.4 Ena/VASP Proteins in Cardiomyocytes _____ 15

1.3.2.5 Do Ena/VASP Family Members Compensate for each other? _ 16

1.4 Localisation and Functions of Spectrins in the Mammalian Heart _____ **16**

1.5 Manipulating the Mammalian Genome by Generating Knockout Mice _____ **18**

1.5.1 The Classical Knockout Method _____ 19

1.5.2 The Conditional Knockout Method _____ 20

1.5.3 Gene-trapping 21

1.6 Ena/VASP Family Knockout Mice 22

1.6.1 VASP Deficient Mice Generated by Homologous Recombination 22

1.6.2 Targeted Disruption of the VASP Gene 23

1.6.3 Targeted Disruption of the Mena Gene 24

1.6.4 Generation of Triple Knockout Mice 24

***2. Materials and Methods* 25**

2.1 Genotyping of Mice 25

2.1.1 DNA Isolation 25

2.1.2 Polymerase Chain Reaction (PCR) 25

2.1.2.1 Mena PCR 25

2.1.2.2 VASP PCR 27

2.1.3 Agarose Gel Electrophoresis 28

2.2 Histological Analysis 28

2.2.1 Preparation of Mouse Organs 28

2.2.2 Cryosections of Mouse Organs 29

2.2.3 X-Gal Staining 29

2.2.4 Immunofluorescence 31

2.3 Protein Analysis 33

2.3.1 Preparation of Mouse Organ Protein Extracts 33

2.3.2 Preparation of Mouse Washed Platelets 34

2.3.3 Analysis of Protein Extracts 34

2.3.3.1 Measuring Protein Concentration by UV-Spectrometry 35

2.3.3.2 Coomassie Staining of SDS-PAGE-Gels 35

2.3.4 Western Blot Analysis 35

2.3.4.1 Sodium Dodecyl Sulfate - Polyacrylamide-Gel-Electrophoresis (SDS- PAGE) 35

2.3.4.2 Semi-Dry Electrophoretic Transfer and Immunolabeling 37

2.4. Cell Culture - Transfection 38

2.4.1 Prearrangements for Transfection 39

2.4.2 Transfection 40

2.4.3 Harvesting Transfected Cells 41

3. Results *42*

3.1 Characterisation of the Mena Ko Mouse **42**

3.1.1 Generation of Mena Deficient Mice 42

3.1.2 Insertion of the Gene Trap Construct with its Consequences for the Mena Gene 43

3.2 Characterisation of the VASP Ko Mouse **44**

3.3 Genotyping Mice Using PCR **45**

3.4 X-Gal Staining **47**

3.4.1 X-Gal Staining of the Brain 48

3.4.2 X-Gal Staining of the Heart 49

3.4.3 X-Gal Staining of the Lung 52

3.4.4 X-Gal Staining of the Gastrointestinal Tract 52

3.4.5 X-Gal Staining of Liver, Spleen, Kidney and Thymus 53

3.4.6 X-Gal Staining of Skeletal Muscle 55

3.4.7 X-Gal Staining of Neonatal Mice 55

3.5 Western Blot Analysis **56**

3.5.1 Mena Protein Expression in Wild-type and Mena Deficient Mice 57

3.5.2 VASP Protein Expression in Wild-type and Mena Deficient Mice 61

3.5.3 Western Blot Analysis with Mena/VASP-Double-Deficient Mice 62

3.6 Analysis of Mena Protein Localisation in Heart and Lung by Confocal Immunofluorescence Microscopy **65**

3.6.1 Immunohistochemical Analysis to Compare Mena and F-Actin Localisation in Cardiomyocytes 65

3.6.2 Immunohistochemical Analysis to Compare Mena and α-Smooth-Muscle-Actin Localisation 67

3.6.3 Immunohistochemical Analysis to Compare Mena and VE-cadherin Localisation in Heart and Lung 72

3.6.4 Immunohistochemical Analysis to Compare Mena and αII-Spectrin Localisation in the Heart 75

3.7 Functional Analysis of Mena-VASP-Double-Deficient Hearts Using Electrocardiography **77**

4. Discussion _____ *79*

4.1 Mena Promoter Activity in Diverse Tissues _____ **79**

4.2 Protein Expression of Ena/VASP Family Members _____ **83**

4.3 Detailed Mena Localisation in the Cardiovascular System ____ **87**

4.4 Functional Analysis Revealed Cardiac Dysfunctions in Mutated Mice _____ **90**

4.5 Conclusions and Future Aspects _____ **91**

Summary _____ *94*

Zusammenfassung _____ *96*

References _____ *98*

1. Introduction

1.1 Actin

1.1.1 Actins are Abundant Proteins in Eukaryotic Cells

Previously published data and results about functions of the Ena/VASP family allude to the importance of these proteins in association with actin. Therefore, the protein actin is dealt with in this chapter.

Actins are globular proteins, which are the main components of actin filaments. Quantitatively, they are the most abundant proteins of eukaryotic cells and humans. The genome contains six functional actin genes. The six actin isoforms are expressed in various muscle and non-muscle tissues and comprise α-cardiac muscle actin, α-skeletal muscle actin, α-smooth muscle actin, β-cytoplasmic actin, γ-cytoplasmic actin and γ-smooth muscle actin (Tondeleir et al., 2009). Together with microtubules and intermediate filaments, actin filaments build up the cytoplasmic cytoskeleton, which is found in every cell and ensures cell stability. In assembly with myosin filaments, actin filaments provide the basis for contraction in skeletal, in smooth and heart muscle cells (Fig. 1-1). But also in non-muscle cells, actin bundles that are tightened by α-actinin and myosin II can facilitate cell contractility. Such contractile bundles are called stress fibres, as they stabilize the cell against shear stress. Especially in endothelial cells (ECs), stress fibres play an important role because these cells are permanently exposed to the bloodstream.

Actin filaments also connect the cytoplasm with the cellular environment. They link the cytoskeleton to protein complexes of the plasma membrane which in turn are connected to adjacent cells (adherens junctions) or with the extracellular matrix (focal adhesions) (Fig. 1-1; A).

1.1.2 Organization of Actin Filaments

Globular actin (G-actin) can polymerise into double-helical actin filaments (F-actin). This polymerisation and actin filament growth is driven by ATP-hydrolysis. Actin filaments have a fast growing end, called “barbed” or (+)-end,

and a slow growing, called “pointed” or (-)-, end. The organization of actin cytoskeleton dynamics is mediated by a large repertoire of over 100 actin-binding proteins (ABPs). This regulation is important to coordinate cell movement and contractility, cell-cell- and cell-matrix-interaction, cell morphology and polarity. The ABPs can be grouped into three classes. The first group comprises proteins that regulate the assembly and disassembly of F-actin. The Arp2/3 (**a**ctin **r**elated **p**roteins) complex mediates filament nucleation and branch formation. Like capZ, tropomodulin and gelsolin, Arp2/3 also acts as capping protein, thereby controlling filament length. The G-actin-binding protein, profilin, facilitates the nucleotide exchange of ADP for ATP, thereby promoting filament polymerisation. Proteins containing poly-proline motifs, such as Ena/VASP, can bind to profilin. By recruiting this component of the actin polymerisation machinery, Ena/VASP facilitate F-actin assembly. The second group of ABPs regulates networks and higher-order F-actin structures. These F-actin structures, which are formed by actin bundling and crosslinking proteins, are crucial for cell shape, adhesion and locomotion. Actin bundling, the alignment of F-actin into linear arrays, is important for the formation of stress-fibres, filopodia and microvilli. It is promoted, for example, by fimbrin, α-actinin and Ena/VASP. Actin-crosslinking, the arrangement of actin filaments into orthogonal arrays, is mediated by filamin, spectrin complexes and Ena/VASP proteins. The third class of ABPs are proteins that utilize F-actin as structural framework to produce movement, force, and cell integrity. Myosins, which are ATP-dependent motor proteins, use actin as a track to move other proteins or vesicles. Annexin and vinculin link actin fibres to the plasma membrane, either directly or by binding to cell adhesion receptors, respectively. Interaction with other cytoskeletal elements is mediated by plectin, which links actin fibres to microtubules and intermediate filaments. (Revenu et al., 2004; Sechi and Wehland, 2004; Winder and Ayscough, 2005)

1.1.3 Actins Ensure Cell Stability

An important precondition for the function of actin filaments is their ability to build up bundles and meshworks. In the cell cortex, adjacent to the plasma

membrane, the membrane skeleton is comprised of a two- or three-dimensional network of actin filaments (cortical actin network), which ensures the stability of the cell membrane. Depending on the cell type, the cortical networks are built up differently, thus diverse actin binding proteins are of importance. Among these are filamin, α-actinin and spectrin.

A unique membrane skeleton is found in erythrocytes. It not only provides stability but also flexibility to the red blood cells. The meshwork consists of spectrin tetramers that are cross-linked by short actin filaments. Association with proteins of the plasma membrane is mediated by the adaptor proteins ankyrin and protein 4.1 (Fig. 1-4).

Also some cellular extensions, such as microvilli of intestinal enterocytes, are stabilised by actin bundles. In microvilli, actin filaments are cross-linked by fimbrin and villin. Special myosins attach the framework to the membrane.

1.1.4 Role of Actin Filaments in Muscle Contraction

1.1.4.1 Skeletal Muscle

A skeletal muscle comprises several muscle fibres that in turn consist of hundreds of myofibrils, which constitute the contractile apparatus. Myofibrils consist of myosin and actin filaments (α-skeletal muscle actin). In between these, cell organelles such as the sarcoplasmatic reticulum (SR) and mitochondria are located. The typical cross-striation is caused by the periodic alignment of the actin and myosin filaments (Fig. 1-1; B). The repetitive basic units are called sarcomeres; two of them are attached at a Z-line. Actin filaments that are cross-linked by α-actinins, originate from these Z-lines. As regulatory proteins, the actin filaments also contain tropomyosin and the troponin complex, which interact with calcium and which initiate muscle contraction after sarcoplasmatic calcium elevation. The myosin filaments are cross-linked at the M-line. Another “super-thin“ filament is titin; it reaches from the Z-line over the M-line and prevents the sarcomer from overexpansion. During a contraction process, in which the actin filaments slide further between the myosin filaments, the sarcomeres shorten to a maximum of 70%. This sliding process results from ATP dependent cross-bridging of myosin head

domains and actin filaments followed by their detachment (sliding filament process). For the contraction of a muscle fibre many cycles of cross-bridging are needed.

The sarcoplasmatic reticulum (SR) contains large stores of calcium. It is composed of longitudinal cisterns (L-system) that surround the myofibrils. It stands in direct contact to transversal tubules (T-system) which are invaginations of the plasma membrane. The T-tubules allow the conduction of electrical impulses from the cell surface into the inside of the cell, leading to the release of calcium out of the SR. This process is important, as relatively high concentrations of calcium are necessary for the activation of the troponin system in order to initiate contraction. Another requirement for contraction of muscle fibres is the linkage of myofibrils to the sarcolemma via the membrane skeleton. In the range of Z-lines, costameres (cytoskeletal aggragations) are aligned circumferentially around myofibrils. They contain actin binding proteins such as dystrophin, spectrin, vinculin and talin. These proteins bind to integrins and destroglycans of the sarcolemma, which are also linked to the extra cellular matrix (ECM). Desmin filaments also link the myofibrils to the sarcolemma.

1.1.4.2 Smooth Muscle

Smooth muscle is non-striated muscle which is found for example in hollow organs of the intestinal tract, in bronchioles, in bladder and uterus and in blood vessels. In smooth muscle, cells are spindle shaped, their actin (α-smooth muscle actin) and myosin filaments are not arranged in sarcomers, and thus the striation pattern is missing. The contractile apparatus contains almost longitudinal oriented myosin and actin filaments being connected to cytoplasmic dense bodies (Fig. 1-1; C). The stabilising cytoskeleton comprises desmin filaments and non-muscle actin. It permeates the cell and is anchored to the dense bodies and focal adhesions of the sarcolemma. Contraction is explained by the filament sliding model but in contrast to skeletal and cardiac muscle, smooth muscle does not contain the calcium-binding protein troponin. Contraction is initiated by a calcium-regulated phosphorylation of myosin through the myosin light-chain kinase, MLCK. On the other hand, contraction is

inhibited by the myosin light-chain phosphatase, MLCP, which dephosphorylates myosin, thereby leading to a relaxation of smooth muscle tissue.

1.1.5 Actin Filaments at Adherens and Tight Junctions and at Focal Adhesions

Actin filaments are linked to adherens and tight junctions (cell-cell adhesion) and to focal contacts (cell-matrix adhesion) (Fig. 1-1; A). Adherens junctions are predominant in epithelial cells where they appear as an apical belt encircling the cell (zonula adherens). In cardiomyocytes, adherens junctions (fascia adherens) are found at the intercalated discs (ID) (see 1.2.2). The transmembrane proteins that mediate the intercellular attachment are cadherins. There exist several isoforms, such as E-cadherins in epithelial layers, N-cadherins in cardiomyocytes and VE-cadherins in vascular endothelial cells. Via plaque proteins (e.g., catenin, α-actinin, and vinculin), a bridge is set up between actin filaments and cadherins. Thus actin filaments serve as a direct connection to the cytoskeleton. Tight junctions appear as zonula occludentes (ZO) in epithelial cells, where they serve as a diffusion barrier. Tight junctions are composed of the transmembrane proteins occludin, claudin and junctional adhesion molecules (JAMs) which are linked to actin filaments via plaque proteins on the cytoplasmic site. Focal contacts are mainly apparent in vascular endothelium. At these contacts integrins are connected to the ECM and, at the cytoplasmic side, to contractile actin filaments (stress fibres) via plaque proteins, such as talin, α-actinin and vinculin.

1.1.6 Actin Dynamics are Important for Cell Motility

Actins, actin binding proteins and myosins play an essential role in cell motility. Cell motility is, for example, important for wound healing, angiogenesis, cancer, and leucocyte migration within the scope of inflammations. Mobile extensions of the cell, lamellipodia, and their sharp tips, filopodia, contain a two-dimensional actin meshwork. The actin filaments are linked to the ECM via focal contacts, thereby the lamellipodia are attached to their substratum. By the

polymerisation of F-actin at the plus-ends and the depolymeristaion at the minus-ends, the protrusion of lamellipodia and filopodia is achieved (Grimm et al., 2003) (see also Fig. 1-3). Similar to this is the motility process of the gram-positive bacterium, *Listeria monocytogenes*, within eukaryotic cells. Here, actin polymerisation is promoted by proteins, such as ActA, Ena/VASP-proteins and profilin (Sechi and Wehland, 2004).

1.2 The Cardiovascular System

The presented work is focussed on the functions of Ena/VASP-proteins in the cardiovascular system. The microscopic anatomy of the main organs of the cardiovascular system is described shortly in this chapter.

1.2.1 Histology of Blood Vessels

Most blood vessels are composed of three layers: intima, media, adventitia (Fig. 1-1; E). This organisation is more distinct in arteries than in veins. The intima mainly consists of the endothelium, a simple squamous epithelium. The endothelial cells (ECs) are connected among each other by adherens junctions (containing VE-cadherin), tight and gap junctions. The attachment on the ECM of the basement membrane is mediated by focal contacts. Stress fibres that anchor at the cytoplasmic site of the focal contacts provide mechanical support so that the ECs can withstand the high shear of the bloodstream. The media is most important for vasoconstriction and -dilation and therefore contains smooth muscle cells and ECM. The external vessel layer, the adventitia, consists of connective tissue. There are two different principal types of arteries, the muscular and the elastic type. The aorta, for example, is an artery of the elastic type and its media contains additional elastic fibres.

1.2.2 Histology of Heart Muscle Tissue

The coordinated contractions of heart muscle cells are triggered by the autonomous nervous system (sinoatrial note is pacemaker). These rhythmic contractions cause bloodstreams from the atria into the ventricles from where blood is pumped into the pulmunary and the systemic circulation. The heart is

composed of striated muscle tissue that resembles principally skeletal muscle. But heart muscle fibres consist of branched individual cells, the cardiomyocytes (Fig. 1-1; D). They contain a single nucleus and are electrically and mechanically connected by intercalated discs (IDs). IDs are usually arranged in a staircase-shaped manner and are composed of three important cell contacts: adherence junction (fascia adherens), desmosome (macula adherens) and gap junctions (nexus). At the fascia adherens, which is important for mechanical transmission, actin filaments are linked to N-cadherins. Desmosomes also have mechanical function. They consist of the cadherins desmoglein and desmocollin, which are connected to desmin intermediate filaments. Gap junctions mediate the electrical coupling of cardiomyocytes. They are composed of two tunnel like protein complexes (connexons) that build a channel through two attached cell membranes. Connexons comprise connexins. In heart muscle, smooth muscle and vascular enothelium the isoform connexin 43 is the predominate isoform. T-tubules in cardiomyocytes are different from those of skeletal muscle fibres. Their diameter is larger in heart muscle and they surround myofbrils at the range of the Z-discs.

1.2.3 Histology of Lungs

Simplified, pulmonary tissue comprises airways (bronchi, bronchioles) and the alveoli, which are essential for the gas exchange. The wall of the bronchioli consists of an internal mucous membrane, the respiratory epithelium, which is a ciliated pseudostratified columnar epithelium (Fig. 1-1; F). It is surrounded by a thin lamina propria (connective tissue) and smooth muscle tissue. In the case of bronchi, the muscle layer is surrounded by seromucous glands and by a scaffold comprising cartilage plaques. Cartilage and glands usually do not exist in bronchioles. The alveoli are the places of gas exchange occurring between the inhaled air and the blood. They consist predominantly of compact capillary endothelium, which is sustained by alveolar epithelium. Alveolar epithelium comprises type I pneumocytes that encase the alveolar walls and type II pneumocytes which produce surfactant.

Fig. 1-1. Localisation and Cellular Functions of Actin and Basic Histology of Cardiovascular Organs (following page).
(A) Structural organization of tight and adherens junctions (cell-cell adhesion) and focal contacts (cell-matrix adhesion). The impermeable tight junctions are composed of the transmembrane proteins occludin, claudin and junctional adhesion molecules (JAMs), whereas adherens junctions consist of VE-cadherins. At focal contacts integrins are connected to the ECM. All these contacts are linked to the actin cytoskeleton through proteins, such as catenins, vinculin and talin, which provide junctional stability. (B) Electron micrograph and schematic illustration of a sarcomere; the basic contractile unit of a skeletal muscle. Actin filaments are anchored at the Z-lines of a sarcomere, whereas the thicker myosin filaments originate from the M-line. The periodic alignment of the filaments causes the typical cross-striation of skeletal muscle fibres. Contraction is explained by the sliding filament model which implies cross-bridging and detachment of myosin heads and actin filaments. (C) Schematic illustration of smooth muscle cells. Cells are attached by adherens junctions, whereas gap junctions allow electrical conduction. The contractile apparatus comprises actin (α-smooth muscle actin), myosin filaments and cytoplasmic dense bodies. Contraction is explained by the filament sliding model which is activated by a calcium-regulated phosphorylation of myosin by MLCK. (D) Electron micrograph of cardiomyocytes, showing the typical striation pattern, mitochondria, T-tubules and intercalated discs (IDs) arranged in a staircase-shaped manner. IDs comprise different types of contacts, such as desmosomes (macula adherens), nexus (gap junctions) and fascia adherens (adherens junction). They provide electrical and mechanical conduction. (E) Schematic cross section of a blood vessel, consisting of three layers: intima (endothelium), media (smooth muscle cells) and adventitia (connective tissue, fibroblasts). (F) Histology of a bronchiole and surrounding alveoles. The respiratory epithelium, which is a ciliated pseudostratified columnar epithelium, is surrounded by connective tissue and smooth muscle fibres. Alveoles consist predominantly of compact capillary endothelium which is sustained by alveolar epithelium, comprising type I and II pneumocytes.
Figures modified from (A) (Mehta and Malik, 2006), (B) http://fajerpc.magnet.fsu.edu/Education/2010/Lectures/37_Muscle_System_files/image010.jpg, (C) http://www.mona.uwi.edu/fpas/courses/physiology/muscles/SmoothMuscle.jpg, (D,F) (Drenckhahn, 2003), (E) http://en.wikipedia.org/wiki/Endothelium

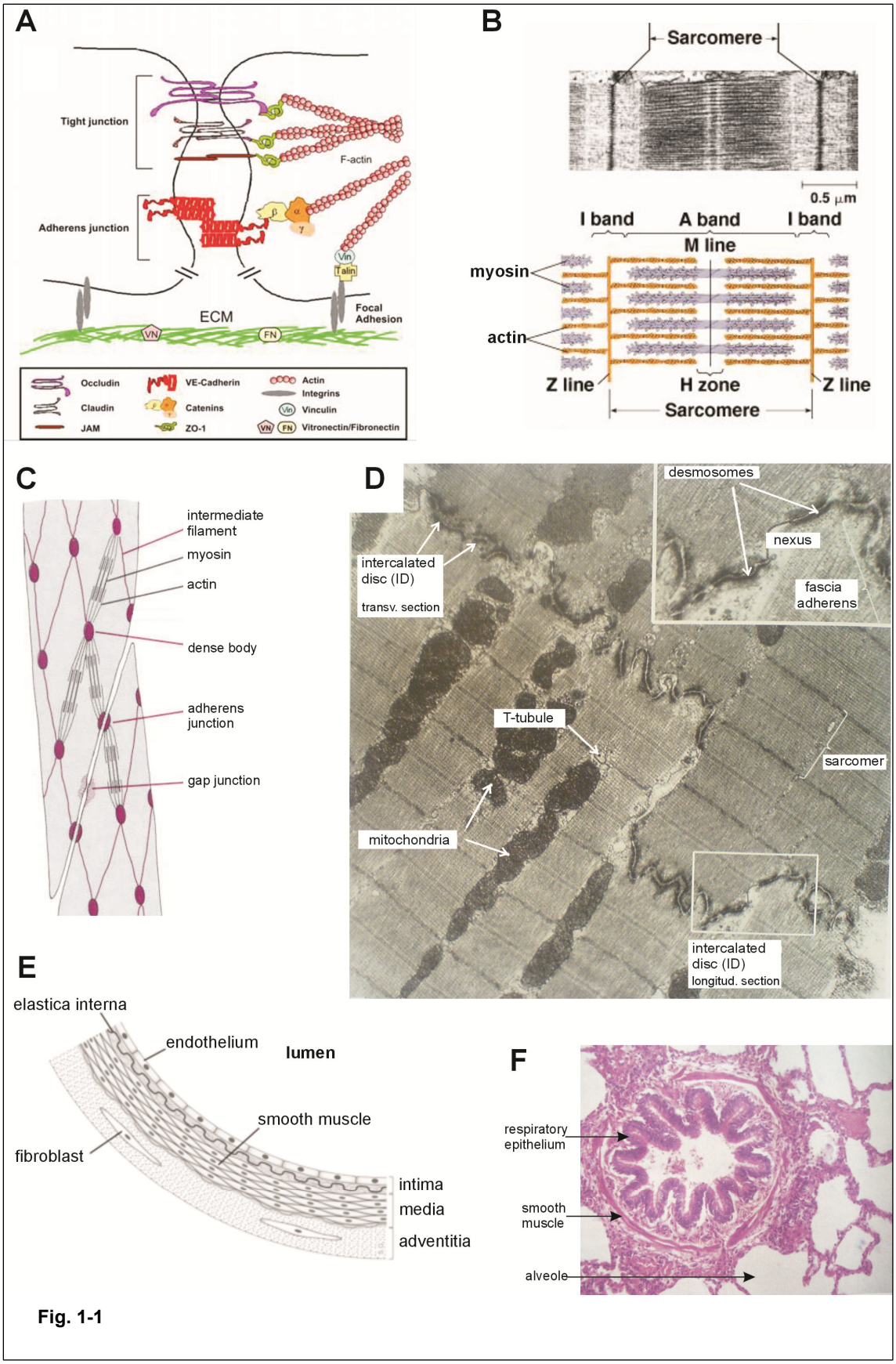
A
Tight junction
F-actin
Adherens junction
Vin
Talin
ECM
Focal Adhesion
VN
FN
Occludin
Claudin
JAM
VE-Cadherin
Catenins
ZO-1
Actin
Integrins
Vinculin
Vitronectin/Fibronectin
B
Sarcomere
0.5 µm
I band
A band
I band
M line
myosin
actin
Z line
H zone
Z line
Sarcomere
C
intermediate filament
myosin
actin
dense body
adherens junction
gap junction
D
desmosomes
nexus
fascia adherens
intercalated disc (ID)
transv. section
T-tubule
sarcomer
mitochondria
intercalated disc (ID)
longitud. section
E
elastica interna
endothelium
lumen
smooth muscle
fibroblast
intima
media
adventitia
F
respiratory epithelium
smooth muscle
alveole

Fig. 1-1

1.3 Ena/VASP Protein Family

1.3.1 Structural Organization of Ena/VASP Family Proteins

The human Ena/VASP family, which links signal transduction pathways to actin cytoskeleton dynamics, is comprised of the proline rich proteins Mena, VASP and EVL. Mena (mammalian enabled) is the mammalian homolog of the *Drosophila* protein Ena (enabled), which is a substrate for Abl (Abelson) tyrosine kinase and is linked to its signalling pathway (Gertler et al., 1995). VASP (vasodilator stimulated phosphoprotein) was first identified in platelets as a substrate of cGMP and cAMP-dependent protein kinases. It was proposed that VASP phosphorylation in response to cyclic-nucleotide elevating vasodilators could inhibit platelet aggregation (Halbrugge and Walter, 1989; Waldmann et al., 1987). The third family member is an Ena-VASP-like protein and therefore called EVL.

In mammals, all family members share a similar structural domain organization consisting of an N-terminal EVH1 (Ena-VASP-homology 1) domain and a C-terminal EVH2 domain which flank a central proline-rich region (PRR) (Fig. 1-2) (Lanier et al., 1999; Sechi and Wehland, 2004). The EVH1 domain serves as a binding interface for the focal adhesion proteins zyxin and vinculin and for the listerial protein ActA (Niebuhr et al., 1997). All three binding partners contain a F/LPPPP sequence, which serves as binding motif (Ball et al., 2002).

The EVH2 domain mediates the multimerisation of Ena/VASP proteins and, harbouring binding sites for G-actin and F-actin, it is also responsible for actin bundling and for filopodia formation (Bachmann et al., 1999; Han et al., 2002). The proline-rich region is binding partner to several ligands. It interacts with the actin-binding protein profilin and with Src homology 3 (SH3) domains of the scaffolding proteins spectrin and IRSp53 and the non-receptor tyrosine kinases Abl and Src (Benz et al., 2008; Sechi and Wehland, 2004). In contrast to Ena, VASP and EVL, Mena also contains a low-complexity sequence called LERER. This is a 5 amino acid repeat region located between the EVH1 domain and the PRR. LERER might function as another binding interface (Gertler et al., 1996). All Ena/VASP-family members are substrates for the cAMP and cGMP

dependent serine/threonine protein kinases, PKA and PKG, respectively. In addition, Mena is phosphorylated by the Abl tyrosine kinase (Fig. 1-2) (Sechi and Wehland, 2004). Human VASP harbours three phosphorylation sites (serine-157, serine-239, and threonine-278). VASP-phosphorylation at S157, preferentially by cAMP-dependent protein kinases, leads to a shift of apparent molecular mass from 46 kDa to 50 kDa in SDS-PAGE (Gambaryan et al., 2001). Mena displays three bands in SDS-PAGE, namely at 80 kDa, 88 kDa and 140 kDa. However, these bands represent different Mena splice variants. Western blot analyses have shown that the 80 kDa form is broadly expressed in various tissues, whereas the 140 kDa form is only expressed in neuronal cells. Therefore, the 140 kDa isoform is also named neuronal Mena or (+)-Mena (Gertler et al., 1996). EVL protein is expressed mainly in hematopoietic cells of thymus and spleen (Lambrechts et al., 2000). It shows single bands at 55 kDa in SDS/PAGE.

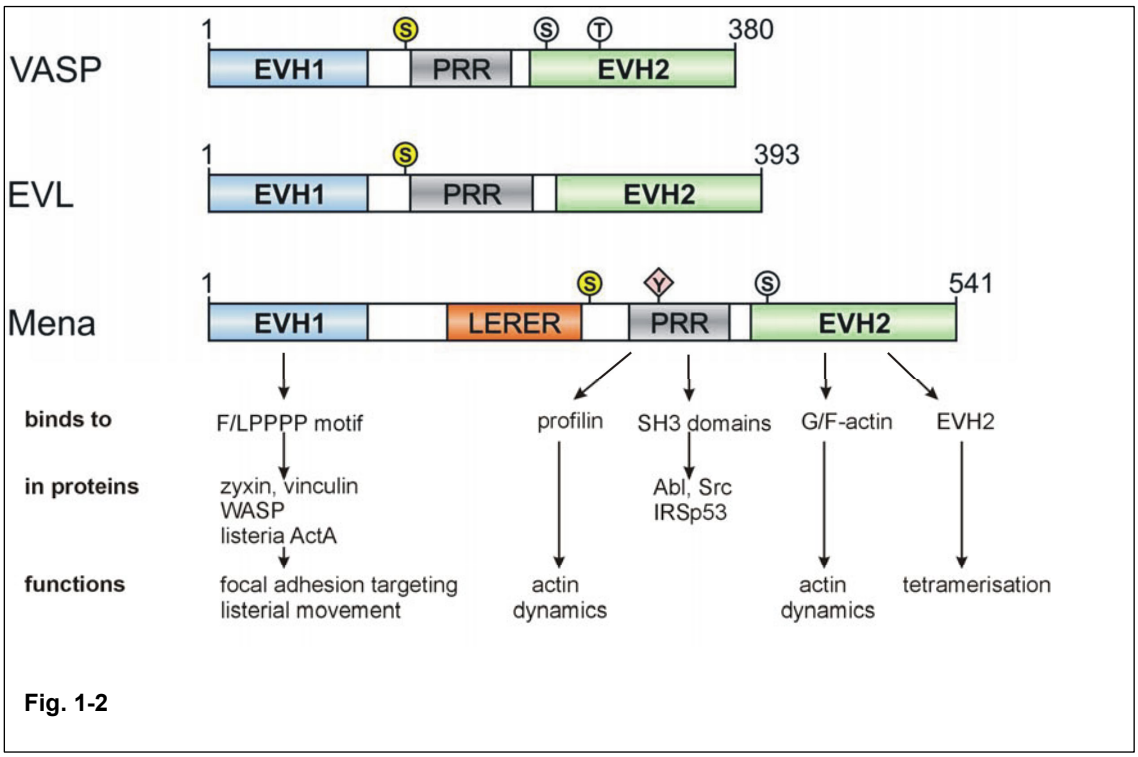

Fig. 1-2

Fig. 1-2. Domain Structure of Ena/VASP Proteins with their Binding Partners and Functions (previous page).
Domain structure of the proteins VASP, EVL and Mena. EVH1: Ena/VASP homology 1, PRR: proline-rich region, LERER: region harbouring LERER repeats, EVH2: Ena/VASP homology 2. Each protein domain binds to different domains and motifs of several proteins (the major ones are listed) and the protein-protein interactions mediate diverse functions of Ena/VASP family.
The letters S and T in circles indicate serine and threonine phosphorylation sites. In VASP, residues S157, S239 and T278 are preferentially phosphorylated by PKA, PKG and AMPK, respectively. The PKA site is conserved among all Ena/VASP family members (highlighted in yellow; VASP S157, Mena S236 and EVL S160). The pink rhombus (Y) indicates the tyrosine phosphorylation site in Mena.
Figure modified from (Sechi and Wehland, 2004).

1.3.2 Functions of Ena/VASP Proteins

Former studies have shown that Ena/VASP proteins are important mediators of actin cytoskeleton dynamics, thereby regulating listerial and cell movement, cell-cell and cell-matrix interactions and cell shape. They are also described as filament elongating factors as their incubation with G-actin leads to actin filament polymerisation, resulting in F-actin. Moreover, Ena/VASP proteins are able to bundle F-actin, hence they increase the stability of actin networks (Sechi and Wehland, 2004).

1.3.2.1 Ena/VASP Proteins are involved in Bacterial and Cell-Movement

The EVH1 domain can bind to the central proline-rich region of ActA, the surface protein of the intracellular bacterium *Listeria monocytogenes* (Chakraborty et al., 1995; Smith et al., 1996), whereas the PRR of Ena/VASP proteins binds to profilin (Reinhard et al., 1995). It is proposed that Ena/VASP family members in association with ActA can recruit profilin-G-actin-complexes which are then targeted to the (+)-ends of growing actin-filaments. Thereby, Ena/VASP proteins support actin polymerisation and the intracellular movement of *Listeria monocytogenes* (Gertler et al., 1996; Sechi and Wehland, 2004). In their ability to mediate listerial movement, Mena, VASP and EVL have been shown to be interchangeable (Lanier et al., 1999).
In a similar way, Ena/VASP proteins are involved in cell-locomotion by regulating the movement of actin- and plasma membrane protrusions of lamellipodia and filopodia. Probably they are targeted by their PRR to the cell

edges via interactions with proteins like Abis, Scar/WAVE and IRSp53. There they recruit profilin-actin complexes which promote the fast filament elongation (Sechi and Wehland, 2004). Studies have revealed that an IRSp53-Mena complex initiates actin filament assembly into filopodia (Krugmann et al., 2001). In analogy to the motility of filopodia, Ena/VASP shall play a role in actin filament dynamics during T-cell activation and phagocytosis (Sechi and Wehland, 2004).

There are some hints that Ena/VASP not only regulate actin dynamics via their assembly with profilin. They seem to protect the barbed ends of F-actin from capping proteins, thereby also promoting actin polymerisation (Applewhite et al., 2007; Barzik et al., 2005). Moreover VASP reduces branching of actin filaments induced by the Arp2/3 complex (Samarin et al., 2003).

A special form of cell protrusion being important for neuronal development is induced only by the 140 kDa form of Mena. It regulates growth cone dynamics and axonal guidance and is required for the formation of several axonal projection pathways in the brain, predominantly in the corpus callosum and in the hippocampus. Although mice lacking Mena are viable, they show a malformation of these pathways (Lanier et al., 1999).This stands in contrast to VASP, as no CNS defects result in VASP deficient mice (Aszodi et al., 1999).

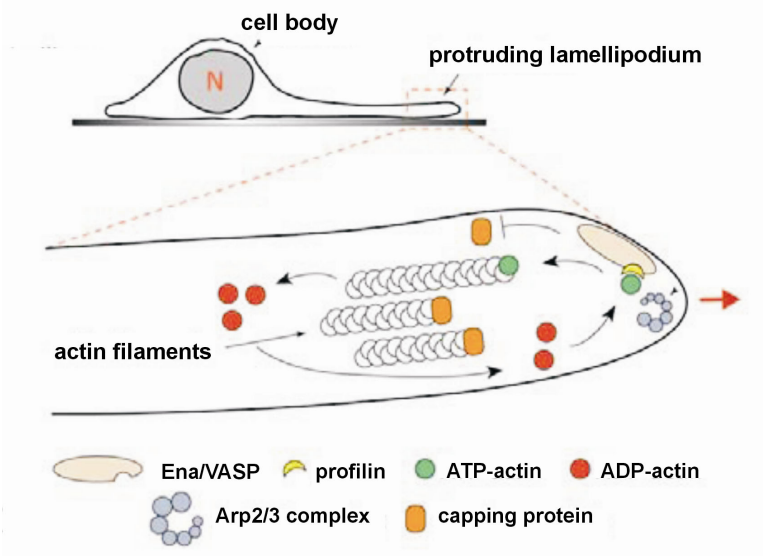

Fig. 1-3

Fig. 1-3. Ena/VASP Proteins Promote Cell Motility (previous page).
Schematic illustration of a lamellipodium. Ena/VASP proteins are recruited to the cell extension where they recruit profilin-actin complexes and thereby promote fast filament elongation. It is presumed that Ena/VASP also enhance the elongation process by blocking capping proteins and they can influence the activity of the Arp2/3 complex.
This movement regulation of Ena/VASP is similar to their influence on Listeria motility. There they are targeted to the bacterial surface protein ActA where they recruit the profilin-actin complex which promotes filament elongation. Figure modified from (Sechi and Wehland, 2004).

1.3.2.2 Ena/VASP Proteins at Cell-Contacts

Ena/VASP proteins promote actin assembly and polymerisation at focal adhesions and cell-cell contacts, thereby modulating cell-migration, cell-matrix- and cell-cell-interactions, respectively (Drees et al., 2000; Scott et al., 2006; Vasioukhin et al., 2000). Focal adhesions are cell surface structures composed of integrins and associated proteins, such as vinculin, that link the ECM to the actin cytoskeleton (see 1.1.5 for further details). Thus focal adhesions are crucial for cell adhesion and locomotion. The EVH1 domain binds to the focal adhesion proteins zyxin and vinculin and thus implicates the importance for Ena/VASP proteins at these contacts (Gertler et al., 1995; Lanier et al., 1999; Reinhard et al., 1995). Studies using zyxin-null mice have shown reduced accumulation of Ena/VASP proteins at focal adhesions. It is presumed that zyxin plays an important role in targeting Ena/VASP to focal adhesions. Furthermore it is assumed that zyxin and Ena/VASP cooperate to influence integrin-dependent cell motility (Drees et al., 2000; Hoffman et al., 2006). Adherens junctions (cell-cell-contacts) are intercellular structures, prominent in epithelial cells. The transmembrane proteins that mediate the intercellular attachments are cadherins (E-cadherins in epithelial cells, VE-cadherins in endothelia). Their cytoplasmic domain binds to α- and β-catenins, which link the actin cytoskeleton to the adherens junction. It is proposed that the formation of adherens junctions requires filopodia induced clustering of cadherins and, additionally, actin reorganization, which is mediated by the interaction of Ena/VASP proteins with zyxin and vinculin (Vasioukhin et al., 2000). Ena/VASP are also important for intercellular adhesion at endothelial cells (EC). Here, αIIb-

spectrin has been shown to colocalize with non-phosphorylated VASP at cell-cell-contacts. In more detail, the SH3 domain of αII-spectrin binds to the triple GP_5-motif of VASP. The resulting complex is important for stabilizing the endothelial barrier. Phosphorylation of VASP at S157 inhibits this assembly (Benz et al., 2008). To date, Mena has not yet been found to be a binding partner to αII-spectrin.

1.3.2.3 Aspects about the Regulation of Ena/VASP Proteins

The phosphorylation of S157 of VASP not only inhibits binding to αII-spectrin, it also prevents fibrinogen binding to the platelet glycoprotein IIb IIIa (= integrin α_{IIb} β_3) resulting in the inhibition of platelet aggregation (Halbrugge and Walter, 1990; Hauser et al., 1999; Horstrup et al., 1994). In addition, VASP phosphorylation may influence actin nucleation and filament bundling negatively, whereas phosphorylation does not seem to affect VASP interactions with profilin, zyxin and vinculin (Harbeck et al., 2000). Recent studies have shown that the PKG- and AMPK-mediated phosphorylation of VASP (S239, T278) impedes F-actin accumulation. In contrast to this, phosphorylation of the structurally and functionally conserved PKA phosphorylation site (VASP S157, Mena S236 and EVL S160) does not affect Ena/VASP-driven F-actin assembly (phosphorylation sites see Fig. 1-2). But it promotes VASP targeting to focal adhesions and lamellipodia as cells spread (Benz et al., 2009).

1.3.2.4 Ena/VASP Proteins in Cardiomyocytes

It is known that mice lacking either Mena or VASP do not show any obvious cardiac abnormalities (Aszodi et al., 1999). Nevertheless, there are hints that these proteins are important for proper heart function. VASP and Mena colocalise with connexin-43, cadherin and vinculin at intercalated discs (ID) (Gambaryan et al., 2001). IDs are essential for cardiac contraction as they mediate the conduction of electrical signals and the transmission of mechanical force between cardiomyocytes. It has been shown that displacement of Mena and VASP from IDs in mice leads to a severe dilated cardiomyopathy (Eigenthaler et al., 2003).

1.3.2.5 Do Ena/VASP Family Members Compensate for each other?

In most of the studies published to date, Mena and VASP exhibit very similar subcellular distribution and functions, indicating that both proteins could compensate for each other. Furthermore, mice lacking either Mena or VASP show no severe phenotype (Aszodi et al., 1999; Hauser et al., 1999; Laurent et al., 1999), whereas the deletion of both genes results in a lethal phenotype during late embryonic development (Bear et al., 2002; Menzies et al., 2004). Further studies have demonstrated that human VASP can partially substitute for a loss of Ena in the developing *Drosophila* embryo (Ahern-Djamali et al., 1998). But there are also some differences between Mena, VASP and EVL, for example concerning their expressions in diverse tissues. Mena and VASP are both localized in heart, lung, blood vessels, smooth muscle cells of stomach and intestine and in glomerular mesangial cells. However, VASP and EVL are highly expressed in platelets and spleen, whereas Mena has not yet been detected in these tissues (Gambaryan et al., 2001; Hauser et al., 1999). Moreover, Mena is different from the other family members because of its neuronal variant. To date, no neuronal splice variants of VASP or EVL have been identified.

To conclude, the hypothesis of compensation has to be explored further.

1.4 Localisation and Functions of Spectrins in the Mammalian Heart

Spectrins are actin-binding proteins that assemble into tetramers, which are composed of two α- and two β-subunits. To date, two α- and five β-isoforms have been identified (Bennett and Baines, 2001). Originally, spectrins were identified in erythrocytes where they are important for the mechanical stabilisation of the plasma membrane. In erythrocytes, the spectrin tetramer is composed of two αIβI-dimers. Actin filaments and spectrin tetramers build up a meshwork which is associated with the plasma membrane by ankyrin and protein 4.1 (Fig. 1-4) (Tse and Lux, 1999).

Whereas the expression of αI- and βI-subunits is restricted to erythrocytes, other subunits like αII-spectrin (also named fodrin) are expressed in most tissues, including heart muscle.

The spectrin cytoskeleton in cardiomyocytes is not only associated with the lateral plasma membrane. Spectrins also localise to T-tubules, to Z-discs, to intercalated discs (IDs) where they shall be important for stabilizing gap junctions and they are enriched at costameres (see 1.1.4.1) (Baines and Pinder, 2005; Thornell et al., 1984; Toyofuku et al., 1998). The subunits localise differently in the mammalian heart. αI-spectrin is found at the lateral plasma membrane. αII-spectrin localises to Z-discs, lateral plasma membrane, IDs and the nucleus. In endothelial layers of vessels, αII-spectrin and non-phosphorylated VASP build up complexes that regulate cortical actin cytoskeleton assembly in endothelial cells. This assembly is important for perijunctional stress fibre formation and to sustain endothelial barrier function (Benz et al., 2008). Concerning both, βI- and βII-spectrin, there exist two subunits, Sigma1 and Sigma2, which are different splice variations on the C-terminal side of each protein (Baines and Pinder, 2005). The βISigma1-isoform is restricted to erythrocytes, whereas the βISigma2-isoform is found at costameres. βII-spectrins, Sigma1 and 2, localise at intercalated discs and Z-discs where they colocalise with α-actinin (Baines and Pinder, 2005). From these results it is presumed that IDs contain $(\alpha II\beta IISigma1)_2$ and $(\alpha II\beta IISigma2)_2$-tetramers. This implies that important functions of spectrins in heart are the promotion of force transduction between cardiomyocytes and the electrical conduction by stabilising the gap junctions (Toyofuku et al., 1998). This role is confirmed by the finding that an alternatively spliced isoform of αII-spectrin, namely αII-SH3i, associates with connexin 43 (Ursitti et al., 2007). αII-SH3i contains a 20-aminoacid-insertion downstream of the SH3 domain and may modulate its binding to proline-rich-regions of target proteins. Also at costameres, spectrins provide for stabilisation of cell adhesions and for transmitting force from the contractile apparatus to the ECM (Bennett et al., 2004).

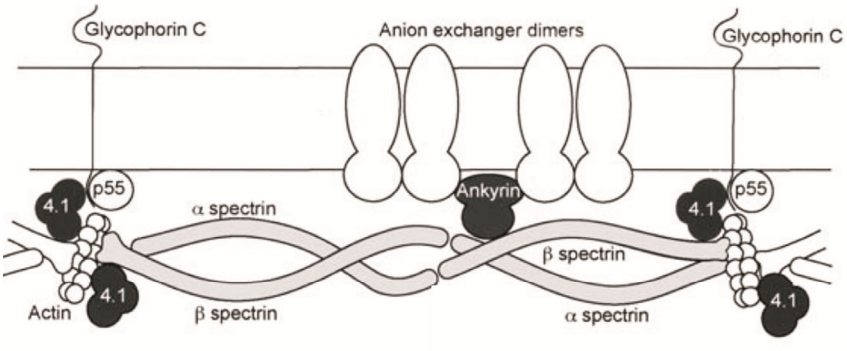

Fig. 1-4. The Spectrin-Based Membrane Skeleton in Erythrocytes.
Schematic illustration of the erythrocyte membrane cytoskeleton. Spectrin tetramers are cross-linked by short actin filaments and protein 4.1. The network is attached to the plasma membrane by ankyrin, which binds spectrin tetramers and the transmembrane anion exchanger band 3 simultaneously. Figure taken from (Bignone and Baines, 2003)

1.5 Manipulating the Mammalian Genome by Generating Knockout Mice

Today, an essential part in biological and medical basic research is the analysis of genetically manipulated mice. As the genome of mice resembles the human genome, the mouse model helps to understand the functions of our genes. This knowledge leads to a better understanding of life processes, diseases, and the development of carcinomas and can be used for improving medical therapy.

The first knockout mouse was created by the work of M. Capecchi, J. Evans and O. Smithies in 1989. They were awarded the Nobel Prize in 2007 “for their discoveries of principles for introducing specific gene modifications in mice by the use of embryonic stem cells” (www.Nobelprize.org). Their work was the breakthrough to classical gene targeting using embryonic stem cells (ES-cells) and homologous recombination. But gene targeting not necessarily implies the inactivation, the knockout = loss-of-function, of a specific gene. With gene targeting it is also possible to exchange a gene sequence by another (knock in) or imply a point mutation in a functional domain (gain-of-function).

1.5.1 The Classical Knockout Method

For the targeted inactivation of a gene, a vector is engineered, which, in the case of knockout mice, contains a non-functional DNA sequence, a positive selection marker (usually *neo* = neomycin resistance gene) and two flanking genes which are homologous to sites of the targeted gene. Outside the region of homology, the generated DNA-construct also harbours a *HSV-tk* (Herpes-simplex-virus-thymidine-kinase) gene as a negative selection marker.

From a mouse blastocyst (e.g. mouse with grey fur) ES-cells are isolated and grown in vitro. The DNA construct is inserted into the ES-cells by electroporation. By homologous recombination, which resembles the process that occurs during meiosis, the targeted gene is exchanged by the generated construct containing the *neo*-sequence (Fig. 1-5). Usually, this exchange leads to the complete loss of the protein function. As homologous recombination occurs quite rarely and sometimes undirected, cells containing the mutated DNA have to be selected. Therefore the ES-cells are grown in antibiotics. Cells having undergone homologous recombination are resistant to neomycin because they contain the *neo*-sequence. In contrast, by homologous integration, the *HSV-tk* is kept outside. ES-cells harbouring *HSV-tk* have undergone undirected recombination (random integration). HSV-tk phosphorylates gancyclovir, a process that in the end leads to cell death. By this, *HSV-tk* serves as a negative selection marker when cells are grown in gancyclovir. Afterwards, selected ES-cells are injected into a new blastocyst (e.g. wt mouse with white fur) which is then implanted into a pseudo pregnant mouse. For identifying the offsprings, the fur colour serves as indicator. Some of the offsprings have white fur, others are chimeric mice, and their cells derive from the white-mouse blastocyst and from the recombinated cells. Chimeric mice are crossbred with white wt mice again. By PCR and Southern blot analysis heterozygous mice are identified and then crossbred. 25% of their offsprings are homozygous, they are knockout mice. (www.bio.davidson.edu/courses/genomics/method/homolrecomb.html)

(Lottspeich and Zorbas, 1998; Melton, 1994; Stanford et al., 2001)

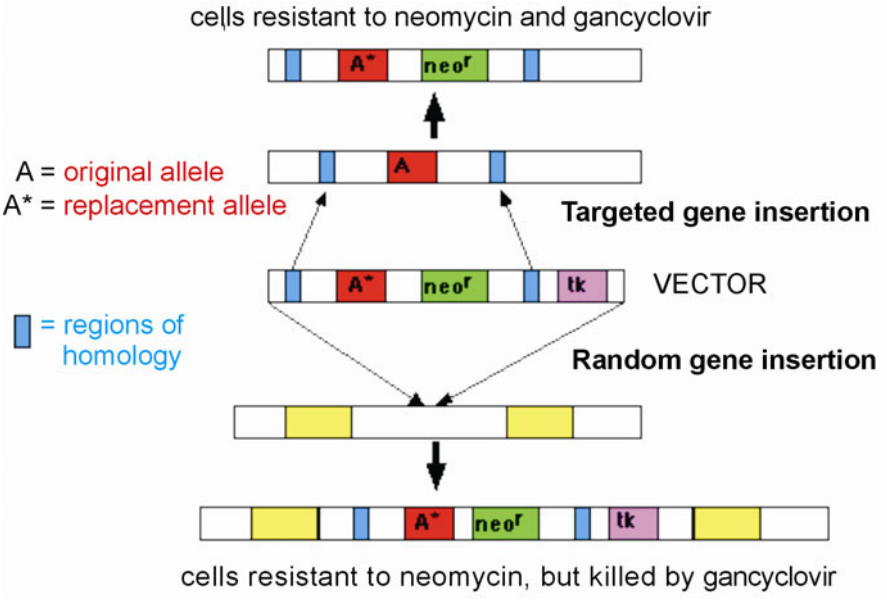

Fig. 1-5. Schematic Illustration of Gene Targeting and Random Gene Insertion, Respectively. By homologous recombination, the targeted allele (A) is exchanged by the generated vector construct containing the *neo*-sequence. Homologous recombination occurs quite rarely and sometimes undirected, thus the cells containing the required mutated DNA have to be selected by growing them in antibiotics. Cells having undergone homologous recombination are resistant to neomycin as they contain the *neo*-sequence, whereas the *HSV-tk* (tk) is kept outside. ES-cells harbouring *HSV-tk* have undergone undirected recombination. *HSV-tk* serves as a negative selection marker when cells are grown in gancyclovir.
Figure modified from: http://users.rcn.com/jkimball.ma.ultranet/BiologyPages/N/Neo.tkVector.gif

1.5.2 The Conditional Knockout Method

Limitations of the classical knockout method can be an embryonic lethal phenotype and the problem that the lesion generated does not always have an easily interpretable effect. Therefore, alternative technologies have been developed; for example the conditional knockout or tissue-specific gene-targeting. The most common is the Cre-LoxP recombinase system. The Cre-recombinase (Cre = cyclization recombination) catalyses DNA recombination between two LoxP sites (LoxP = locus of X-over P1). Depending on the relative orientation of the LoxP-recognition sites, the Cre-recombinase may catalyse deletion (same orientation) or inversion of the DNA segment lying between those two LoxP sites. A targeted gene sequence that is flanked by two LoxP sites is called a floxed allele. By crossing two strains of transgenic mice, one carrying the floxed alleles, the second one carrying a Cre-recombinase encoding sequence under the control of a tissue-specific promoter (e.g. of a

neuronal specific gene), conditional knockout mice can be obtained. (Cohen-Tannoudji and Babinet, 1998; Lottspeich and Zorbas, 1998).

1.5.3 Gene-trapping

Whereas gene-targeting relies on rare homologous recombination between a DNA construct and the targeted DNA sequence, gene-trapping relies on random integration of a promoterless reporter construct. Thus, compared to gene-targeting, it is usually a faster method because it leads to a broad availability of ES-cell clones with identified trapped genes (Ullrich, 2009).

A gene-trap vector is introduced into ES-cells by electroporation or retroviral infection. The insertion, which often takes place in introns, usually leads to the inactivation of the trapped gene. The gene-trap vector construct which is put under control of the endogenous promoter, usually contains a splice acceptor site upstream of the reporter gene and a polyadenylation signal at the other end. As reporter or selection genes serve, amongst others, *lacZ*, *β-geo* and *neo*. *lacZ* encodes for β-galactosidase, an enzyme that can be used for staining (e.g. of cryosections) in order to analyse the expression pattern of the gene. *β-geo* encodes β-galactosidase and neomycin resistance. The transcription of the trapped gene is followed by a splicing process of the mRNA resulting in a fusion protein which contains the selection- and/or reporter protein and a fragment of the original protein (Fig. 1-6). To identify the trapped gene, PCR based strategies such as 5`RACE are used (Skarnes, 2005; Stanford et al., 2001).

Today, libraries of ES-cell lines harbouring gene-trap insertions have been generated (a database of available gene trap lines at *International Gene Trap Consortium*, www.genetrap.org). For example, until 2008 Bay Genomic, a consortium of research groups in San Francisco, used gene-trap vectors to inactivate thousands of genes in ES-cells of mice to generate knockout mice. They have made all of their ES-cell lines available to the scientific research community.

More sophisticated is the method of targeted trapping (Friedel et al., 2005). It is a technique that combines gene-trapping with gene-targeting (homologous

recombination). Therefore the gene-trap cassette is flanked with homologous gene sequences.

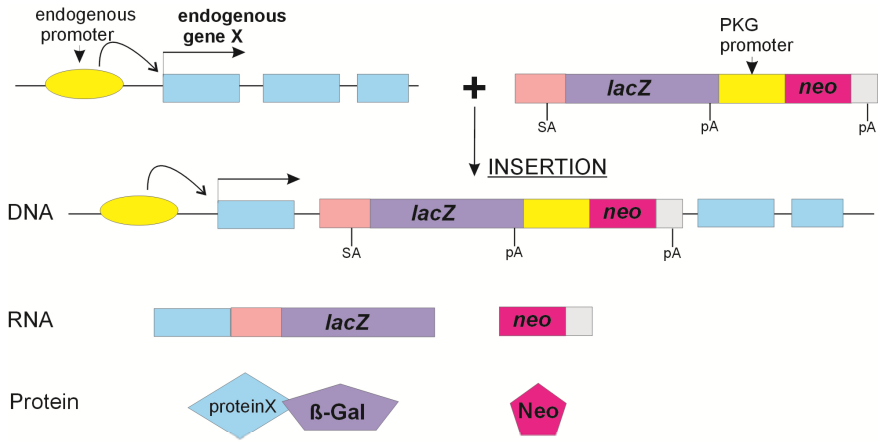

Fig. 1-6. Schematic Illustration of a Gene-Trap Method.
The constructed vector contains a splice acceptor (SA) upstream of the *lacZ* reporter gene, followed by the neomycin resistance gene (*neo*), which is under control of the phosphoglycerate kinase (PGK) promoter. The vector integrates in intron 1 of the endogenous gene X, resulting in a fusion transcript between exon 1 of the endogenous gene and the l*acZ* reporter. The translation of the spliced mRNA leads to neomycin resistance and to a fusion protein comprising β-galactosidase (β-Gal) and a part of protein X. Usually by this method, protein x becomes non-functional. The enzyme β-galactosidase can be used for staining methods. Figure modified from (Stanford et al., 2001)

1.6 Ena/VASP Family Knockout Mice

1.6.1 VASP Deficient Mice Generated by Homologous Recombination

Hauser et al. 1999, explored the function of VASP in platelet activation. For this purpose they generated VASP deficient mice using homologous recombination. The targeting vector (p19TV) contained a neomycin resistance gene and a *HSV-tk* gene which served as positive and negative selection markers, respectively. By homologous recombination the *neo* cassette replaced exons 4-11. This part of the allele, encoding the PRR and the proximal part of the EVH2 domain, was deleted by this (Fig. 1-7). The targeting construct was electroporated into ES-cells of 129Sv/ola mice. The selection of correctly recombined cells was performed using antibiotics and the result was verified by

Southern blot analyses. Finally an ES-cell clone was injected into a C57Bl/6 blastocyst resulting in chimeric offsprings. By germline transmission, homozygous VASP$^{-/-}$ mice were obtained.

In this study, we used the VASP$^{-/-}$ mice from *Hauser et al*. For genotyping of these mice we performed PCR, the method is described in detail in 2.1.2.2.

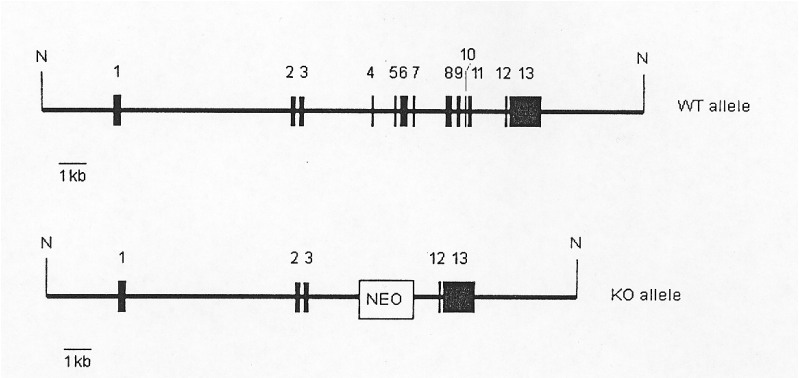

Fig. 1-7. VASP Deficient Mice Generated by Homologous Recombination.
Schematic illustration showing the VASP wild-type (WT) allele and the knocked-out (KO) allele bellow. The targeting vector (p19TV) is inserted into the allele by homologous recombination. *The neo* cassette (neomycin resistance gene) replaces exons 4-11, the part which usually encodes the PRR and the proximal part of the EVH2 domain. Figure modified from (Hauser et al., 1999)

1.6.2 Targeted Disruption of the VASP Gene

Aszodi et al 1999, also analysed the role of VASP in platelet aggregation. VASP$^{-/-}$ mice were obtained by targeted disruption. For this purpose they used a gene trap vector with a *geo*-DNA sequence which was inserted into exon 2. The *geo*-cassette was flanked by genomic DNA that was homologous to a part of intron 1 and a part of exon 13, respectively. By homologous recombination almost the hole VASP gene, precisely exons 2-13, was exchanged by the vector construct. Selection of the correctly targeted ES-cells was performed using neomycin and Southern blot analysis. The selected cells were transferred into blastocysts and by crossbreeding, homozygous VASP deficient mice were obtained in the end.

1.6.3 Targeted Disruption of the Mena Gene

Lanier et al., 1999, analysed the function of Mena in the central nervous system using Mena deficient mice. These mice were generated by targeted disruption of the Mena gene. The targeting vector contained a *β-geo*-cassette harbouring a splice acceptor at the one end and a polyadenylation site at the other end. This cassette was flanked by DNA fragments that were homologous to the first intron and to the third intron respectively. As a negative selection marker served a PGK diphtheria toxin cassette. The targeting vector was electroporated into AK7 ES-cells. After selection steps, ES-cell clones were injected into mice blastocysts in order to generate chimeras.

1.6.4 Generation of Triple Knockout Mice

As mentioned above, knocking out an individual Ena/VASP family member results in a relatively minor phenotype (Aszodi et al., 1999; Hauser et al., 1999; Lanier et al., 1999), whereas Mena/VASP double deficient mice die perinatally (Menzies et al., 2004). *Furman et al., 2007*, have analysed the importance of Ena/VASP in endothelial barrier function. Therefore they generated Ena/VASP triple deficient mice (mmvvee). Because of their perinatal death, only the embryos could be inspected. For the generation of mmvvee-mice, *Furman et al.* followed the descriptions of Kwiatkowski (Kwiatkowski et al., 2003). They used homologous recombination to disrupt the EVL gene. Their targeting vector contained a *neo*-cassette flanked by genomic DNA. The insertion led to a deletion of EVL-exons 2 and 3, and, as in case of VASP and Mena, the EVL deficient mice revealed no obvious phenotype. The generated $EVL^{-/-}$ mice were crossbred to existing $Mena^{-/-}$ - and $VASP^{-/-}$ -lines (Aszodi et al., 1999; Lanier et al., 1999). Triple-null offsprings were never born alive. Lethality occurred between E16.5 and P0 (Furman et al., 2007).

2. Materials and Methods

2.1 Genotyping of Mice

2.1.1 DNA Isolation

DNA was isolated from mouse tail biopsies using the Qiagen DNeasy Tissue Kit. The instructions of the protocol „Purification of Total DNA from Animal Tissues (Spin Column Protocol)" were followed.

Briefly, a 1 cm length tail piece of each mouse was chopped, placed into a microcentrifuge tube, 180 µl Buffer ATL and 20 µl proteinase K were added and mixed by vortexing. Incubation at 56°C was performed overnight using a thermomixer. After the tissue was completely lysed, 200 µl Buffer AL and 200 µl ethanol were added. The samples were vortexed and the mixture was loaded into a DNeasy Mini spin column. After centrifugation at 6000 x g for 1 min, the column was washed once with 500 µl Buffer AW1 and 500 µl Buffer AW2. To dry the DNeasy membrane, the column was centrifuged for 3 min at 20000 x g. Differing from the protocol, for DNA elution, 150 µl H_2O were pipetted onto the membrane and centrifuged for 1 min at 6000 x g.

2.1.2 Polymerase Chain Reaction (PCR)

PCR was used to amplify DNA fragments, which can be visualized by agarose gel electrophoresis.

2.1.2.1 Mena PCR

The following primer sequences were used:

Mena Forward Pimer

me_F3: 5' – TGG GCA GAA AGA TTC AAG ACC – 3'

Mena Reverse Pimer WT-PCR

me_in2_R2: 5' – CCA GTT TCA ATG CCC ATT CCT T – 3'

Mena Reverse Pimer KO-PCR

pGT0Lxf_R2: 5' – CGG ATC TCA AAC TCT CCT CC – 3'

The Mena forward primer hybridizes to the 3'-end of Mena exon 2, the wt reverse primer to the Mena intron 2, whereas the Mena ko reverse primer hybridizes to the RRG138 gene trap construct (Baygenomics, San Francisco, USA). The ko-PCR-product has a size of 824 bp, the wt-PCR-product a size of 1123 bp.

For each sample a PCR master mix with an end volume of 50 µl was mixed as follows:

5 µl	10x Taq buffer
10 µl	Q-Solution
1 µl	10 mM dNTP Mix
0.5 µl	Taq (Qiagen Taq DNA Polymerase, Cat. No. 201207)
1.5 µl	10 µM me_F3 primer
1.75 µl	10 µM me_in2_R2
1 µl	10 µM pGT0Lxf_R2
10 µl	Isolated DNA of mouse tail biopsy
19.25 µl	dH_20

The DNA samples were amplified in 32 cycles, using a thermocycler (Biometra, Göttingen, Germany). Each cycle included a denaturation (94°C), a primer annealing (56°C) and an elongation step (72°C).

Step	Temperature	Time	
1	94°C	4 min	
2	94°C	1 min	Repeat 32x
3	56°C	30 sec	
4	72°C	90 sec	
5	72°C	10 min	
6	15°C	forever	

2.1.2.2 VASP PCR

The following primer sequences were used:

VASP Forward Primer KO-PCR

GIK 273 5´–CGA ATA GCC TCT CCA CCC AAG CGG CCG GAG AAC–3´

VASP Reverse Primer KO-PCR

GIK 274 5´–GGC CAG CAG AAC AGT ATT GGA GAA CAT CCA GG–3´

VASP Forward Primer WT-PCR:

GIK 269 5´–TTA GCT TGG TTT GGG GAC TGA ACC AGC CTC CTT TC-3´

VASP Reverse Primer WT-PCR:

GIK 270 5´–CAG CCA CTC CCT GGT ACT TCC TTA CCT TGC TCA C–3´

The VASP forward ko primer hybridizes to the *neo* cassette, the reverse ko primer to the VASP intron between the *neo* cassette and exon 12, resulting in a PCR-product-size of approximately 600-700 bp.
The VASP forward wt primer hybridizes to the VASP intron 5' to exon 5 and the reverse wt primer to exon 6, resulting in a PCR-product-size of 450-500 bp.

For each sample, a PCR master mix with an end volume of 50 µl was mixed as follows:

5 µl	10x Taq buffer
10 µl	Q-Solution
1 µl	10 mM dNTP Mix
0.5 µl	Taq (Qiagen Taq DNA Polymerase, Cat. No. 201207)
1 µl	10 µM GIK 273 primer
1 µl	10 µM GIK 274 primer
1.75 µl	10 µM GIK 269 primer
1.75 µl	10 µM GIK 270 primer
10 µl	Isolated DNA of mouse tail biopsy
18 µl	dH_20

The thermocycler (Biometra) was programmed as follows:

Step	Temperature	Time	
1	95°C	5 min	
2	95°C	1 min	Repeat 35x
3	65°C	1 min	
4	72°C	2 min	
5	72°C	10 min	
6	15°C	forever	

2.1.3 Agarose Gel Electrophoresis

An 1% agarose gel (1 x TAE [40 mM Tris-acetate and 1 mM EDTA] and 1% of ultra pure agarose, obtained from Roth, Karlsruhe, Germany) with a final concentration of 0.08% of ethidium bromide (Aplichem, Darmstadt, Germany) was prepared and poured into a gel rack with an appropriate comb. After 30 min, the comb was removed and the gel was transferred to a TAE-filled electrophoresis chamber. The PCR samples (25 µl each), and a sample that contained water instead of genomic DNA, for reference, and 6 µl of a GeneRuler™ DNA Ladder Mix (Fermentas) were loaded into the pockets. 120 V were applied to the electrophoresis chamber for approximately 40 min, the DNA fragments in the gel were visualised under ultraviolet light and documentation was performed using KODAK Gel Logic 100 Imaging System.

2.2 Histological Analysis

2.2.1 Preparation of Mouse Organs

Mice were sacrificed with carbon dioxide followed by cervical dislocation. Tissues (heart, lung, liver, spleen, kidneys, stomach, large intestine, small intestine, femoral skeletal muscle, testis/ovaries, brain, eyes, lymph nodes) were dissected using forceps and scissors and briefly rinsed in 1 x PBS (Phosphate-buffered saline; 137 mM NaCl, 0.3 mM KCl, 8.1 mM Na_2HPO_4, 6.7

mM KH_2PO_4, pH 7.4). The organs were then snap frozen in 2-methylbutan (Sigma-Aldrich), which had been pre-cooled on dry ice or in liquid nitrogen. The frozen organs were then stored in Falcon tubes at -80°C. In some cases, the tissues were embedded in -and in the cases of hallow organs also filled with- Tissue-Tek®.

2.2.2 Cryosections of Mouse Organs

The tissues were cut with a microtome (Mikrotom-Kryostat HM 500 OM, Microm Int., Walldorf and Leica Jung CM 3000, Bensheim) into 10 µm sections at -20°C and collected on SuperFrost Plus object slides (Menzel-Gläser, Braunschweig, Germany). Subsequently, the sections were either used for X-gal staining or immunohistochemistry.

2.2.3 X-Gal Staining

Our Mena deficient mice were generated by gene-trapping, using the gene-trap construct RRG138 provided by Baygenomics, San Francisco, USA.

With X-gal staining the vector insertion and the β-galactosidase expression of these Mena $^{-/-}$ mice were confirmed. X-gal staining was performed as described in the "X-gal staining protocol" of the Sanger Institute (http://www.sanger.ac.uk/PostGenomics/genetrap/protocols/XGalStaining.pdf).

Organ cryosections of Mena$^{-/-}$ mice with the gene trap insertion and of wt mice as negative controls were used.

The following reagents were prepared and used as stock solutions:

0,1M phosphatase buffer (ph 7.3)	3.75 g NaH_2PO_4- H_2O (MW = 137.99) 10.35 g Na_2HPO_4 (MW = 141.96) dissolved in 1 litre dH_2O
Fix buffer for X-gal staining	0,1 M phosphatase buffer (ph 7.3) 5 mM EGTA, pH 7.3 2 mM $MgCl_2$ 0.2% glutaraldehyde
Wash buffer for X-gal staining:	0.1 M phosphate buffer (pH 7.3) 2 mM $MgCl_2$

X-gal staining buffer:	0.1 M phosphate buffer (pH 7.3) 2 mM $MgCl_2$ 5 mM $K_4Fe(CN)_6$ -$3H_20$ 5 mM $K_3Fe(CN)_6$ before use: X-gal (5-bromo-4-chloro-3-indolyl-β-D-galactoside) added to a final concentration of 1 mg/ml
X-gal stock solution (50 mg/ml):	10 ml dimethylformamide (Roth, Karlsruhe, Germany) 500 mg X-gal

Approximately 2 - 4 hours before staining, X-gal solution was added to X-gal staining buffer to a final concentration of 1 mg/ml and mixed thoroughly. Prior to use, this solution was filtered with a folding filter in order to remove any precipitate.

Straight after the collection of the cryosections, the object slides were transferred to a glass chamber with fix buffer. After 15 min of fixation, the object slides were washed twice with wash buffer, each time for 5 min. Finally, the cryosections were covered with the filtered X-gal staining buffer, and incubated for 13 to 15 hours at 37°C. The next day, object slides were washed twice, and then mounted with 100 µl of Mowiol and a cover slip. After air-drying at room temperature overnight, stained sections were stored at 4°C until inspection using a Nikon microscope. Images were acquired using the ACT-1 software (Nikon).

Mowiol + Dabco (stored at -20°)	2,4 g Mowiol 4-88 (Hoechst) 6 g Glycerol 6 ml H_2O 12 ml 0,2M Tris (pH 8,5) 2,5% 1,4-diazobicyclo-octane

2.2.4 Immunofluorescence

Cryosections were prepared as described in 2.2.1 and 2.2.2, using Mena$^{-/-}$ and wt mouse organs.

The following reagents were prepared and used as stock solutions:

4% PFA	8 g paraformaldehyde 200 ml PBS mixed under cooking
20% Triton stock solution	20 ml Triton X-100 (Sigma) 80 ml dH_20
10% NGS/PBS	1 ml Normal Goat Serum (NGS) 9 ml 1 x PBS

Each organ section on the object slides was encircled with a PAP pen (DAKO pen), fixed in ice-cold 4% PFA for 7 min and then thrice washed in PBS for 10 min each at room temperature. The sections were permeabilized with 0.1% Triton X-100 for 20 min at room temperature, washed again twice and blocked for 1 hour with 10% Normal Goat Serum (NGS). Incubation with primary antibodies in 10% NGS was performed overnight in a humid chamber at room temperature.

The next day, sections were washed thrice in 1 x PBS, incubated with fluorescence-conjugated secondary antibodies in 10% NGS/PBS for 1 – 2 hours in the dark in a humid chamber. The slides were washed three times and finally mounted with Mowiol (see 2.2.3) and cover slips.

After air-drying overnight, the sections were investigated by using a Nikon Eclipse E600 microscope with a C1 confocal scanning head and a 60-fold oil immersion objective. Images were acquired and prepared using the EZ-C1 software (Nikon, V. 3.00).

Primary Antibodies (AB) Used in this Study for Immunofluorescence Labelling

Primary AB	Description	Source	Dilution
anti-mena 438, affinity purified 2,16 mg/ml	rabbit, antibody against LERER repeat	Dr. P. Benz, University of Würzburg	1:500
anti-mena 438	rabbit, FITC-conjugated	Dr. P. Benz, University of Würzburg	1:200
anti-VASP M4, 19728, serum	rabbit, polyclonal	Immunoglobe	1:500
anti-EVL AB109, purified	rabbit	Immunoglobe	1:500
Phalloidin-TRITC, P1951, 1 mg/ml		Sigma	1:500
anti-α-smooth-muscle-actin, F3777	mouse, monoclonal, FITC conjugated	Sigma	1:500
anti-VE Cadherin, hybridoma supernatant	rat	Kind gift from Dr. J. Waschke, University of Würzburg	1:10, **pure**
anti-αII-spectrin, sc-7465, 200 µg/ml	goat	Santa Cruz, USA	1:50
alpha-Fodrin, #2122	rabbit	Cell Signaling, USA	1:50
alpha-Fodrin, ab11755, tissue culture supernatant, 1 mg/ml	mouse, monoclonal	Abcam, Cambridge, USA	1:100
Anti-Fodrin, α, clone AA6, MAB1622, purified, 0,1 mg/ml	mouse, monoclonal	Chemicon (Millipore), USA	1:200

Secondary Antibodies (AB) used in this Study for Immunofluorescence Labelling:

Secondary AB	Source	Dilution
Alexa Fluor 488 goat anti-rabbit IgG	Molecular Probes, Invitrogen, USA	1:500
Alexa Fluor 594 goat anti-rabbit IgG	Molecular Probes, Invitrogen, USA	1:500
goat-anti-rat GART Cy2, #112-225-003	Dianova	1:600
Alexa Fluor 488 goat anti-rat IgG	Molecular Probes, Invitrogen, USA	1:500
Alexa Fluor 594 donkey anti-goat IgG	Molecular Probes, Invitrogen, USA	1:400

2.3 Protein Analysis

The expression of Mena protein in diverse tissues was analysed by Western blots, comparing Mena deficient and wild-type mice.

2.3.1 Preparation of Mouse Organ Protein Extracts

The mouse was sacrificed and organs excised using scissors and forceps. Every organ was weighed and 80 – 150 mg of tissue were transferred into a round bottom bacteria tube (Hartenstein #KU59, Würzburg, Germany). Then 2 ml lysis buffer per 100 mg tissue were added.

Lysis Buffer:

Final Concentrations	For 25 ml Lysis Buffer
2% SDS	5 ml of 10% stock solution
1 x PBS	2.5 ml of 10 x PBS
2 x Complete EDTA free protease inhibitors cocktail tablets (Roche Applied Science, Indianapolis, USA)	2 ml of 25 x stock solution

1 x PhosSTOP phosphatase inhibitor cocktail tablets (Roche Applied Science, Indianapolis, USA)	2.5 ml of 10 x stock solution
dH_2O	13 ml

Tissues were homogenized in an IKA Ultra Turrax T25 and afterwards incubated for 30 min at room temperature. The resulting suspension was transferred into Eppendorf tubes and centrifuged for 30 min at room temperature at 20 000 x g. The supernatant was then transferred into new tubes, and 250 – 500 µl aliquots were snap frozen in liquid nitrogen and stored at -80°C.

2.3.2 Preparation of Mouse Washed Platelets

Mouse blood was obtained by retroorbital blood collection. Briefly, mice were anaesthetised by intraperitoneal aventin injection and venous blood was collected from the mouse's orbital sinus using a glass capillary, which was inserted between the eyeball and the medial orbita wall. Blood was collected into a 1 ml microtube (9NC, Sarstedt, Nümbrecht, Germany) filled with citrate buffer to prevent coagulation. After centrifugation for 5 min at 400 g at room temperature, the white phase, which contains most of the platelets, was transferred into a new tube. With an additional quick run (1500 g) more platelets were harvested. The sample was then centrifuged for 8 min at 100 g, the platelet rich plasma (PRP) was collected into a new tube. The platelets were resuspended in 1 ml PBS and then in 2% SDS in PBS.

2.3.3 Analysis of Protein Extracts

In order to compare Mena protein expression of different tissues or mice, respectively, equal protein loading on the SDS-PAGE-gels was necessary. To analyse the concentration of the protein extracts, the following methods were used:

2.3.3.1 Measuring Protein Concentration by UV-Spectrometry

First the spectrometer was zeroed with a solvent blank (5 µl lysis buffer + 95 µl dH_2O). Then the cleaned cuvette was filled with protein extract (5 µl protein sample + 95 µl dH_2O) and extinctions of the sample were recorded at 260 nm, 280 nm and 320 nm. Protein concentrations were estimated according to E. Layne (Layne, 1957):

Protein concentration [mg/ml] $= 1.55 \times (A_{280} - A_{320}) - 0.76 \times (A_{260} - A_{320})$

Or simplified: $= 1.55 \times A_{280} - 0.76 \times A_{260}$

2.3.3.2 Coomassie Staining of SDS-PAGE-Gels

Coomassie staining of protein containing gels can be used to estimate and compare the concentrations of loaded protein samples. The protein samples of interest were loaded on a Sodium Dodecyl Sulfate-Polyacrylamide-Gel-Electrophoresis (SDS-PAGE-gel see 2.3.4.1). After protein separation was completed, the gel was stained for at least 2 h with Coomassie solution.

Coomassie solution:

Isopropyl alcohol	25% (v/v)
acetic acid	10% (v/v)
Coomassie brilliant blue R250	0.025% (w/v)

Afterwards the gel was destained overnight in 20% (v/v) methanol and 10% (v/v) acetic acid.

2.3.4 Western Blot Analysis

Western blotting is a method to detect proteins by using antibodies. Briefly, the proteins are first separated by SDS-PAGE, then transferred onto a membrane and finally detected by using antibodies.

2.3.4.1 Sodium Dodecyl Sulfate–Polyacrylamide-Gel-Electrophoresis (SDS-PAGE)

larger than 110 kDa to 12% for those SDS-PAGE is a technique, which separates proteins electrophoretically by molecular mass. According to the size of the

expected proteins, the separating gel contained different amounts of acrylamide, ranging from 6% for proteins of molecular weight being smaller than 40 kDa.

Separating gel

Acrylamide mix (Rotiphorese Gel 30 (37.5/1) Roth, Germany)	6% - 12% (w/v)
Tris-HCl pH 8.8	375 mM
SDS	0.1% (w/v)
APS	0.1% (w/v)
TEMED	0.04% (v/v)
dH_2O	

SDS= sodium dodecyl sulfate, APS= ammonium persulfate, TEMED= Tetra-Methyl-Ethylene-Diamine

This acrylamide solution was poured between the glass plates of the apparatus and overlaid with isopropanol, which created a barrier to oxygen. After 30 min the gel had set, its top was cleared with distilled water, the solution for the stacking gel was poured on the separating gel and a comb was placed into the stacking gel solution.

Stacking gel

Acrylamide mix	5.1% (w/v)
Tris-HCl pH 6.8	130 mM
SDS	0.1% (w/v)
APS	0.1% (w/v)
TEMED	0.1% (v/v)
dH_2O	

The gel was placed into a gel box with running buffer (25 mM Tris, 192 mM glycine and 0,1% (w/v) SDS). Referring to the results of 2.3.3.1 and 2.3.3.2, the gel was loaded using a Hamilton syringe with 30 µg of total protein mixed with 10 µl Laemli-loading buffer (250 mM Tris-HCl pH 6.8, 10% SDS (w/v), 30 – 40% Glycerol (v/v), 0.05% Bromphenol-blue (w/v), 5% (v/v) β-mercaptoethanol). For size comparison, 12 µl of PageRuler™ Plus Prestained Protein Ladder

(Fermentas) were loaded. Electrophoresis was started at 100 – 120 V for approximately 20 minutes. After the dye front had moved into the separating gel, voltage was increased to 150 – 200 V. Depending on the size of proteins, electrophoresis was performed for 45 to 80 min.

2.3.4.2 Semi-Dry Electrophoretic Transfer and Immunolabeling

For blotting the proteins from the gel onto a membrane we used a methanol activated polyvenylidenfluorid membrane (PVDF, Westran Clear Signal, Sigma), six sheets of Whatmann papers (Protran, Schleicher & Schuell, Dassel, Germany) and transfer buffer (1 x SDS Running buffer, 20% (v/v) methanol). The transfer was performed with a semi dry transfer unit at 2 mA/cm² and 12 V for 50 min. Subsequently, the PVDF membrane was blocked for 1 h in 5% fat free milk/PBS. Primary antibodies prepared in 5% fat free milk/PBS were usually applied overnight at 4°C. Afterwards the membrane was washed thrice in PBS-T (0.05% Tween-20 (v/v) in PBS). Secondary conjugated antibodies were incubated for 1-3 h at room temperature. After another 3 washing steps, the blots were developed using self-made Enhanced Chemiluminescence substrate (ECL): Solution A: 2.5 mM Luminol, 400 µM p-Coumaric acid, 0.1 M Tris-HCl pH 8.5. Solution B: 5.4 mM H_2O_2, 0.1 M Tris-HCl pH 8.5. Both solutions were mixed in equal parts.). The blots were incubated with ECL for 1-2 min, covered with Saran wrap and exposed to X-ray films (XBA, Fotochemische Werke Berlin) for 5 sec to 10 min. Finally the PVDF membranes were washed with PBS-T and sometimes stained with Ponceau S (Sigma-Aldrich) to confirm transfer of protein bands from SDS-PAGE on to the membrane.

Primary Antibodies (AB) used for Western Blotting Analysis

Primary AB	**Description**	**Source**	**Dilution**
anti-Mena 438, affinity purified, 2,16 mg/ml	rabbit, antibody against LERER repeat	Dr. P. Benz, University Würzburg	1:2000, **1:4000**
anti-EVL AB-109,	rabbit	Immunoglobe	1:1000, 1:200

anti-GAPDH, MAB 374, 1,0 mg/ml	mouse	Chemicon (Millipore), USA	1: 10000, **1:20000**
anti-GAPDH, 14C10	rabbit	Cell signaling	1:2000
anti-VASP M4, 19728	rabbit	Immunoglobe	**1:2000**, 1:500

Secondary AB used for Western Blotting Analysis in this Study

Secondary AB	Source	Dilution
goat-anti rabbit IgG + HRP	Dianova, Jackson ImmunoResearch, Hamburg, Germany	1:5000, 1:15000, **1:20000**
goat-anti mouse IgG	Dianova, Jackson ImmunoResearch, Hamburg, Germany	**1:10000**, 1:5000
anti-Mouse IgG + HRP	Mouse TrueBlot™ ULTRA, eBioscience, San Diego, USA	1:1000

2.4. Cell Culture - Transfection

In this study, cell culture was used to generate positive and negative controls for Western blot analysis. These controls ensured the specifity of the applied antibodies (anti-mena 438, anti-VASP19728, anti EVL AB-109).

Briefly, eukaryotic cultivated cells were transfected with plasmids. In case of negative controls, empty vectors were transfected, whereas in case of positive controls vectors with Mena-, VASP-, and EVL-specific cDNA sequences were transfected. 24 hours after transfection, cells were lysed and protein extracts were analysed by Western blotting.

The following table gives an overview on the plasmid-constructs, transfected cells and the protocols that were used.

Plasmid	Transfected cells	Protocol	Amounts
sport-6 (neg. control) Clone nr.: IRAVp968D066D (RZPD)	HEK cells (no detectable EVL-expression)	PolyFect (Quiagen)	8 µg DNA, 80 µl Polyfect
sport6- EVL			
pcDNA3 (neg. control)	MyEnd$^{-/-}$ cells (VASP-deficient Myocardial Endothelial cells; mouse)	Lipofectamine 2000 (Invitrogen)	24 µg DNA, 60 µl Lipofectamine
pcDNA+His_6-WT-VASP			
pCEP4 (neg. control)	CHO-S cells (no detectable Mena expression)	Lipofectamine 2000 (Invitrogen)	8 µg DNA, 20 µl Lipofectamine
pCEP4 -Mena			
pcDNA3 (neg. control)			
pcDNA3 - Mena			

2.4.1 Prearrangements for Transfection

Human embryonic kidney 293 cells (HEK-cells) were cultivated in Dulbecco´s modified Eagle´s medium (DMEM) containing 10% FCS. One day prior to transfection, HEK-cells were washed with EDTA, detached with trypsin-EDTA and resuspended in DMEM. Two 10 cm-wells (for sport6 and sport6-EVL transfection) with each 15 ml of cell-suspension were incubated at 37°C overnight, yielding in 80% confluent cells on the day of transfection.

VASP deficient Murine microvascular myocardial endothelial cells (MyEnd$^{-/-}$ cells) were cultivated on gelatinized tissue culture plates with DMEM. One day prior to transfection, one confluent 10 cm plate of MyEnd$^{-/-}$ was washed with

EDTA and cells were detached with trypsin-EDTA. After centrifugation (1000 rpm, 5 min), cells were resuspended in 30 ml DMEM and equal halves were plated onto new 10 cm plates. Cells were incubated overnight at 37°C to 90% confluence on the day of transfection. Chinese hamster ovary cells (CHO-S cells) (Gibco, Invitrogen) were cultivated in serum-free medium CHO-S-SFM II (#12052, Gibco, Invitrogen). One day prior to transfection, cells of one dense 10 cm plate of CHO-S cells were resuspended, spinned down and split onto four 6 cm plates.

2.4.2 Transfection

In this study, transfection of HEK-cells was performed similar as described in the PolyFect - "Protocol for Transient Transfection of 293 Cells" (PolyPect Transfection Reagent Handbook 09/2000, Quiagen, Hilden, Germany).

Briefly, for each reaction (sport6 and sport6-EVL transfection), 8 µg DNA were mixed with OptiMem-medium (OptiMem + GlutaMax, Cat.No. 51985, Gibco, Invitrogen) resulting in a 300 µl solution. 80 µl of PolyFect Transfection Reagent were added to the DNA solution and mixed by pipetting up and down. Incubation at room temperature was performed for 10 min to allow complex formation. Meanwhile, the medium of the prepared 10 cm HEK-cell plates was aspirated. 7 ml of fresh high glucose 4.5 g/l DMEM medium with serum were pipetted on each plate and 1 ml of this medium was also added to each DNA-PolyFect solution and mixed. The DNA solution was then dispersed on the plates (resulting in 8 ml of medium per plate). Incubation was performed overnight at 37°C.

Transfection of MyEnd$^{-/-}$ and CHO-S cells was performed as detailed in the Lipofectamine 2000 – protocol (Lipofectamine 2000, Cat.No.11668-019, Invitrogen).

Briefly, 24 µg of pcDNA and pcDNA-VASP were used for MyEnd$^{-/-}$ transfection, using 10 cm - wells. DNA was diluted in 1.5 ml of OptiMem-medium, and 60 µl Lipofectamine 2000 for each reaction were mixed with 1.44 ml OptiMem-medium and incubated for 5 min at room temperature. Subsequently, the diluted DNA and diluted Lipofectamine were combined, mixed and incubated for 20 min

(to form complexes). Meanwhile, differing from the protocol, medium of the prepared 10 cm – plates was changed. On each plate 15 ml of high glucose 4.5 g/l DMEM medium were added. 3 ml of DNA-LF2000-complexes were added to each well, mixed gently and then incubated overnight at 37°C.

For transfecting the plasmids pCEP4, pCEP4-Mena, pcDNA, pcDNA-Mena into CHO-S cells the Lipofectamine protocol was used. Differing from the above mentioned, for each reaction a 6 cm – well, 8 µg of DNA, 20 µl LF2000 and the adopted amounts of OptiMem medium were used. Complexes were dispersed on the wells without changing medium of the day before.

2.4.3 Harvesting Transfected Cells

When harvesting, HEK cells had to be handled with extreme care. Apart from this, HEK and MyEnd cells were harvested likewise. Medium was drained carefully, cell-plates were washed with 10 ml prewarmed PBS each and 2 ml of 2% SDS/PBS were poured onto each plate. With a cell scrape the viscous solution was harvested and then transferred into a 15 ml Falcon tube.

Transfected CHO-S cells were harvested differently. The cell suspension was transferred into a 15 ml Falcon tube, remaining cells on the plates were harvested with 1 ml PBS and then added into the tube. The Falcon tube was then filled up with PBS to a final volume of 15 ml. After centrifugation at 1000 rpm for 4 min, the supernatant was aspirated and the cell pellet was resuspended with 1 ml PBS and 1 ml 2% SDS/PBS. All lysates were stored at -20°C.

3. Results

3.1 Characterisation of the Mena Ko Mouse

3.1.1 Generation of Mena Deficient Mice

At the beginning of my studies, Mena$^{-/-}$ mice had already been generated. However, the principle process for generating our Mena$^{-/-}$ mice is described here. For the generation of Mena deficient mice, the RRG138 embryonic stem cell clone (Baygenomics, San Francisco, USA) was used. In this RRG138 ES clone the gene-trap vector pGT0Lxf is inserted between exon 2 and exon 3 of the Mena gene which is located on chromosome 1, resulting in a targeted mutation (Fig. 3-1).

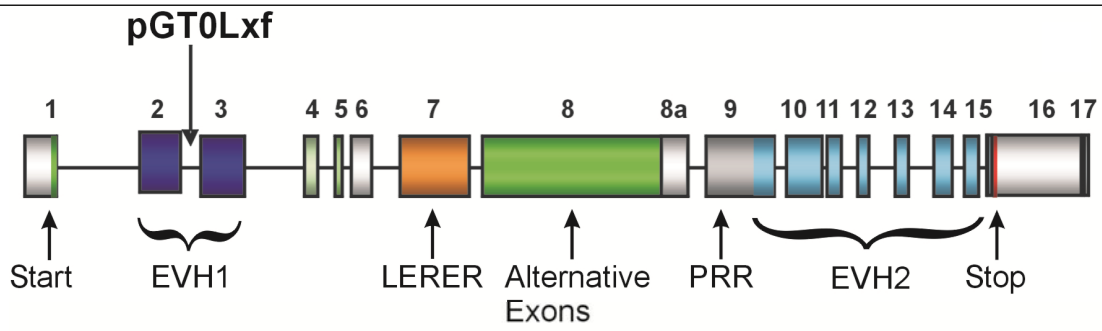

Fig 3-1. Insertion of Gene-Trap Vector pGT0Lxf.
In the RRG138 ES clone the gene-trap vector pGT0Lxf inserts between exon 2 and 3 of the Mena gene, which is located on chromosome 1. The gene contains 16 exons and has a total genomic size of 114214 bp. Start- and stop-codons are localised in exons 1 and 15, respectively. The EVH1 domain, comprising exons 2 and 3, is disrupted by the vector insertion. The EVH2 domain comprises exons 9 to 15. The LERER-repeat is localised in exon 7, the proline-rich region (PRR) in exon 9. Exons 4, 5 and 8 are alternative exons. The fusion transcript consists of exons 1 and 2 and the gene-trap construct.

The RRG138 ES-cells of a brown mouse (129ola, genotype: A/A; M/m) were injected into a blastocyste stage embryo of a black female (C57/BL6; genotype: a/a;M/M) (A = brown fur; a = black fur; M = Mena gene; m = mutated Mena gene). Accordingly, an embryo developed in a surrogate mother's uterus. The newborn mouse with brown-black brindled fur showed a chimeric phenotype as a result of carrying cells of two different mouse strains (Fig. 3-2).

The mature chimera (genotype: a/a;M/M plus A/A;M/m) was crossbred with a C57/BL6 mouse. This led to offsprings with following genotypes: a/a;M/M,

A/a;M/m, A/a;M/M. Crossbreeding two of the ones with genotype A/a;M/m, resulted, apart from others, in Mena deficient mice (genotype: m/m) with brown fur, showing a normal phenotype (Fig. 3-2).

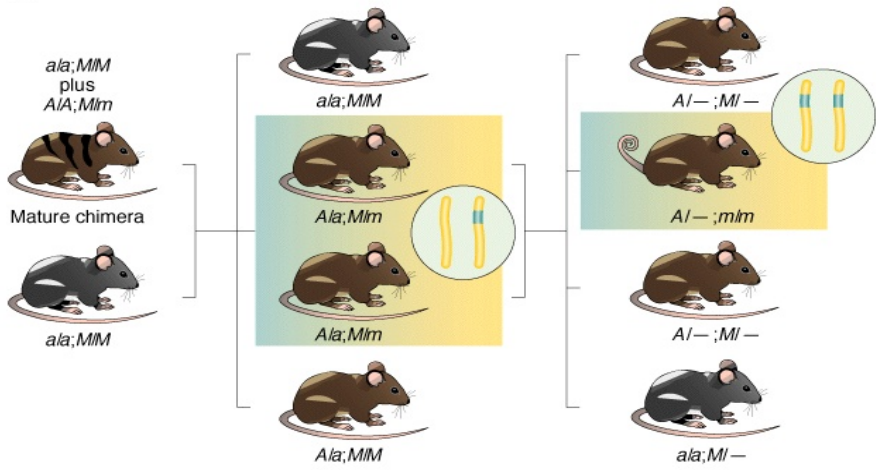

Fig. 3-2. Crossbreeding Mice.
The mature chimera (genotype: a/a;M/M plus A/A;M/m) was crossbred with a C57/BL6 mouse (genotype: a/a;M/M). Crossbreeding two mature Mena-heterozygous mice led, amongst others, to Mena deficient mice (m/m). A=brown fur; a=black fur; M=Mena gene; m=mutated Mena gene.
Figure taken from http://fig.cox.miami.edu/faculty/dana/knockout.html

3.1.2 Insertion of the Gene Trap Construct with its Consequences for the Mena Gene

In the RRG138 ES clone, the pGT0Lxf gene trap vector is inserted in intron 2 of the Mena gene. Thereby the construct is brought under control of the endogenous Mena promoter. The gene trap construct contained a *β-geo* gene (encodes β-galactosidase and neomycin resistance) flanked by a splice acceptor (*SA*) sequence and a polyadenyline termination sequence (*polyA*). The gene trap insertion led to a fusion transcript that connected exons 1 and 2 to the *β-geo* cassette, encoding for β-galactosidase. Thus, the gene trapping resulted in the disruption of the Mena gene but also provided the gene trap sequence tag, β-galactosidase (Fig. 3-3). In this study, the promoter activity of Mena was analysed by detecting β-galactosidase expression with X-gal staining.

Exons 2 and 3 both encode for the EVH1 domain of the Mena gene. The disruption in between them made this domain non-functional and led to the inactivation of the Mena gene. The exact insertion site of the gene trap was determined by genomic PCR and sequencing showing the intronic part of the trap vector starts 682 bp downstream of Mena exon 2. To confirm that the RRG138 cell line contains the splice product of Mena exon 2 splice donor and splice acceptor (SA in Fig. 3-3) of the gene trap vector, a reverse transcriptase PCR (RT-PCR) was performed and the PCR product was confirmed by sequencing. Southern blot analysis, using BgIII as restriction enzyme, verified the singular insertion the of gene trap.

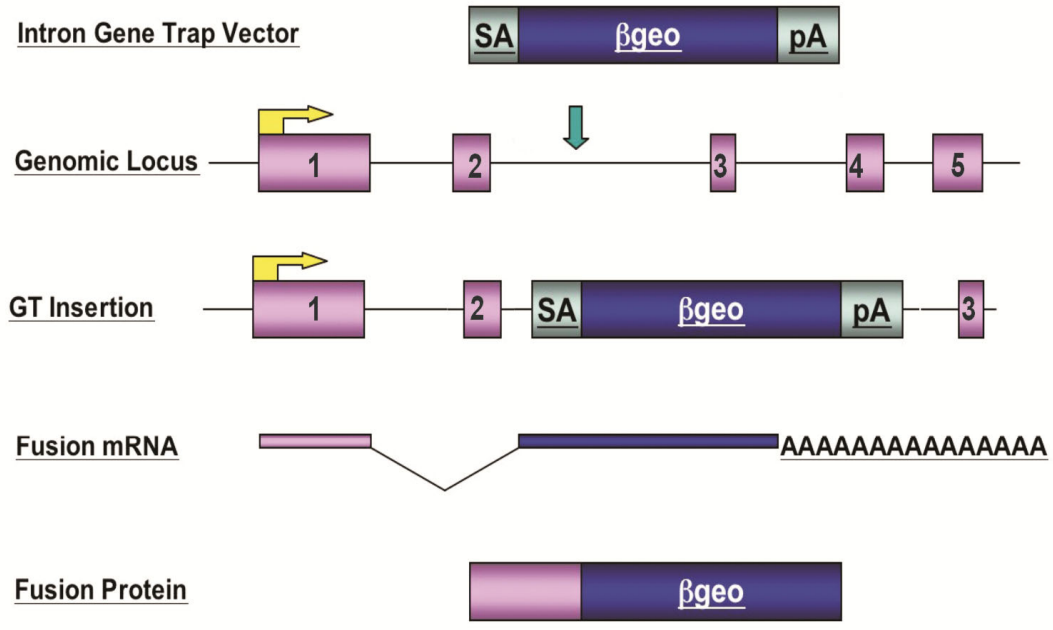

Fig. 3-3. Generating Mena$^{-/-}$ Mice Using the Method of Gene-Trapping.
The gene-trap construct containing a *β-geo* gene (encodes β-galactosidase and neomycin resistance) flanked by an *SA*- and a *polyA*-sequence, inserts between exons 2 and 3. The construct is thereby brought under control of the endogenous Mena promoter. This leads to a fusion transcript connecting exons 1 and 2 to the *β-geo* cassette, encoding for β-galactosidase. X-gal staining detects β-galactosidase, thereby showing Mena promoter activity.

3.2 Characterisation of the VASP Ko Mouse

For this work, VASP-deficient mice were generated by homologous recombination as described by *Hauser et al. 1999.* For further details, see 1.6.1.

3.3 Genotyping Mice Using PCR

12 mice with targeted mutations in the Mena and/or VASP gene were genotyped by PCR.

For detecting the Mena wild-type (wt) gene, the Mena forward primer me_F3 (Mena exon 2) and the Mena reverse primer me_in2_R2 (Mena intron 2) were used. Performing the PCR with these primers led to the amplification of the "Mena wt"-DNA product of 1123 bp (Fig. 3-4). For the PCR-amplification of the mutated Mena gene, the same forward primer me_F3 and the reverse primer pGT0Lxf_R2 were used. This reverse primer hybridizes to the gene trap insertion vector (pGT0Lxf). Using this primer allowed to distinguish wt from ko mice and also confirmed the successful insertion of the gene trap construct. Using me_F3 and pGT0Lxf_R2 resulted in the Mena ko PCR product of 824 bp (Fig. 3-4). This difference in product size was used to determine the genotype by analysing the bands on the agarose gel.

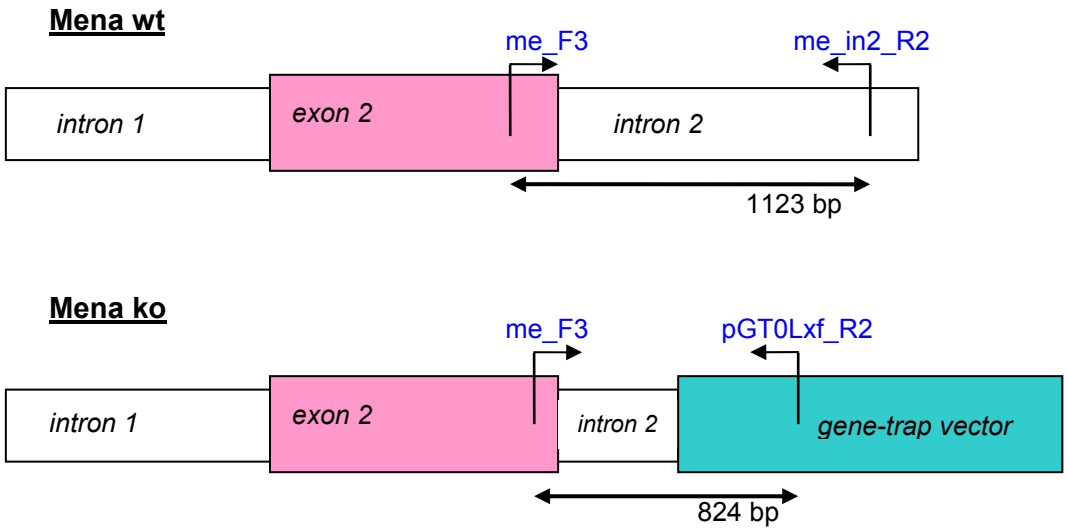

Fig. 3-4. Schematic Illustration of Primer Localisation Used for Mena PCR Genotyping.
Section of Mena wt allele: forward primer me_F3 and reverse primer me_in2_R2 hybridize to exon 2 and intron 2, respectively; PCR product size 1123 bp.
Section of Mena ko allele: forward primer me_F3; reverse primer pGT0Lxf_R2 hybridizes to the inserted gene trap construct; PCR product size 824 bp.

Quite similar to this, VASP PCR was performed. For amplifying a specific wt gene sequence, the primers GIK269 (forward) and GIK270 (reverse) were used. These primers locate to the intron 4 and to exon 6, yielding in a PCR product of approximately 450 bp (Fig. 3-5). In the VASP ko allele, a large gene sequence between exon 3 and exon 12 had been replaced by the *neo*-cassette, thus using primers hybridizing in intron 4 and and exon 6 was specific for detecting the VASP wt gene. To obtain a VASP ko PCR product, the forward primer GIK273 and the reverse primer GIK274 were used, resulting in a PCR product size of approximately 700 bp (Fig. 3-5). GIK273 hybridizes in the *neo*-cassette, whereas GIK274 hybridizes in the intron between this cassette and exon 12.

The PCR products were loaded on agarose gels, followed by electrophoresis for separating DNA products according to their size (see 2.1). With the knowledge of the PCR product sizes, the genotypes could easily be determined (Fig. 3-6).

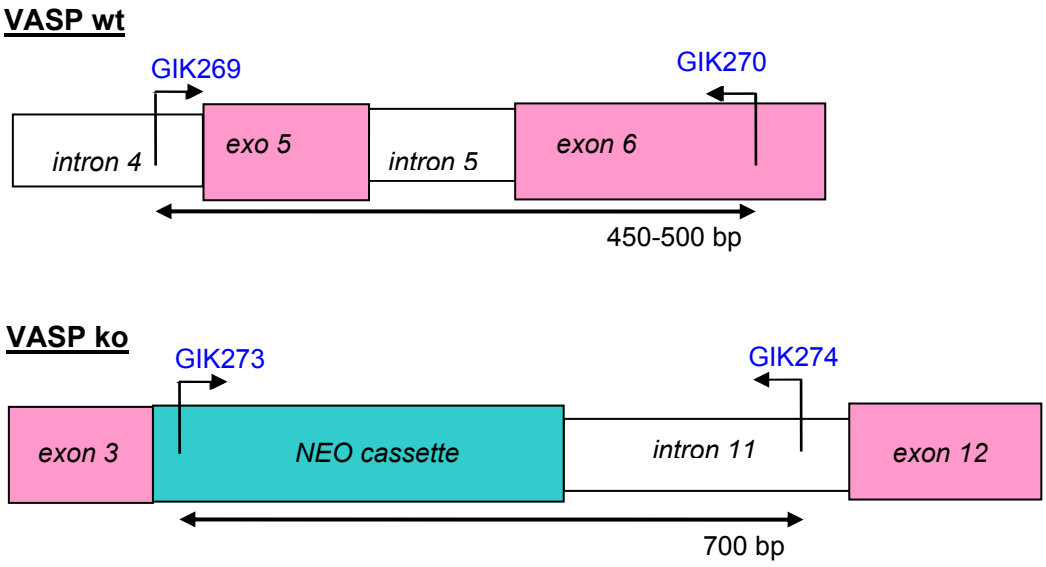

Fig. 3-5. Schematic Illustration of Primer Localisation Used for VASP PCR Genotyping.
Section of VASP wt allele: forward primer GIK269 and reverse primer GIK270 hybridize to intron 4 and exon 6, respectively; PCR product size ~400-500 bp.
Section of VASP ko allele: forward primer GIK273 hybridizes in the *neo*-cassette; reverse primer GIK274 hybridizes to intron 11, respectively. PCR product size ~700 bp.

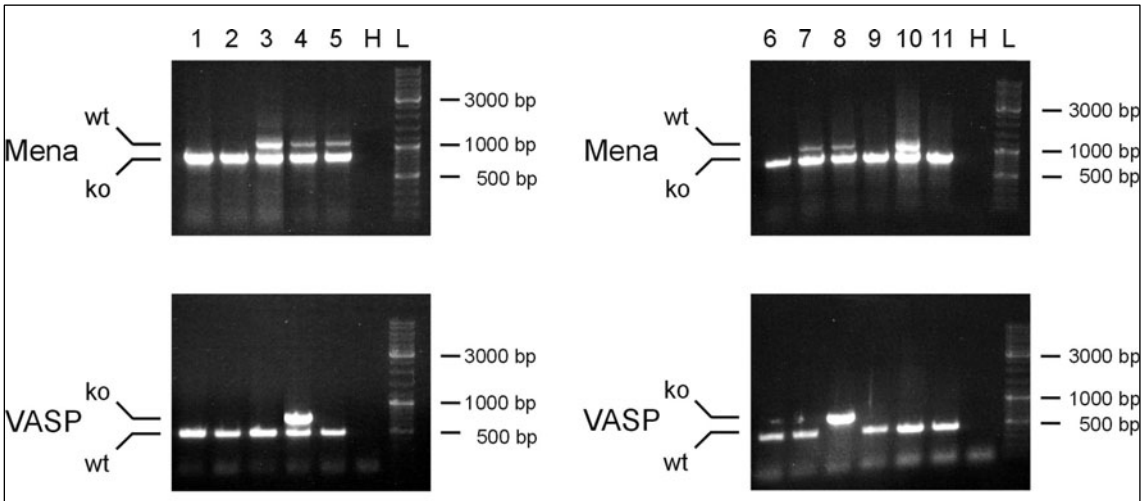

Fig. 3-6. Mena/VASP PCR Results.
PCR samples of different mice (1-11), water probes (H) and DNA ladders (L) were loaded on 1% agarose gels. DNA was isolated from mouse tails. Electrophoresis separated the DNA products according to their size. The resulting DNA bands were visualized under ultraviolet light and photographed. The DNA ladder mix allowed estimating the size of the bands. With the knowledge of the PCR product sizes, the genotypes could be determined.
1: $m^{-/-}$ $v^{+/+}$, 2: $m^{-/-}$ $v^{+/+}$, 3: $m^{+/-}$ $v^{+/+}$, 4: $m^{+/-}$ $v^{+/-}$, 5: $m^{+/-}$ $v^{+/+}$, 6: $m^{-/-}$ $v^{+/+}$,
7: $m^{+/-}$ $v^{+/+}$, 8: $m^{+/-}$ $v^{-/-}$, 9: $m^{-/-}$ $v^{+/+}$, 10: $m^{+/-}$ $v^{+/+}$, 11: $m^{-/-}$ $v^{+/+}$. m = Mena, v = VASP

3.4 X-Gal Staining

To analyse the Mena gene promoter activity, X-gal staining of several cryosections was performed. Diverse organs of $Mena^{-/-}$ mice, which contained the gene-trap vector, but also of wt mice as negative controls were investigated. X-gal is a substrate analogue, which is cleaved by β-galactosidase, an enzyme, which is encoded by the *β-geo* cassette, the main part of the insertion vector. It is known that this enzymatic reaction yields in two products, namely galactose and 5-bromo-4-chloro-3-hydroxyindole, which is then oxidized into insoluble indigo (Huang et al., 2009; Simmer et al., 2009). Subsequently, β-galactosidase activity leaves a blue stain that localises in the cytoplasm of the cell. Accordingly, by using this method, it is not possible to determine the exact localisation of the β-galactosidase fusion protein within the cell. The staining of cryosections demonstrated Mena promoter activity in diverse tissues.

3.4.1 X-Gal Staining of the Brain

For the analysis of the brain, frontal and sagittal sections were made. Incubation of the sections in X-gal staining solution was performed for approximately 15 hours. In contrast to the wt preparations, the ko cryosections indicated β-galactosidase expression (Fig. 3-7). Slightly blue staining could be seen in isolated cells of the cortex. But the density of stained cells differed; in some cell layers the density was much higher than in others. Compared to this, staining of brain vessels, for example of arteries in the subarachnoid space (Fig. 3-7; E, F) or of the capillaries in the plexus choroideus of the lateral ventricle (Fig. 3-7; B) was strong positive. By closer inspection of the vessels, a predominant staining of the media layer was observed. But with this staining method, it was impossible to discriminate between Mena promoter activity in the intima or the adventitia because the layers could not be distinguished clearly. To differentiate between Mena expression in these two vessel layers, immunofluorescent staining was performed later on (Fig. 3-17, Fig. 3-21). Striking about the X-gal stained brain sections was the strong positive signal in certain cell layers of the hippocampus. Thus, structures like the pyramidal cell layer, the cornu ammonis (ca) and the dentate gyrus (*gyrus dentatus* = gd) could be distinguished (Fig. 3-7; A-C).

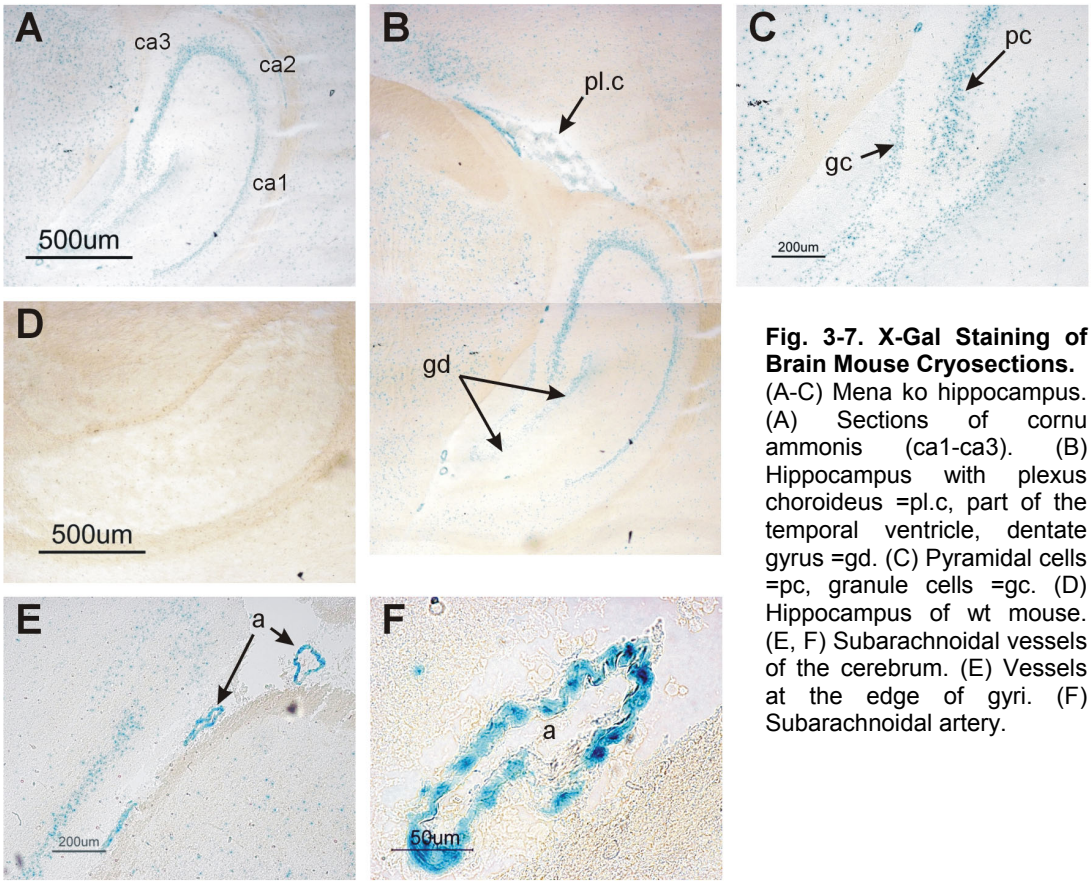

Fig. 3-7. X-Gal Staining of Brain Mouse Cryosections. (A-C) Mena ko hippocampus. (A) Sections of cornu ammonis (ca1-ca3). (B) Hippocampus with plexus choroideus =pl.c, part of the temporal ventricle, dentate gyrus =gd. (C) Pyramidal cells =pc, granule cells =gc. (D) Hippocampus of wt mouse. (E, F) Subarachnoidal vessels of the cerebrum. (E) Vessels at the edge of gyri. (F) Subarachnoidal artery.

3.4.2 X-Gal Staining of the Heart

X-gal staining of heart cryosections was performed with Mena$^{-/-}$, Mena$^{-/+}$ and wt mice. Strong blue staining was seen in the walls of big vessels, e.g. the aorta or the coronary arteries (Fig. 3-8; A-E). Again, thorough analysis suggested a stronger Mena promoter activity in the media compared to the flanking layers, intima or adventitia (Fig. 3-8; C). Due to the intense blue staining, also smaller branches of the coronary arteries toward the apex of the heart could clearly be distinguished from the surrounding heart tissue (Fig 3-8; H, I). The cardiomyocytes were stained too, but less than the vessels. Interestingly, the intensity of staining differed in different parts of the ventricle walls (Fig. 3-8, D). On closer inspection of the cardiomyocytes, punctual indigo stain within each -cell could be seen (Fig. 3-8, F). The atrioventricular valves were not stained blue (Fig. 3-8, D). X-gal stained sections of Mena$^{-/+}$ hearts showed the expected diminished colour intensity (Fig. 3-8, L). Cardiomyocytes and heart

vessels of the wt mice heart sections remained completely unstained after the incubation in X-gal solution (Fig. 3-8, M-O). This confirmed the specific indigo staining as a result of β-galactosidase activity in mice containing the gene-trap construct.

Fig. 3-8. X-Gal Staining of Mouse Heart Cryosections (following page)**.**
(A) Mena$^{-/-}$ mouse; transversal section of the aorta, at the level of the heart base. (B) Enlargement of the indicated area in A; blue stained vessel wall. (C) Enlargement of the indicated area in B; slightly distinguishable vessel wall layers: intima, media, adventitia; blue staining predominant in the media. (D) Mena$^{-/-}$ mouse; transversal section of the left ventricle; Vessels and heart muscle tissue are stained blue, valves remain unstained. (E) Enlargement of the indicated area in D; Walls of coronary arteries and cardiomyocytes are stained clearly. (F) Enlargement of E; Punctual accumulations of β-galactosidase, indicated by indigo stain, in heart muscle cells. (G-I) Mena$^{-/-}$ mouse; Heart muscle tissue and coronary vessels show blue staining. (J, K) Enlargements of the indicated areas in H and I; walls of small coronary arteries are stained. (L) Mena$^{+/-}$ mouse; staining intensity of heart tissue is reduced as compared to Mena$^{-/-}$ preparations. (M) wt mouse; wall of left ventricle. (N) Enlargement showing branches of coronary arteries, completely unstained. (O) Enlargement of the indicated area in N, showing also erythrocytes.
a=arteries, ad=adventitia, ao=aorta, ca=coronary arteries, cm=cardiomyocytes, e=erythrocytes, i=intima, lu=lumen, m=media, va=valve.

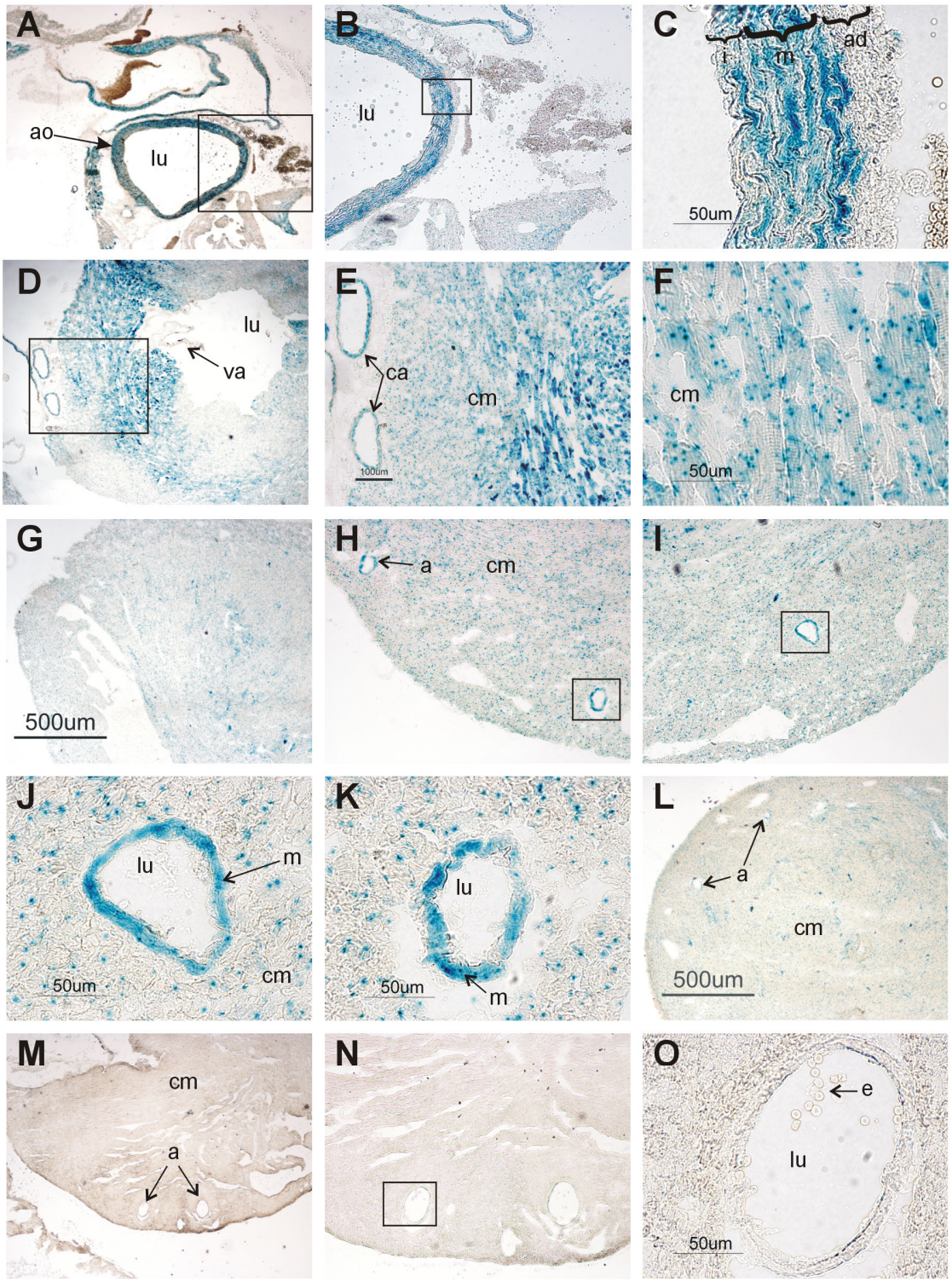
A
ao
lu
B
lu
C
ad
m
50um
D
lu
va
E
ca
cm
100um
F
cm
50um
G
500um
H
a
cm
I
J
lu
m
cm
50um
K
lu
50um
m
L
a
cm
500um
M
cm
a
N
O
e
lu
50um

Fig. 3-8

3.4.3 X-Gal Staining of the Lung

Also X-gal staining of pulmonary tissue of Mena$^{-/-}$ mice showed striking Mena promoter activity in the vessel walls (Fig. 3-9; A, B). In the bronchioles, primarily the respiratory epithelium was stained blue (Fig. 3-9; D). In contrast, the alveolar tissue, mainly consisting of pneumocytes and the endothelium of capillaries, remained largely unstained. Again, X-gal incubation of wt lung sections was performed as negative control (Fig. 3-9; E, F). As expected, this did not result in any blue staining, confirming the specifity of this method.

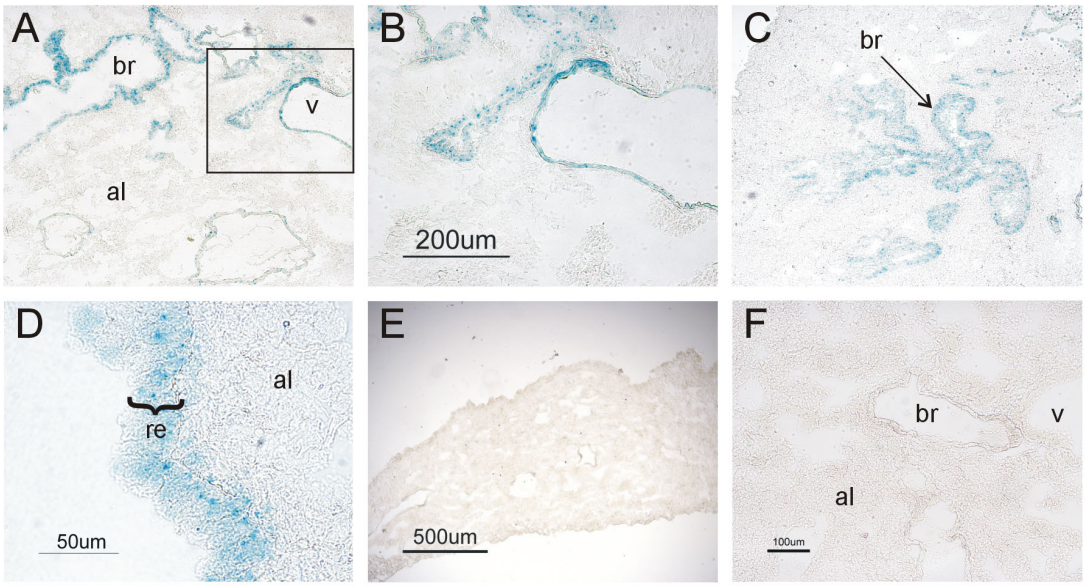

Fig. 3-9. X-Gal Staining of Cryosections of the Lung.
(A) Mena$^{-/-}$ mouse; walls of bronchioles and vessels show Mena promoter activity, alveolar tissue is not stained. (B) Enlargement of the indicated area in A. (C) Mena$^{-/-}$; blue stained bronchioles. (D) Enlargement of a bronchiole wall; demonstrating Mena promoter activity in the respiratory epithelium. (E) wt mouse, cryosection of pulmonal tissue. (F) Bronchioles, vessels and alveolar tissue are shown. However, it is hard to distinguish between these structures because none of them got stained (negative control). al=alveolar tissue, br=bronchiole, re= respiratory epithelium, v=vessel.

3.4.4 X-Gal Staining of the Gastrointestinal Tract

For X-gal staining of stomach and large intestine (colon), transversal sections of these organs of Mena$^{-/-}$ and of wt mice were made. The results showed clearly that the muscularis, circular and longitudinal muscle layer, but also the lamina muscularis mucosae were stained blue after incubation (Fig. 3-10; A, B, D, E).

This became even more apparent by looking at the pylorus (Fig. 3-10; E). Vessels going through the submucosa and adventitia showed β-galactosidase expression as well. The mucosa of the stomach consisting of the surface epithelium and the gastric glands (foveolae), and the submucosa showed no detectable Mena promoter activity. Equally, the colon epithelium with its characteristic intestinal crypts remained unstained. For comparison, the X-gal experiments with stomach and colon sections were also performed with wt mice cryosections (Fig. 3-10; C, F).

3.4.5 X-Gal Staining of Liver, Spleen, Kidney and Thymus

First, by macroscopic analysis of the X-gal treated Mena$^{-/-}$ cryosections of kidneys, liver and spleen, we observed no difference compared to the wt controls. Under the microscope, however, isolated blue stained spots on the Mena$^{-/-}$ sections could be detected. Punctual staining appeared in some kidney tubules (Fig. 3-10; H), but it could not be distinguished between proximal and distal tubules. More evident was the Mena promoter activity in the renal arteries (Fig. 3-10; H). In spleen, liver and thymus, β-galactosidase expression was exclusively detected in the vessel walls (Fig. 3-10; I, J and O, respectively). The wt cryosections remained unstained after incubation (data not shown).

Fig. 3-10. X-Gal Staining of Cryosections of Abdominal Organs, Skeletal Muscle and Thymus (following page).
(A) Mena$^{-/-}$, transversal section of the colon; intense blue colour indicates Mena promoter activity in the muscle layer. (B) Enlargement of the indicated area in A; showing blue stained vessels, lamina muscularis mucosae, circular and longitudinal muscle layer. (C) wt colon section; negative control. (D) Mena$^{-/-}$; Section of stomach wall (fundus/corpus area) showing Mena promoter activity in the muscle layer. (E) Mena$^{-/-}$; stomach wall (pylorus area). (F) Wt stomach section, negative control. (G) Mena$^{-/-}$; section of the kidney (renal cortex). (H) Enlargement of the indicated area in G; β-galactosidase expression is found in renal vessels and in some tubules. (I) Mena$^{-/-}$; cryosection of the spleen; Mena promoter activity only detected in vessels. (J) Mena$^{-/-}$; liver-cryosection; Mena-promoter activity only detected in vessels. (K) Mena$^{-/-}$; femoral skeletal muscle. (L, M) Enlargements of the indicated area in K; β-galactosidase expression appears only in vessels not in the muscle tissue. (N) wt skeletal muscle. (O) Mena$^{-/-}$; section of thymus gland; Mena promoter activity only detected in vessels.
cm=circular muscle layer, e=epithelium, lm=longitudinal muscle layer, lmm=lamina muscularis mucosae, lu=lumen, t=renal tubule, v=vessel.

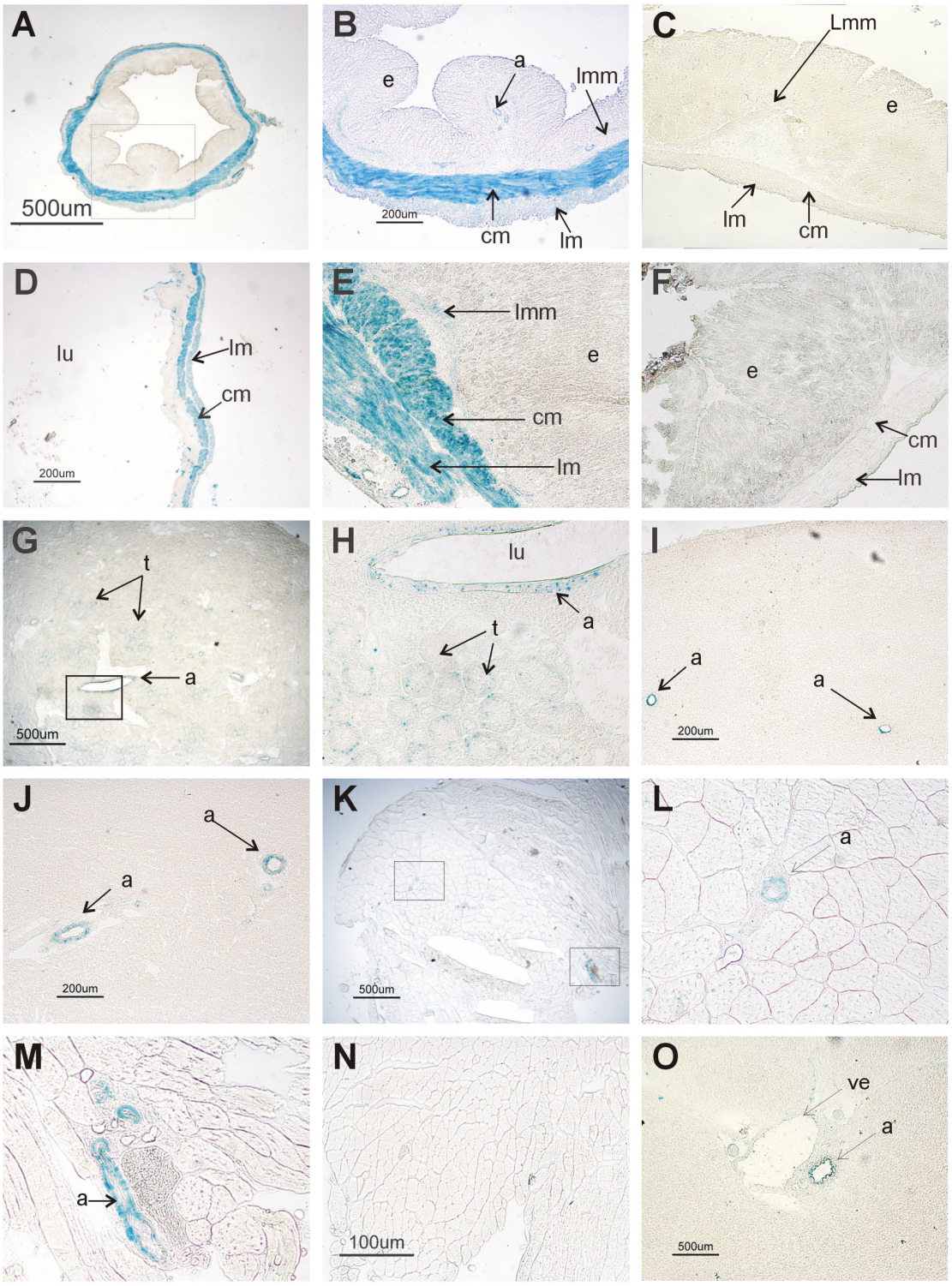
A
500um
B
e
a
lmm
200um
cm
lm
C
Lmm
e
lm
cm
D
lu
lm
cm
200um
E
lmm
e
cm
lm
F
e
cm
lm
G
t
a
500um
H
lu
a
t
I
a
a
200um
J
a
a
200um
K
500um
L
a
M
a
N
100um
O
ve
a
500um

Fig. 3-10

3.4.6 X-Gal Staining of Skeletal Muscle

For these X-gal experiments, cryosections of femoral skeletal muscle tissue of Mena$^{-/-}$ and wt mice were used. The striated muscle tissue itself of Mena$^{-/-}$ mice exhibited no blue staining. Only the walls of vessels supplying the muscle cells, showed Mena promoter activity (Fig. 3-10; K, L, M). The wt sections showed the expected negative results (Fig. 3-10; N).

3.4.7 X-Gal Staining of Neonatal Mice

Previous studies have already shown that Mena protein expression is increased during embryonic development and during the neonatal period in comparison to adult mice (Gambaryan et al., 2001; Lanier et al., 1999). To study differences in Mena expression of adult and neonatal tissue, we analysed the Mena promoter activity of neonatal mice using the X-gal staining method. Strong β–galactosidase expression was already observed by macroscopic analysis of the cryosections. Striking blue staining appeared in the intestinal tract (Fig. 3-11; A, B, E, F, G). In contrast to adult Mena$^{-/-}$ mice, not only the muscle layer but also the mucosa of the neonatal intestinal tract showed Mena promoter activity. Also the wall of the so called milk stomach exhibited blue colour. A bit less blue staining was observed in heart, lung and kidney. Liver and spleen remained unstained. In the head, multiple structures displayed β-galactosidase expression. Most notably blue stained were the muscular tongue, the brain, the photoreceptors and the ganglion cell layer in the eye (Fig. 3-11; H, I). Striking positive were also parts of the hair follicles, especially in the region of the head.

Fig. 3-11. X-Gal Staining of Cryosections of Neonatal Mena$^{-/-}$ Mice (following page).
(A-D) Diverse neonatal Mena$^{-/-}$ mice; images showing whole bodies; Intestinal tract, heart, lung, kidneys, stomach wall, tongue and brain show Mena promoter activity. (E) Blue stained diaphragm and intestinal tract. (F, G) Enlargements of the indicated area in E; Not only the intestinal muscle layer, but also the mucosa express β-galactosidase protein. (H, I) Eye-sections of a Mena$^{-/-}$ mouse; By closer looking, parts of the retina (photoreceptors and ganglion cell layer) and a layer surrounding the whole eye show blue staining. In addition, parts of hair follicles were stained blue.
ce=cerebrum (brain), ch=choroidea, di=diaphragm, e=eye, gc=ganglion cell layer, he=heart, hf= hair follicle, int=intestinal tract, ir=iris, ki=kidney, le=lens, li=liver, lu=lumen, lun=lung, m=muscularis, mu=mucosa, pr=photoreceptors, re=retina, ri=rips, rpe=retinal pigment epithelium, sp=spleen, st=stomach, t=tongue.

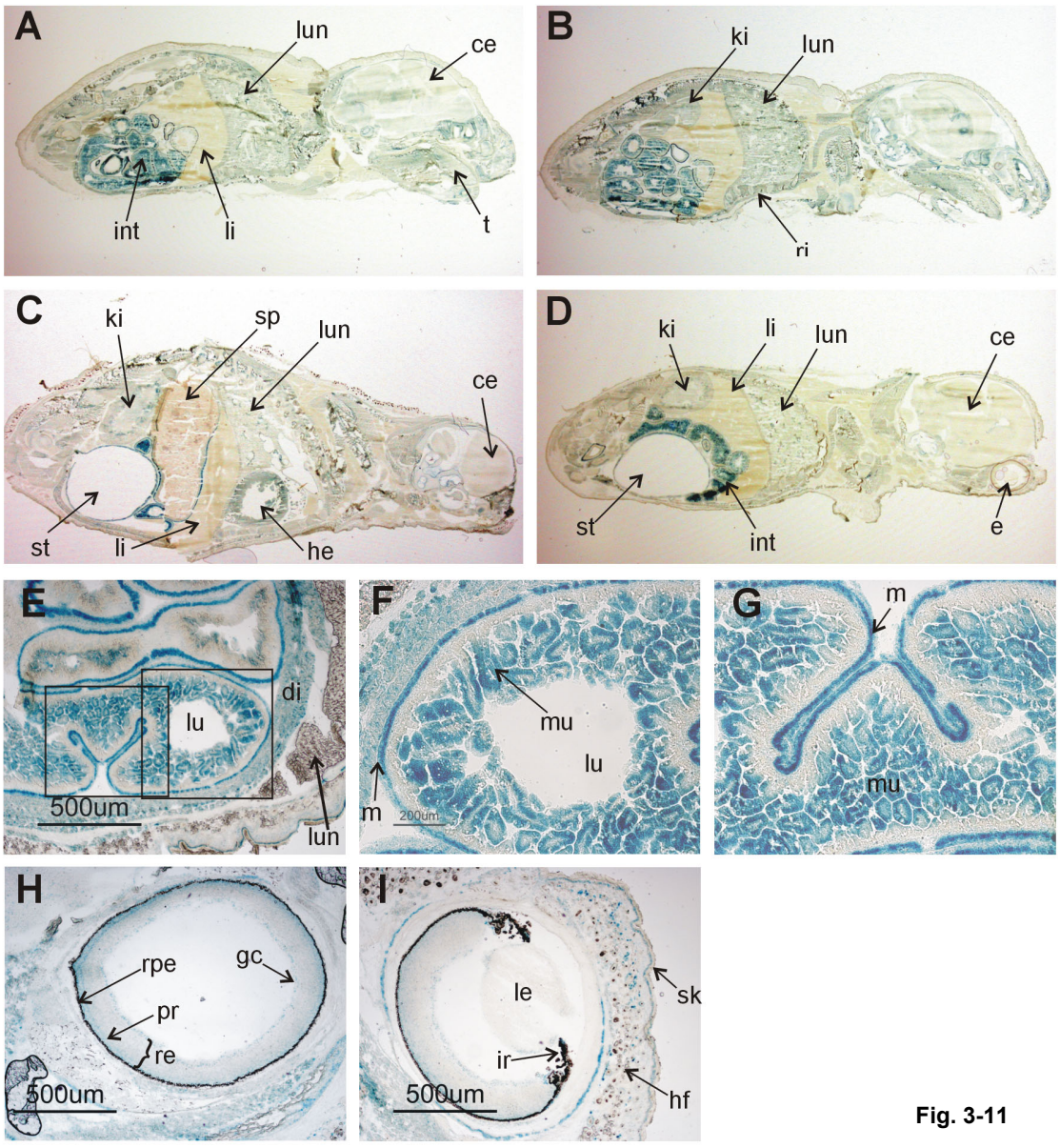

Fig. 3-11

3.5 Western Blot Analysis

Protein expression of Ena/VASP family members was investigated by Western blot analysis. Protein lysates of diverse organs of wt, Mena ko and Mena-VASP-double-deficient (dko) mice were prepared and proteins were separated by SDS-gel electrophoresis. After transferring the protein bands onto PVDF-membranes, Mena, VASP and EVL were identified by incubating the membranes with protein specific primary antibodies. Binding of horseradish

peroxidase-(HRP-) conjugated secondary antibodies was detected by using ECL solution containing luminol. The results were made visible on x-ray films.

3.5.1 Mena Protein Expression in Wild-type and Mena Deficient Mice

To analyse the levels of Mena protein expression in organs of wt and Mena mutated mice, protein lysates of the following adult tissues were prepared: heart, lung, liver, spleen, kidney, brain, eyes, stomach, femoral skeletal muscle, large intestine, testis, lymph nodes, salivary gland and thrombocytes. For the results shown in Fig. 3-12 and Fig. 3-13, gels were prepared with different amounts of acrylamide (Fig. 3-12: continuous 10%, Fig. 3-13: discontinuous step gradient 5.5 ml 7% upper part, 2.5 ml 12% lower part). Per lane, 30 µg of total protein lysate were loaded onto the gels and anti-GAPDH antibody MAB 374 (GAPDH = glyceraldehyde 3-phosphate dehydrogenase) was used as loading control.

Mena protein bands were expected at 80 kDa and 88 kDa and the neuronal Mena variant at 140 kDa (Fig. 3-12, 3-13). An additional band at approximately 120 kDa which was observed in these results, is unspecific and does not label the Mena protein. However, since the intensity of this band is independent of the Mena genotype, it most likely represents an unspecific binding to a different protein. All accomplished Western blots showed that the Mena mutated mice had not been knocked out completely by the gene trap because the protein signal of the $Mena^{-/-}$ probes was indeed generally diminished but did not lack completely.

Our Western blot analyses demonstrated that in wt heart all three Mena isoforms were expressed (Fig. 3-12, 3-13). The signal of the 80 kDa band was strongest, being at least twice as strong as the 88 kDa and the 140 kDa isoform, respectively. Comparing wt and $Mena^{-/-}$ heart, the 140 kDa and 80 kDa forms were almost erased in the $Mena^{-/-}$ heart probe, whereas the signal of the 88 kDa isoform was only slightly decreased. In wt lung probes, the 80 kDa signal was observed. It was at least twice as high as the 80 kDa signal of wt heart (although the GAPDH signal of the lung tissue extracts was even lower).

The Mena$^{-/-}$ signal of the lung probe was reduced to one third, approximately. In wt liver probes, only a very slight signal of the 80 kDa splice variant could be detected (Fig. 3-12). In wt spleen probes, the 80 kDa signal was rather strong, and almost vanished in the ko control (Fig. 3-12, 3-13). No Mena isoform could be detected in kidney tissue extracts (Fig. 3-12). Wt stomach probes showed very strong 80 kDa Mena expression (Fig. 3-12, 3-13). This signal was reduced to approximately one half in the ko control. Rather slight protein bands could also be observed at 88 kDa and 140 kDa of the wt probe (Fig. 3-13). These bands did not appear in the Mena$^{-/-}$ control. The signal intensity of the 80 kDa isoform of wt large intestine probes was similar to the intensity of stomach probes. However, the 88 kDa and 140 kDa splice variants were not expressed clearly in large intestine (Fig. 3-12, 3-13). Skeletal muscle tissue extracts implicated expression of the 80 kDa and the 88 kDa Mena isoforms, with a stronger signal intensity of the 80 kDa isoform. In the ko control, hardly any Mena signal could be observed (Fig. 3-12, 3-13). Strongest Mena bands of all analysed tissues were perceived in testis. All three isoforms were detected in the wt probes. In the Mena$^{-/-}$ controls, Mena signals were still of very high intensity (Fig. 3-12). In tissue extracts of wt lymph nodes, expression of 80 kDa Mena was high; it was diminished to approximately one fifth in the ko control (Fig. 3-12, 3-13). Expression of 80 kDa Mena was also observed in wt salivary gland. The signal was almost erased in the ko control (Fig. 3-12). Rather low expression of 80 kDa Mena was perceived in wt thrombocyte extracts. Whereas the 88 kDa and 140 kDa isoforms were not detectable in this tissue, there appeared a new band at approximately 75 kDa. Both protein bands, the 75 kDa and the 80 kDa band were erased in the Mena$^{-/-}$ thrombocyte extracts (Fig. 3-13). Very high expression of 80 kDa and even higher of 140 kDa Mena was observed in wt brain. These signal intensities were only slightly reduced in the ko controls. In tissue extracts of wt eyes, 80 kDa Mena expression was also relatively high. Signal intensity of neuronal Mena was comparable to the one of wt heart probes (Fig. 3-12, 3-13).

An unknown protein band at 70 kDa was observed in tissue extracts of wt lung, spleen, stomach, large intestine, lymph nodes, brain, eye, testis and salivary

gland. The signal intensity was remarkably high in probes of salivary gland and lung. Expression of this isoform was lower (salivary gland) and even completely erased in the corresponding Mena$^{-/-}$ probes, respectively (Fig. 3-12, 3-13).

Fig. 3-12. Western Blot Analysis to Investigate Mena Protein Expression (following page).
Wt (+/+) mice were compared to Mena mutated (-/-) mice. SDS gels with an amount of 10% acrylamide were prepared. 30 µg of tissue extracts were loaded per lane, followed by electrophoretic separation and blotting. Mena protein was labeled using the primary antibody anti-mena 438 (1:4000) and the secondary antibody goat-anti-rabbit (1:10000). Anti-GAPDH antibody MAB 374 (1:10000) was used as loading control. GAPDH appeared at 35 kDa. The results show that neuronal Mena (140 kDa) is expressed in heart, brain and eyes of wt mice. 80 kDa Mena variant is detected in all wt protein lysates shown, except for kidney. Also in the liver only very small amounts seem to be expressed. Some ko protein lysates also show Mena bands, which proposes that the Mena gene is not completely "knocked out". The 88 kDa variant can not be clearly distinguished from the 80 kDa one. Bands at approximately 120 kDa probably represent unspecific crossreaction with an unrelated protein.
sk.mus.=skeletal muscle, l.int.=large intestine, lymph=lymph nodes, saliv.gl.=salivary gland

Fig. 3-13. Western Blot Analysis to Investigate Mena Protein Expression (following page).
Wt (+/+) mice were compared to Mena mutated (-/-) mice. Two-phase SDS gels with different amounts of acrylamide (part detecting Mena: 5 ml volume of a 7% gel, part detecting GAPDH: 2.5 ml volume of a 12% gel solution). 30 µg of tissue extracts were loaded per lane, followed by electrophoretic separation and blotting. Mena protein was detected by using the primary antibody anti-mena 438 (1:4000) and the secondary antibody goat-anti-rabbit (1:10000). Anti-GAPDH antibody MAB 374 (1:20000) was used as loading control. As a result of the lower amount of acrylamide in this gel, compared to Fig. 3-12, the protein bands were easier to distinguish. Neuronal Mena (140 kDa) was not only expressed in heart, brain and eyes but also in stomach (and slightly in large intestine) of wt mice. 80 kDa Mena variant was detected in all wt-protein lysates shown, except for kidney. Protein extracts of heart, stomach and skeletal muscle contained, apart from the 80 kDa variant, also the 88 kDa isoform. Protein expression of Mena was not completely eliminated in the gene-trapped mice (-/-), as Mena bands also appear in the (-/-)-lanes. Bands at approximately 120 kDa represent unspecific binding.
sk.mus.=skeletal muscle, l.int.=large intestine, lymph=lymph nodes, thromb.=thrombocytes

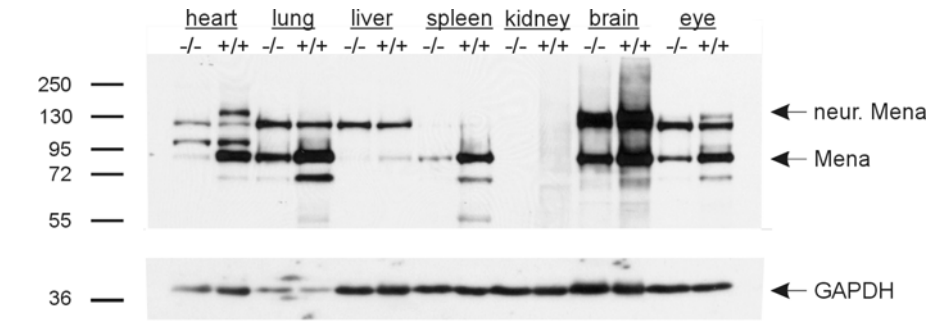

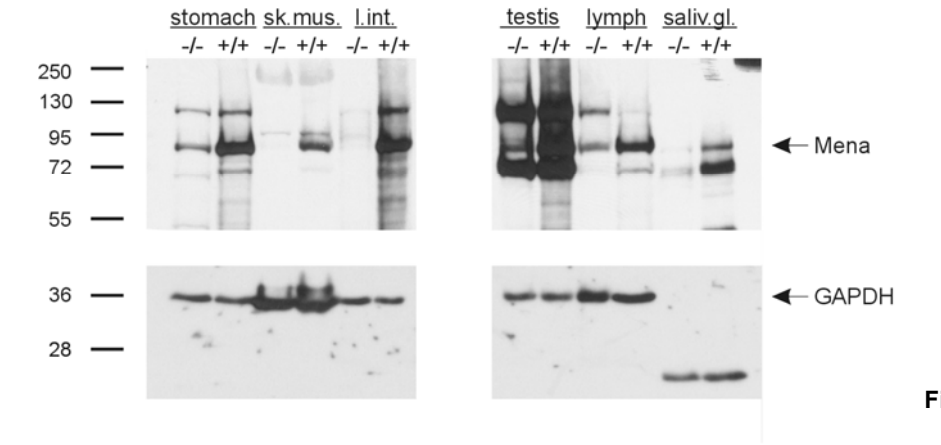

Fig 3-12

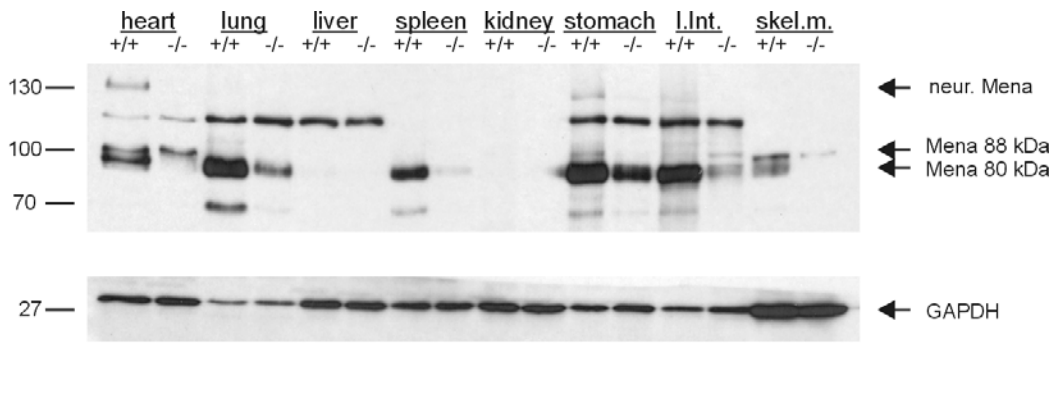

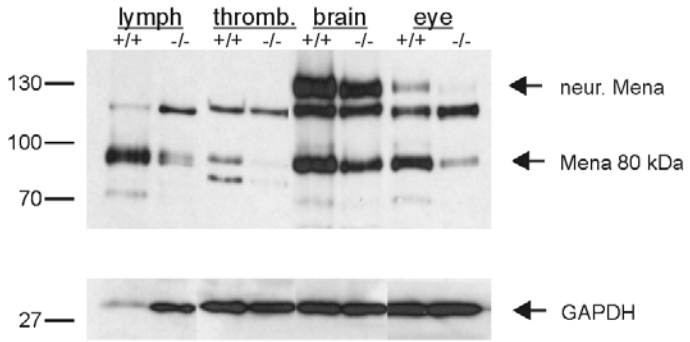

Fig. 3-13

3.5.2 VASP Protein Expression in Wild-type and Mena Deficient Mice

Similar as described above, Western blot analysis was performed to investigate the expression of VASP in wt and Mena ko mice (Fig. 3-14). This experiment should help to answer the question, whether Mena and VASP could compensate for each other. In the case of compensation, VASP protein expression may be increased in tissues of mice lacking Mena.

SDS gels were prepared (10% acrylamide) and loaded with 30 µg of tissue extracts per lane. In Western blots, VASP protein appeared as the doublet of 46 kDa (unphosphorylated VASP) and 50 kDa (phosphor-S157 VASP). Expression patterns of VASP and Mena were quite different (compare Fig. 3-12, 3-13, 3-14). Whereas Mena was broadly expressed in most organs, VASP was predominantly seen in spleen and thrombocytes. It was also detected in lymph nodes, large intestine and slightly in lung. Comparing the VASP protein lanes of wt with Mena deficient mice, no difference in VASP expression could be observed (e.g. Fig. 3-14; protein bands of spleen and thrombocytes), arguing against functional compensation of Mena and VASP.

Fig. 3-14. Western Blot Analysis to Investigate VASP Protein Expression in Wt (+/+) and Mena Deficient (-/-) Mice (following page).
SDS gels with an amount of 10% of acrylamide were prepared, 30 µg of tissue extracts were loaded per lane, followed by electrophoretic separation and blotting. Anti-VASP antibody 19728 was used for labelling (1:2000) VASP protein. Equal protein loading was verified using anti-GAPDH antibody MAB 374 (1:10000). VASP protein appeared as the doublet of 46 kDa (unphosphorylated) and 50 kDa (phosphorylated at serine-157). VASP expression was predominant in spleen and thrombocytes, but was also detected in lymph nodes, large intestine and slightly in lung. When comparing wt with Mena deficient mice, no difference in VASP expression could be observed (e.g. protein bands of spleen and thrombocytes).
Abbreviations: see previous figure.

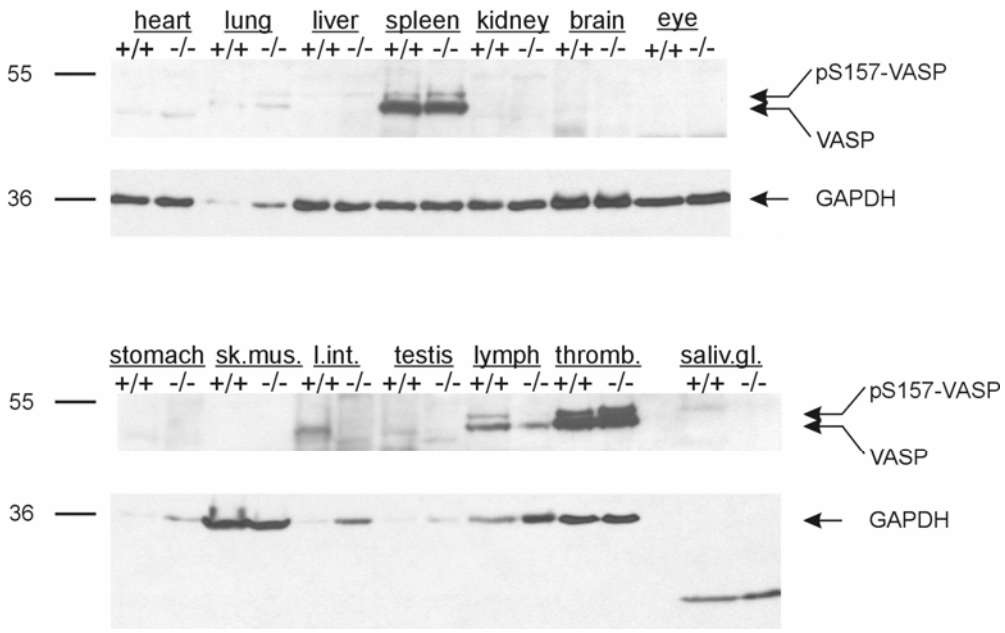

Fig. 3-14

3.5.3 Western Blot Analysis with Mena/VASP-Double-Deficient Mice

Western blot analysis of double-deficient mice (dko) compared to wt mice, were performed with tissues of heart, lung, brain and spleen. Three SDS gels were loaded (25 µg protein per lane) in order to incubate each resulting membrane with another primary antibody, namely anti-mena 438, anti-VASP 19728, anti-EVL109 (Fig. 3-15). In advance, we transfected mammalian cells to generate positive and negative controls for specifity testing of each employed antibody. For negative controls, cells were transfected with empty expression vectors. For positive controls, cells were transfected with constructs encoding Mena, VASP or EVL (see 2.4 for details). The resulting cell lysates were also loaded on the gels (Fig. 3-15).

The result of the Mena-immunoblot (Fig. 3-15) was quite similar to the one described in 3.5.1 and the incomplete knockout of the Mena gene in the dko mice was confirmed. The pCEP-Mena-construct containing cell lysates showed the Mena-protein band at 80 kDa. As expected, the negative-control (cells with pCEP-construct) remained without a signal, confirming the specifity of the employed Mena-antibody. Altogether, this Mena-immunoblot revealed that in

heart and brain, not only the 80 kDa but also the neuronal variant are expressed. In lung, Mena expression is much stronger than in spleen.

The positive control employed for the VASP-immunoblot, lead to the doublet appearing at 46 kDa and 50 kDa, representing the unphosphorylated (VASP) and the phosphorylated (pS157-VASP) form. This experiment showed that the VASP knockout was complete because the dko tissue extracts hardly displayed any signal. Tissue extracts of spleen showed strong expression of VASP. In this case, a signal was also detected in lung and slightly also in heart lysates. No VASP-expression was observed in brain.

Results of the EVL-immunoblot were not really convincing (Fig. 3-15). Although the Sport6-EVL-positive control showed the expected band at 55 kDa which did not appear in the negative control, protein-signals of the tissue extracts were rather fragmented and appeared also between the lanes. Hence, these might be unspecific signals or artefacts of Western blotting. In wt heart and brain lysates strong bands at approximately 70 kDa and 90 kDa were observed. Both protein bands were diminished in the corresponding Mena-VASP-dko lysates, however, the identity of these proteins is unknown.

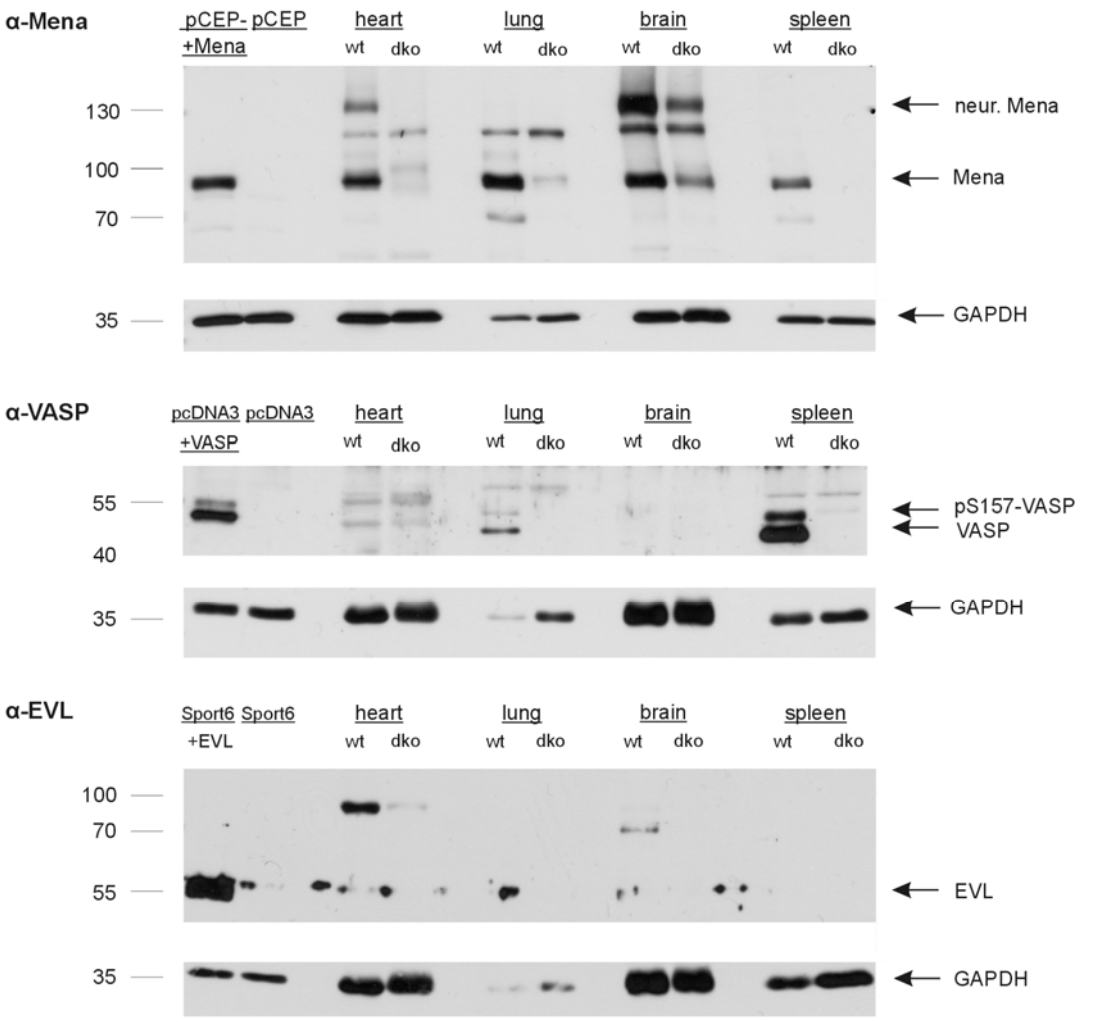

Fig. 3-15. Western Blot Analysis with Wild-type (wt) and Mena/VASP-Double-Defcient (dko) Mouse Organs.
Three immunoblots to analyse protein expression of Mena, VASP and EVL in heart, lung, brain, spleen of wt and dko mice. 25 µg protein of each tissue extract was loaded per lane.
α-Mena: two-phase SDS gel (7%, 12% acrylamide), positive control: pCEP-Mena, negative control: pCEP (each 5 µg total protein of whole cell lysates), antibody: anti-mena 438 (1:4000). 80 kDa variant is expressed in all displayed wt organs, diminished in dko organs. Neuronal Mena is detected in brain and heart.
α-VASP: SDS gel (9% acrylamide), positive and negative controls: pcDNA3-VASP and pcDNA3 (each 10 µg total protein of whole cell lysates), antibody: anti VASP 19728 (1:500). Doublet of 46 kDa and 50 kDa (phosphorylated and unphosphorylated VASP) was very strong in the positive control (pcDNA3-VASP) and in spleen. Slight VASP-expression was detected in lung and heart, no VASP expression in brain and the dko probes.
α-EVL: SDS gel (9% acrylamide), positive and negative controls: Sport6+EVL and Sport6 (each 5 µg total protein of whole cell lysates), antibody: anti-EVL109. Positive control showed expected protein expression at 55 kDa. Results of tissue extracts unclear.

3.6 Analysis of Mena Protein Localisation in Heart and Lung by Confocal Immunofluorescence Microscopy

To identify the exact localisation of Mena protein in the cardiovascular system of mice, we used the method of indirect immunofluorescence. Cryosections of heart and lung of wt and ko mice were incubated with a primary antibody against Mena and a further primary antibody against smooth muscle cells, endothelial cells and αII-spectrin. Some were also incubated with phalloidin, a marker for F-actin. This was followed by the incubation with fluorescence-conjugated secondary antibodies. The resulting double stained immunofluorescence images were analysed using a confocal microscope.

3.6.1 Immunohistochemical Analysis to Compare Mena and F-actin Localisation in Cardiomyocytes

Ena/VASP-family members are known to play an important role in actin regulation, for example in actin polymerisation. Thus, we proposed colocalisation of Mena and actin inside the cells. To test this, we performed double immunofluorescent staining with cryosections of hearts of wt mice. We used the primary antibody anti-mena 438 to detect Mena protein and TRITC-conjugated phalloidin which binds specifically to F-actin (Fig. 3-16). Mena (green fluorescence) was enriched at intercalated discs which connect cardiomyocytes (Fig. 3-16; A), at cardiac vessels (D) and also at Z-discs, which link adjoining sarcomeres within the muscle cells (G). In contrast, TRITC-Phalloidin (red fluorescence) labelled filamentous actin, which is highly important for contraction (Fig. 3-16; H). Colocalisation of Mena and F-actin was detected only at intercalated discs (Fig. 3-16; I, indicated by *).

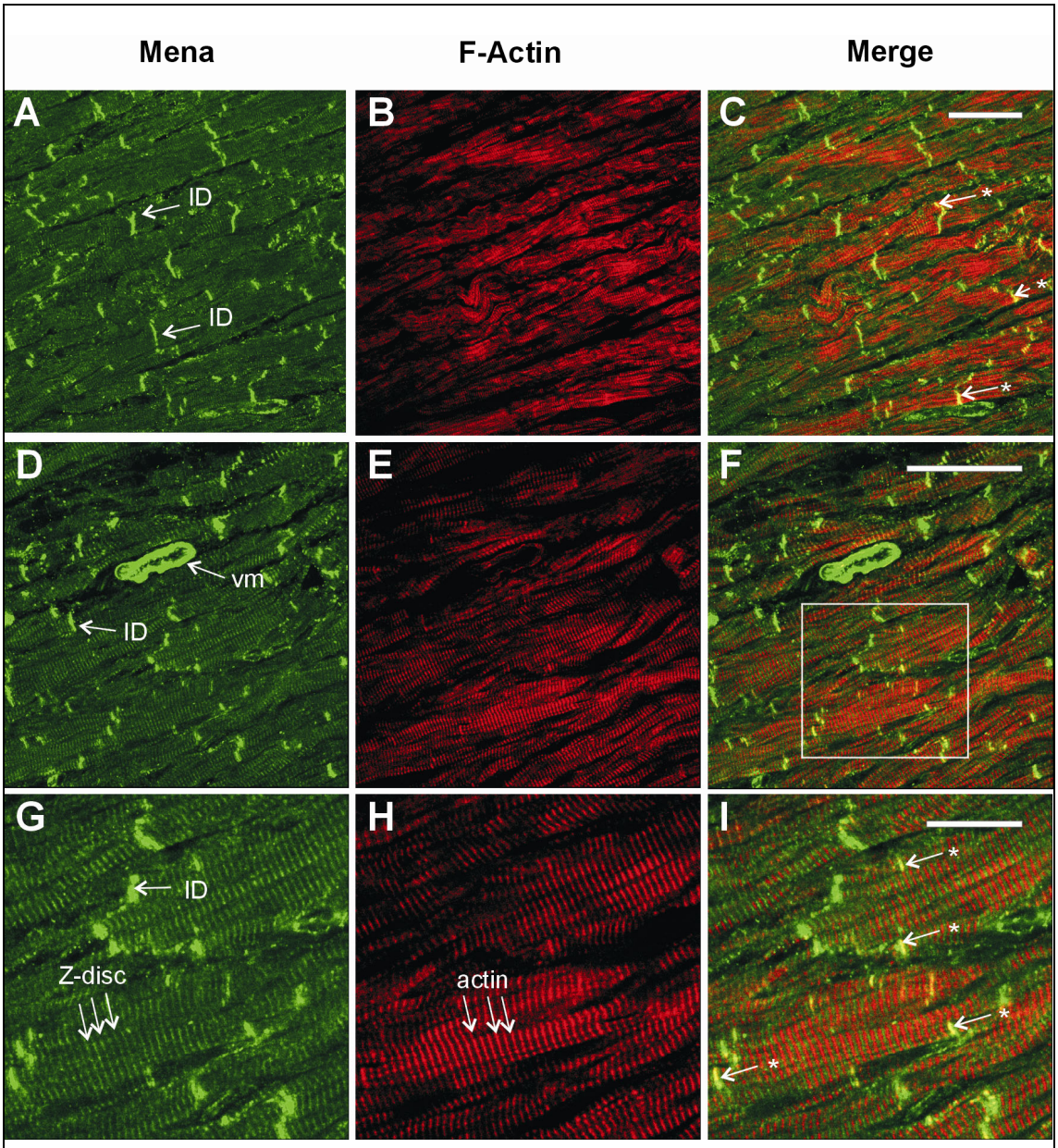

Fig. 3-16. Fluorescent Images of Cryosections of Wild-type (wt) hearts, labeled for F-actin (red) and Mena (green).
(A) Mena protein was enriched at intercalated discs of cardiomyocytes. (D,G) Mena was also detected in cardiac vessels and at Z-discs of cardiomyocytes (striation). (B, E, H) Actin fibres of the contractile apparatus, showing the typical striation pattern. (I) Colocalisation (indicated by *) of F-actin and Mena was observed at intercalated discs (yellow clolour). Antibodies: anti-mena 438 (1:500) with Alexa 488 goat-anti-rabbit (green, 1:500), TRITC-phalloidin (red, 1:500)
a=artery, ID=intercalated discs, vm=vascular smooth muscle. Bars: (C) 50 µm, (F) 50 µm, (I) 20 µm.

3.6.2 Immunohistochemical Analysis to Compare Mena and α-Smooth-Muscle-Actin Localisation

The X-gal results had shown strong Mena promoter activity in muscle layers of the intestines and of vessels. To investigate in more detail, we performed double-immunofluorescence staining of cryosections using anti-mena 438 and the FITC-conjugated anti-α-smooth-muscle-actin antibodies (Fig. 3-17 – Fig. 3-20). Staining was performed with wt and ko mice serving as a control and also for a semi-quantitative assessment of the remaining Mena protein levels in knockout organs. For all corresponding images identical gain and saturation settings were used, thus wt images could be compared to their corresponding $Mena^{-/-}$ images. Fig. 3-17 and Fig. 3-18 show double stained small and larger vessels of the heart. Anti-α-smooth-muscle-actin labelled the smooth muscle tissue of the vessel walls (green fluorescence). Mena protein was detected there as well (red fluorescence). The yellow colour in the merged images demonstrates colocalisation of Mena and α-actin in the smooth muscle vessel wall (Fig. 3-17 C, I; Fig. 3-18 F). Fig. 3-17 B and 3-18 B show that intercalated discs were strikingly labelled by anti-mena 438. Fig. 3-17 D-F and K-L show immunfluorescence images of Mena ko mice. Red fluorescence (Mena protein) was at least diminished to a half compared to wt sections, whereas the intensity of green fluorescence (smooth muscle) remained the same.

Figures 3-19 and 3-20 show double immunofluorescence staining (as described above) of lung cryosections, again comparing wt to Mena ko mice. Displayed are bronchioles and pulmonal vessels. The anti-α-smooth-muscle-actin antibody not only labelled vascular smooth muscle of blood vessels but also smooth muscle of the bronchiole walls. Mena not only localised to vascular and bronchiole muscle, but also to the respiratory epithelium of the bronchioles. The surrounding alveolar tissue was not detected by these antibodies. Again, in these fluorescent images, we observed the expected signal reduction of Mena (red fluorescence), by comparing wt and Mena ko images. The signals of vascular and bronchiole muscle tissue were reduced to approximately 20%, whereas the signal of respiratory epithelium was reduced to approximately 30%.

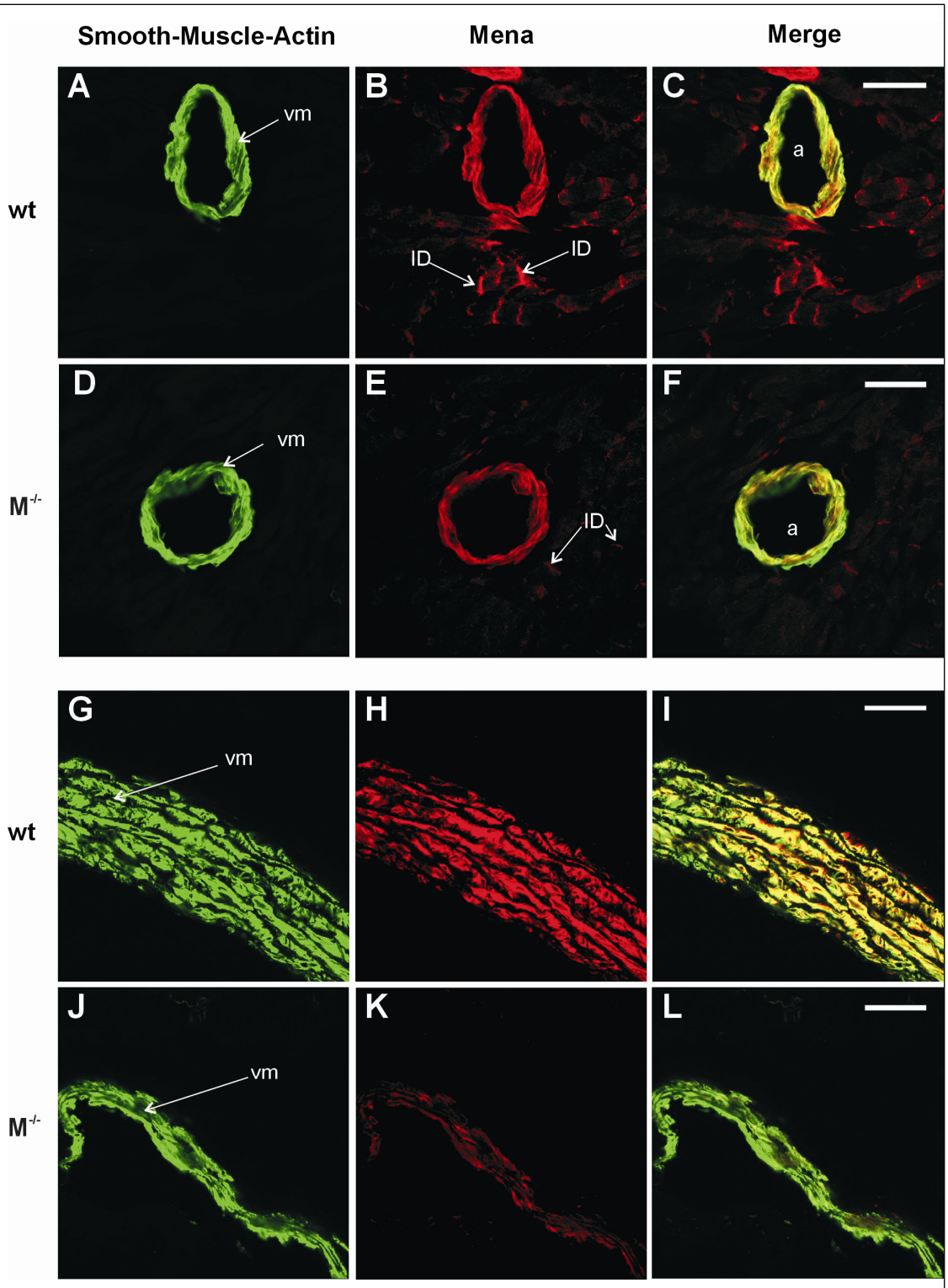

Fig. 3-17

Fig. 3-17. Fluorescent Images of Cryosections of Wild-type (wt) and Mena knockout ($M^{-/-}$) Hearts, Labeled for Mena (red) and α-smooth-muscle-actin (green) (previous page).
(A-C) Small coronary vessel of wt heart: Anti-mena 438 and anti-α-smooth-muscle-actin both labeled vascular smooth muscle; colocalisation is seen in C (yellow). (B) Mena is also enriched at intercalated discs. (D-F) Small coronary vessel of Mena ko heart: diminished Mena expression is seen in E, compared to B. For figures 3-17; A-F same gain and saturation settings were used.
(G-I) Aorta of wt heart: Strong colocalisation in the vessel wall. (J-L) Large vessel of Mena ko heart: Mena protein almost absent. For figures 3-17; G-L same gain and saturation settings were used.
Antibodies: anti-mena 438 (1:500) with goat-anti-rabbit (red, 1:500), FITC-anti-α-smooth-muscle-actin (green, 1:500)
a=artery, ID=intercalated discs, vm=vascular smooth muscle. Bar: 50 µm

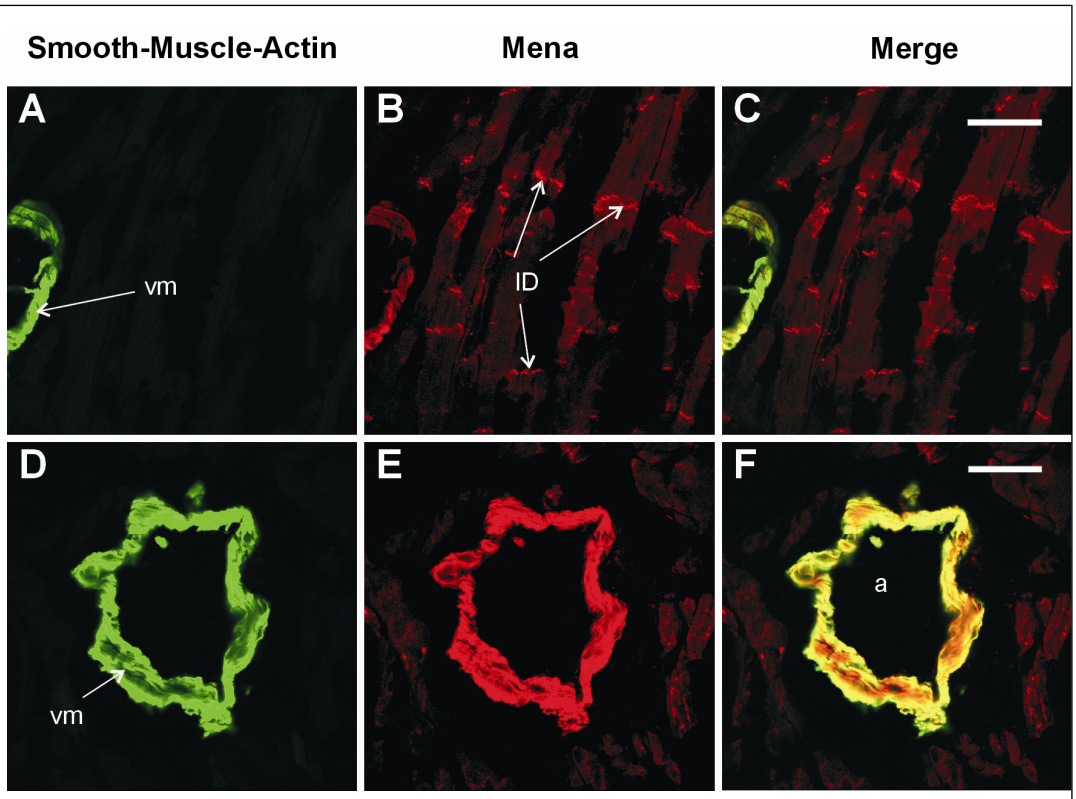

Fig. 3-18. Fluorescent Images of Cryosections of Wt hearts, Labeled for Mena (red) and α-smooth-muscle-actin (green).
(A-C) Small coronary vessel and myocytes of wt heart: Anti-mena 438 and anti-smooth-muscle-α-actin both labeled vascular smooth muscle; slight colocalisation in C (yellow). (B) Mena is enriched at intercalated discs of myocytes. (D-F) Coronary artery of wt heart: Strong colocalisation of Anti-α-smooth-muscle-actin and Mena protein is seen in F. Antibodies: anti-mena 438 (1:500) with goat-anti-rabbit (red, 1:500), FITC-anti-smooth-muscle-α-actin (green, 1:500)
a=artery, id=intercalated discs, vm=vascular smooth muscle. Bar: 50 µm

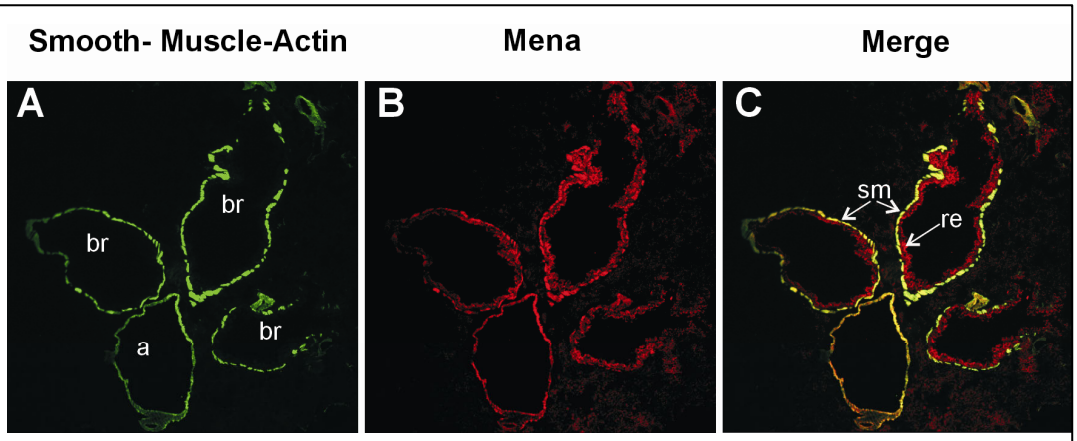

Fig. 3-19. Fluorescent Images showing Cryosections of Wild-type Lung, Labeled for Mena (red) and α-smooth-muscle-actin (green) (previous page).
(A-C) Three adjacent bronchioles and a pulmonal artery. Both antibodies labeled the muscular tissue of bronchioles and of the vessel. (B) Anti-Mena detected also the respiratory epithelium (C) Colocalisation (yellow) is seen only in the vessel wall of the artery and in smooth muscle surrounding the bronchiole but not in the respiratory epithelium. Antibodies: anti-mena 438 (1:500) with Alexa goat-anti-rabbit (red, 1:500), FITC-anti-α-smooth-muscle-actin (green, 1:500) a=artery, br=bronchiole, sm=smooth muscle. Enlargement x4

Fig. 3-20. Fluorescent Images Showing Cryosections of Lung, Labeled for Mena (red) and α-smooth-muscle-actin (green) (following page).
(A-C, G-I) Wt; Pulmonal vessel next to a bronchiole. (D-F, J-L) Ko control. (A, G) Smooth muscle actin is enriched in vascular and bronchiole walls. (B, H) Mena localises to the respiratory epithelium and to smooth muscle tissue of the vessel and the bronchiole. (C, I) Colocalisation of Mena and α-smooth-muscle-actin is detected in muscle layers of vessels and bronchioles. (E, K) Mena-signal is diminished in the images of the mutated mouse, compared to B and H, respectively. For figures 3-20; A-F and for G-I same gain and saturation settings were used.
Antibodies: anti-mena 438 (1:500) with Alexa goat-anti-rabbit (red, 1:500), FITC-anti-α-smooth-muscle-actin (green, 1:500)
br=bronchiole, re=respiratory epithelium, sm=smooth muscle, vm=vascular smooth muscle, v=vessel.
Bar: 50 µm

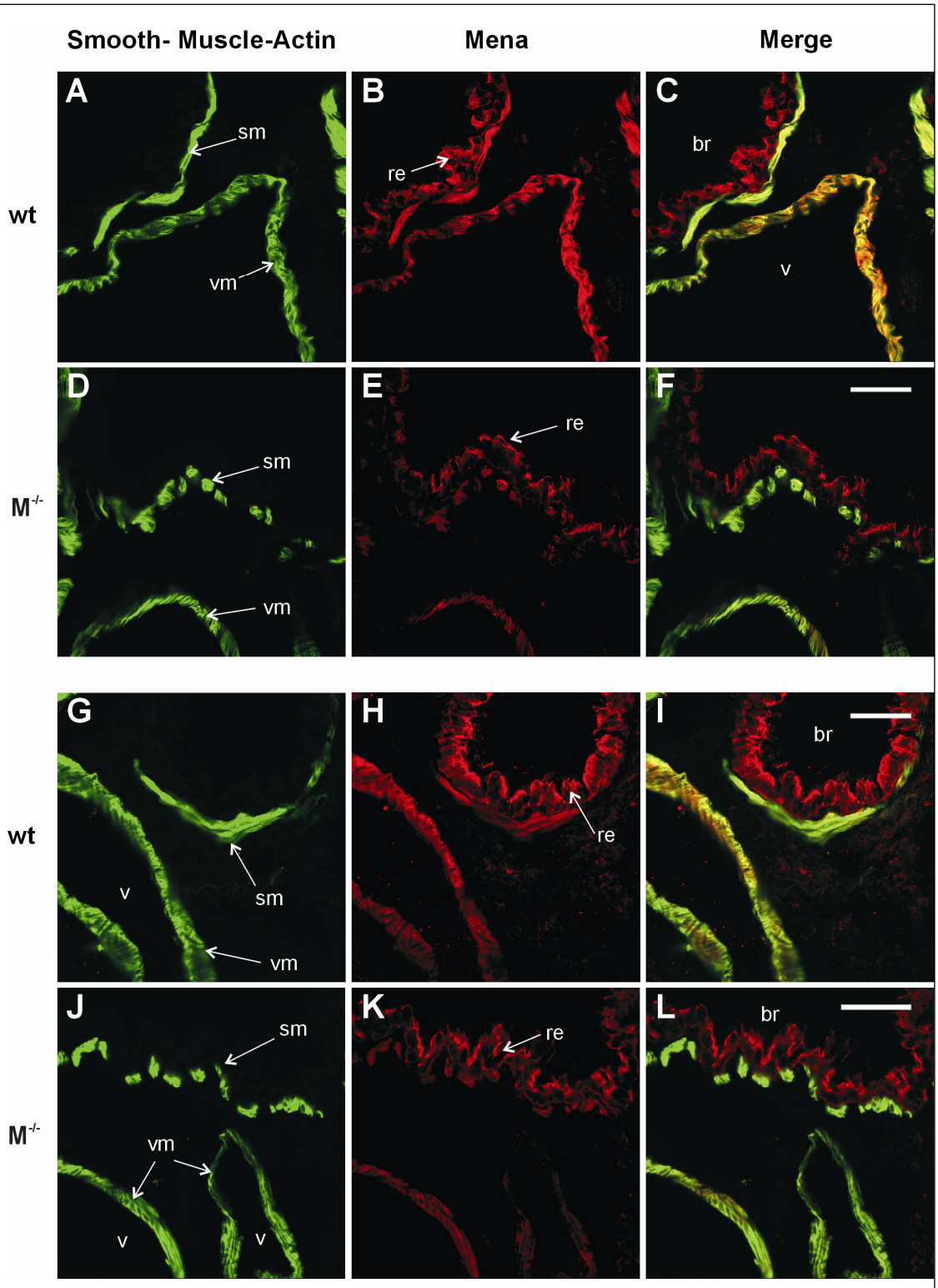
Smooth- Muscle-Actin
Mena
Merge
wt
M-/-
wt
M-/-
A
B
C
D
E
F
G
H
I
J
K
L
sm
re
br
vm
v

Fig. 3-20

3.6.3 Immunohistochemical Analysis to Compare Mena and VE-cadherin Localisation in Heart and Lung

To determine whether Mena is expressed in the vascular endothelium, double immunofluorescence labelling was performed using the primary antibodies anti-mena 438 and anti-VE-cadherin. VE-cadherin is a transmembrane cell-cell adhesion protein, specific for endothelial cells. Figures 3-21; A-I show fluorescent images of small and large vessels in the heart. Anti-VE-cadherin (green fluorescence) labelled the endothelium. Green fluorescent spots in between cardiomyocytes indicate small capillaries (Fig. 3-21; A, D, G). Mena (red fluorescence) was again observed at intercalated discs (IDs) and at vascular smooth muscle (Fig. 3-21; B, E). Colocalisation of Mena and VE-cadherin was not clearly detected in this experiment (Fig. 3-21; C). The intensity of VE-cadherin signal was the same in cryosections of wt and of Mena ko mice. In contrast, the red fluorescence of Mena was clearly reduced to 20% (small vessel, Fig. 3-21; E) and 10% (large vessel, Fig. 3-21; H), respectively, in the ko images.

Figure 3-22 shows immunofluorescence results of lung tissue, stained with the above mentioned antibodies. VE-cadherin localised at the endothelium of the pulmonary arteries but also at the alveolar tissue, which consists predominantly of capillaries (meaning lots of endothelial cells) and pneumocytes. The Mena antibody strongly stained the respiratory epithelium of bronchioles and the vascular smooth muscle. Again, a considerable colocalisation of VE-cadherin and Mena could rather be excluded. Mena did not localise to alveolar tissue. Mena expression was remarkably reduced to approximately 5% in Mena$^{-/-}$ sections (B and H), compared to the corresponding wt sections (E and K).

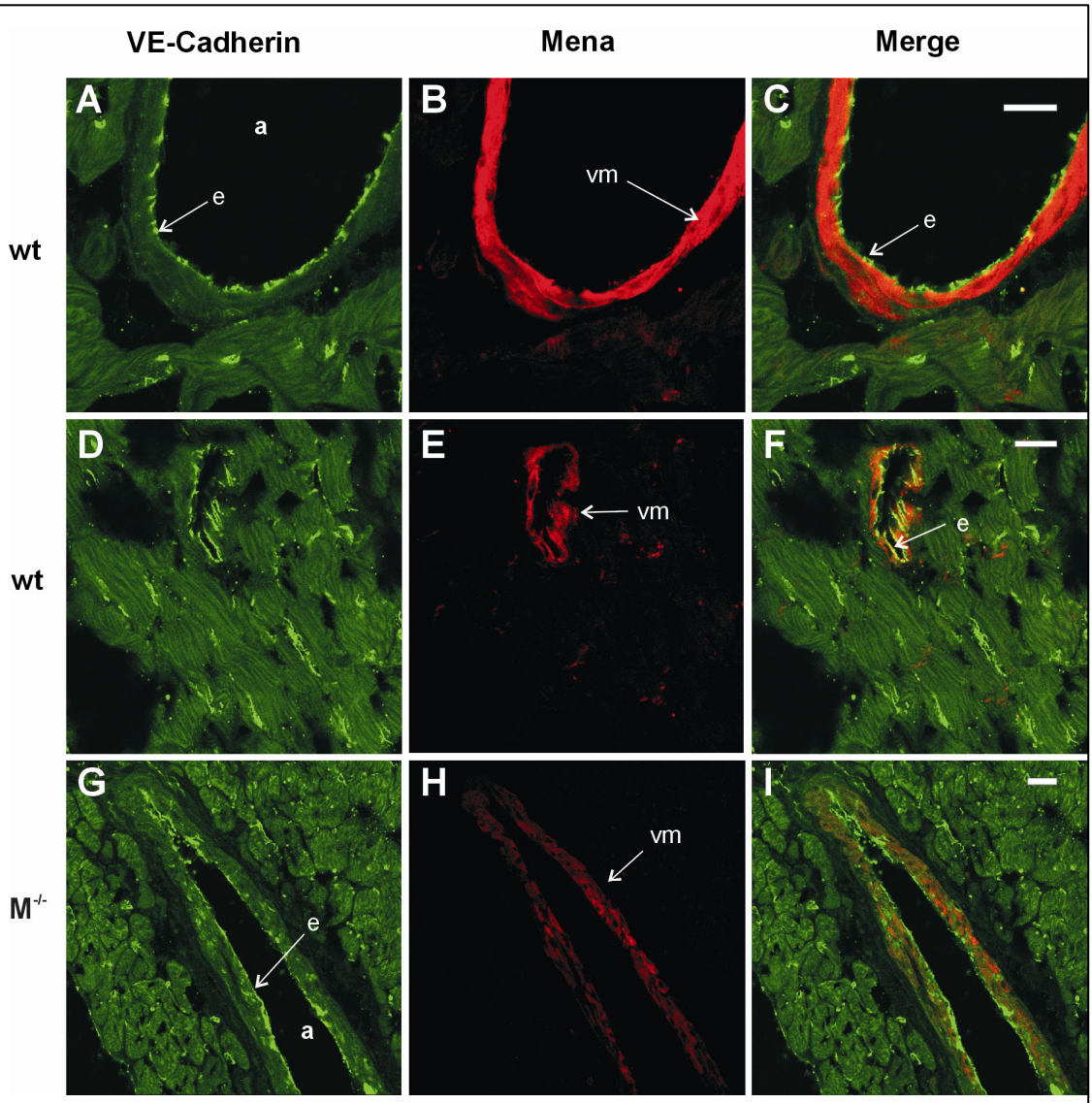

Fig. 3-21. Fluorescent Images of Cryosections of Wild-type (wt) and Mena knockout ($M^{-/-}$) Hearts, Labeled with Antibodies to Mena (red) and VE-cadherin (green).
(A-C) Large coronary vessel of wt heart: anti-VE-cadherin labeled endothelial cells, whereas anti-mena 438 localised to vascular smooth muscle. (C) Colocalisation of VE-cadherin and Mena was not clearly detectable. (D-F) Small cardiac vessel, surrounded by cardiomyocytes. (G-I) Large coronary vessel of a Mena mutated mouse. The knockout was hereby verified as the Mena signal (red) is clearly diminished, comparing images B and H. For all images in Fig 3-21 identical gain settings were used and also saturation was changed equally.
Antibodies: anti-mena 438 (1:500) with goat-anti-rabbit 594 (red, 1:500), anti-VE-cadherin (pure) with goat-anti-rat 488 (green, 1:500)
a=artery, e=endothelium, vm=vascular smooth muscle. Bar: 20 µm

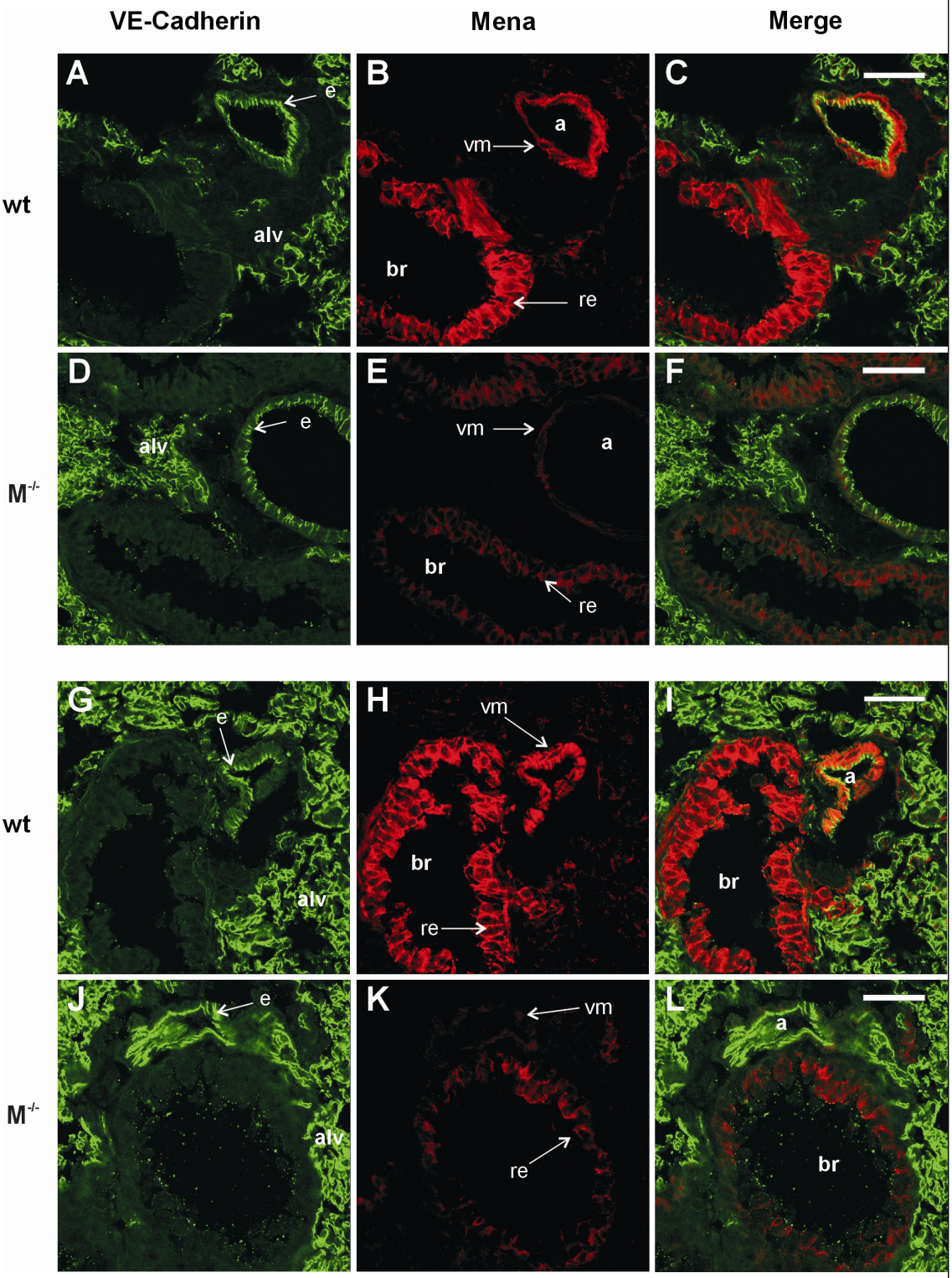

Fig. 3-22

Fig. 3-22. Fluorescent Images of Cryosections of Wild-type (wt) and Mena knockout ($M^{-/-}$) Lung, Labeled with Antibodies to Mena (red) and VE-cadherin (green) (previous page).
(A, D, G, J) In the wt and Mena ko images, VE-cadherin labeled the endothelium of pulmonary arteries and alveolar tissue. (B, H) In wt pulmonary tissue, Mena-antibody localised to vascular smooth muscle and respiratory epithelium. (E, K) Fluorescence intensity analysing Mena localisation was diminished in the Mena-deficient pulmonary tissue. (C, I) Considerable colocalisation could rather be excluded.
For figures 3-22; A-F and G-L identical gain and saturation settings were used.
Antibodies: anti-mena 438 (1:500) with goat-anti-rabbit 594 (red, 1:500), anti-VE-cadherin (pure) with goat-anti-rat 488 (green, 1:500). Bar: 50 µm
a=artery, br=bronchiole, e=endothelium, re=respiratory epithelium, vm=vascular smooth muscle.

3.6.4 Immunohistochemical Analysis to Compare Mena and αII-Spectrin Localisation in the Heart

Spectrins are actin binding proteins, which assemble a two-dimensional meshwork, for example the membrane skeleton (see 1.4), which is associated with the plasma membrane. Thus spectrins are important for cell stability, cell dynamics and transmembrane signal transduction (Bennett and Baines, 2001). Several spectrin subunits are expressed tissue specifically. The αII-spectrin subunit (also named alpha Fodrin) is found at lateral plasma membranes, at Z-discs and IDs (Bennett et al., 2004). Former studies have shown that αII-spectrin colocalises with unphosphorylated VASP at cell-cell contacts and that both proteins are important for the endothelial barrier function (Benz et al., 2008). Therefore we wondered, whether there is also an interaction between Mena and αII-spectrin and performed double immunofluorescence labelling with a FITC-conjugated anti-mena 438 antibody and an alpha-Fodrin antibody (Fig. 3-23).

In wt heart, Mena localised at IDs (Fig. 3-23; A-C) and at vascular smooth muscle (Fig. 3-23; G-I) and these signals were almost erased in the Mena ko controls. Alpha-Fodrin labelled the lateral plasma membranes of cardiomyocytes and the endothelium (Fig. 3-23 B, E, H, K). Because the used antibody is not well suited for immunofluorescence microscopy, αII-spectrin was hardly detectable at IDs. Accordingly, there was no clear colocalisation with Mena at these sites.

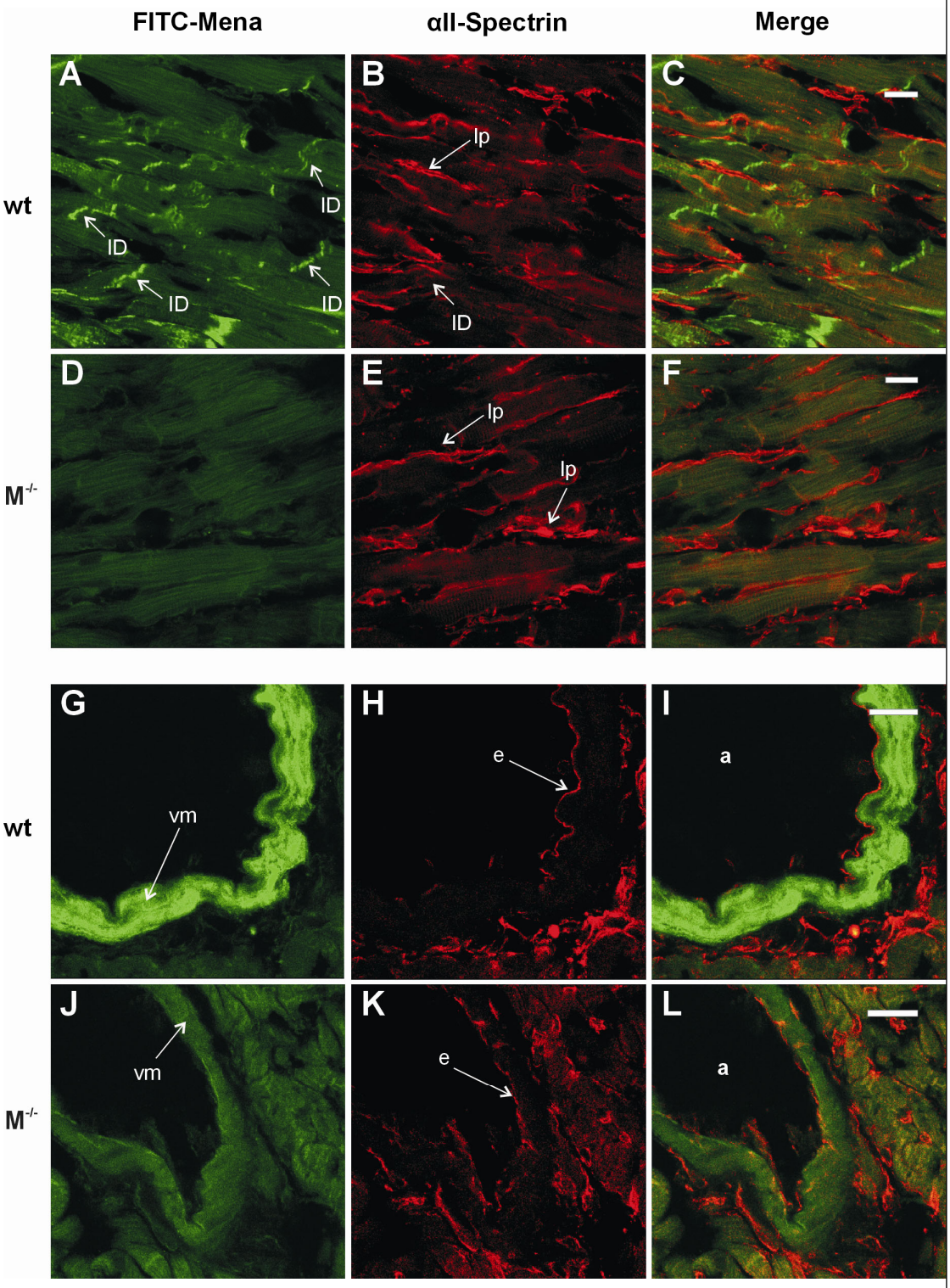

Fig. 3-23

Fig. 3-23. Fluorescent Images of Cryosections of Wild-type (wt) and Mena ko ($M^{-/-}$) Heart, Labeled for Mena (green) and αII-Spectrin (red) (previous page).
(A) Mena localises at IDs of wt heart tissue. (B, E) Anti-αII-spectrin labels the lateral plasma membrane of cardiomyocytes in wt and Mena ko images. (C) Colocalisation of Mena and αII-spectrin in cardiomyocytes is not clearly detectable. (G) Mena localises at the vascular smooth muscle of cardiac vessels. (H) The antibody to αII-spectrin slightly stains vascular endothelium. (I) No detectable colocalisation of αII-spectrin and Mena in cardiac vessels. (J) Vessel wall and surrounding cardiomyocytes of a $Mena^{-/-}$ mouse.
Equal gain and saturation settings were used for images A-F and G-L.
Antibodies: FITC conjugated anti-mena 438 (1:500), alpha Fodrin (Cell signaling, 1:50). Bar: 20 µm
a=artery, e=endothelium, lp=lateral plasma membrane, ID=intercalated disc, vm=vascular smooth muscle

3.7 Functional Analysis of Mena-VASP-Double-Deficient Hearts Using Electrocardiography

Functional cardiac defects of mice lacking the Mena and VASP gene, respectively, were explored by performing electrocardiographic (ECG) analysis. In this assay we compared wt, $Mena^{-/-}$, $VASP^{-/-}$ and Mena-VASP-double-deficient mice (dko). Five animals per group were analysed. All mice were anesthetised with intraperitoneal injection of avertin (10 µl/g). Afterwards mice were placed on a rectal-temperature controlled pad and ECG electrodes were attached. Resting ECGs were recorded for two minutes. Then 2 mg/kg BW of isoprenaline (sympathicomimetic) were injected in order to record stress ECGs for the following five minutes. Recording of all ECGs was performed with Hardware Powerlab, ADInstruments, using the software Chart 5.5.6. ECG interpretation was carried out by ECGAuto 2.5.1.3, EMKA Technologies.

Overall, the results showed striking differences between wt and dko mice, as the resting heart rate (0 – 120 sec) of dko mice was approximately 20 % higher than the heart rate of wt controls (Fig. 3-24). Accordingly, the R-R-intervals of analysed dko mice were shorter. The accelerated heart rate might be due to dysfunctional heart contraction, which requires a higher rate to maintain an adequate cardiac output rate. The $Mena^{-/-}$ and $VASP^{-/-}$ resting heart rates did not differ much from the wt controls. After isoprenaline injection (after 120 sec), the heart rate of dko mice was still a bit higher, compared to single ko and wt mice. However, the heart rate of dko mice was increased by only 7%, whereas heart rates of wt, $VASP^{-/-}$ and $Mena^{-/-}$ mice were elevated by approximately

20%. Concerning dko mice, it seems that at a heart rate of approximately 670 bpm, a limit was reached, thus the heart rate could not be increased further.

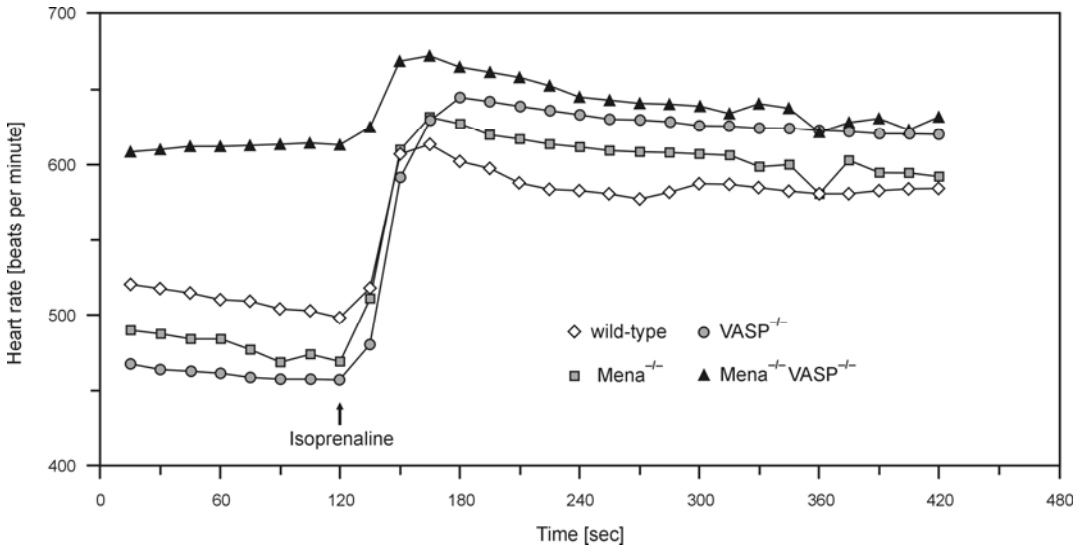

Fig. 3-24. Heart Rate Progression of Wt, Mena$^{-/-}$, VASP$^{-/-}$ and Double-Deficient Mice.
Heart rates of wild-type, VASP$^{-/-}$, Mena$^{-/-}$, and Mena$^{-/-}$ VASP$^{-/-}$ mice under resting condition and after injection of isoprenaline. The resting heart rate of double-deficient (dko) mice is approximately 20% higher than of wt mice. Mena$^{-/-}$ and VASP$^{-/-}$ heart rates do not differ much from those of wt mice. At rest their heart rates are even a bit lower. After isoprenaline injection, the heart rate of dko mice was increased by only ~7%. Whereas heart rates of wt, VASP$^{-/-}$ and Mena$^{-/-}$ mice were elevated by ~20%.

4. Discussion

Proteins of Ena/VASP family participate in cell-cell- and cell-matrix-adhesions (Gambaryan et al., 2001; Gertler et al., 1996; Scott et al., 2006; Vasioukhin et al., 2000). Furthermore, they promote actin polymerisation and it is proposed that they regulate actin nucleation, bundling, branching and capping (Applewhite et al., 2007; Barzik et al., 2005; Schirenbeck et al., 2006). VASP was originally identified in platelets. Its phosphorylation by cGMP- and cAMP-dependent protein kinases correlates with platelet inhibition (Halbrugge and Walter, 1990; Hauser et al., 1999; Horstrup et al., 1994). Mena, on the other hand, contains an additional neuronal isoform (140 kDa) which regulates neuronal migration and axonal outgrowth (Kwiatkowski et al., 2007; Lanier et al., 1999).

One aim of this study was to get a broad overview of the localisation of Mena promoter activity in several tissues using X-gal staining. The closer investigation of Mena localisation in the cardiovascular system was performed by immunofluorescent staining. Additional Western blot analyses with antibodies to Mena, VASP and EVL and functional analysis of mice with different genotypes should help to reveal the functions of Ena/VASP family proteins. Thereby we aimed to identify functional consequences resulting from a gene or protein defect. Moreover, the question was raised whether Mena, VASP and EVL could compensate for each other.

4.1 Mena Promoter Activity in Diverse Tissues

X-gal staining of cryosections of gene-trapped mice served as a method to localise Mena promoter activity. X-gal staining detected β-galactosidase protein, which was encoded by the *β-geo* cassette, a part of the insertion vector which disrupted the original Mena gene between exons 2 and 3. The microscopically detectable blue stain, indigo, is a reaction product generated by the reaction of X-gal with β-galactosidase. Therefore, the subcellular localisation of indigo stain does not correlate with Mena localisation. The figures of section 3.4 show images of microscopic pictures.

We closely investigated brain sections of Mena mutants. Mena promoter activity (blue staining) was detected in isolated cells of the cortex, in the hippocampus and in vessels (Fig 3-7). This is consistent with findings of *Lanier et al.* analysing Mena expression in adult brain (Lanier et al., 1999).
The hippocampus is the main part of the archicortex and belongs to the limbic system. The organ is composed of the cornu ammonis (ca) and the dentate gyrus (gyrus dentatus; gd). It is important for the integration of visceral, endocrine and emotional processes. Therefore it is linked to the hypothalamus, the gyrus cinguli and it receives information from the sense organs.
The cornu ammonis (ca, Fig. 3-7; A) resembles to an enrolled band. It contains predominantly pyramidal cells (pc) which represent the efferent system of the brain. According to their size, the cornu ammonis is structured into sections: ca1- ca3. The dentate gyrus contains granule cells which embrace the tip end of the pyramidal cell layer. The hippocampus receives most afferent fibres from the entorhinal cortex via the perforant path. The fibres run to the cornu ammonis and end at dendrites of the pyramidal and granule cells. These are connected to each other by mossy fibres. These facts show that the hippocampus is well connected by neuronal fibres. Our results verify Mena promoter activity in important hippocampal sections which corresponds to the hypothesis that Mena promotes formation of axonal pathways (Lanier et al., 1999). The positive X-gal staining in the cortex is consistent with the finding that the loss of Ena/VASP prevents axon fibre tract formation in the cortex (Kwiatkowski et al., 2007). High Mena promoter activity at the stated areas is surely due to the importance of Ena/VASP proteins in axonal growth and neuronal migration as they promote the bundling of essential actin filaments and the formation of cellular outgrowths like filopodia. The blue staining that was detected in subarachnoidal vessels and in the plexus choroideus (mainly consisting of capillaries) indicates the localisation of Mena in vessel walls.

X-gal staining of heart cryosections of mutated mice suggested Mena protein expression in cardiomyocytes and coronary vessels and their branches,

respectively (Fig. 3-8). Consistent with this expression pattern, it is presumed that the lack of Mena in cardiomyocytes could lead to cardiac diseases such as cardiac myopathy (Eigenthaler et al., 2003; Pula and Krause, 2008). Closer inspection of large vessels indicated that Mena promoter activity was predominant in the media (Fig. 3-8; C), which consists mainly of smooth muscle cells. This is in good agreement with Ena/VASP function for actin filament formation and actomyosin contractility (Furman et al., 2007; Gertler et al., 1996). Several studies have proposed the role of Ena/VASP family proteins in endothelial cells (Benz et al., 2008; Furman et al., 2007; Sheldon et al., 2009). However, Mena promoter activity in the endothelium of vessels could not be confirmed by X-gal staining of cryosections. Therefore we applied immmunofluorescence analysis to specify Mena localisation. By this we observed clear colocalisation of Mena and α-smooth-muscle-actin in vessels. But a colocalisation of Mena with VE-cadherin at endothelia was not clearly detectable (Fig. 3-21).

X-gal staining of lung sections of Mena mutated mice showed β-galactosidase expression in the respiratory epithelium of bronchi and bronchioles and in pulmonary vessel walls (Fig. 3-9). It appears that the blue staining was predominantly located at the respiratory epithelium which is a ciliated pseudostratified columnar epithelium. Cilia are motile cell extensions. Their motility is enabled by microtubules. Mena may influence cilia function as previously described for other cell extensions, such as lamellipodia. In contrast to lamellipodia and filopodia, which are actin-rich structures, however, microtubules are composed of linear tubulin polymers. But Mena could also regulate actin dynamics, which promote the function of microtubules. Moreover, it is suggestible that Mena supports intercellular adhesion of the respiratory epithelial cells. Mena promoter activity was not detected in alveolar tissue which comprises mainly endothelial cells. This argues against findings, which support Ena/VASP function in endothelial cells (see above). Detailed analysis of Mena localisation in pulmonary tissue was performed by immunofluorescent staining.

Analysing X-gal stained cryosections of intestines displayed Mena promoter activity in intestinal muscle layers, such as the lamina muscularis mucosa and the muscularis, consisting of circular and longitudinal muscle layers (Fig. 3-10). Again, indigo stain was detectable in vessel walls. These results support the hypothesis of Mena function in smooth muscle cells (Gambaryan et al., 2001). However, the intestinal epithelium of Mena$^{-/-}$ sections showed no blue staining after treatment with X-gal solution. This is a bit surprising as former studies have stated the localisation of Ena/VASP proteins at epithelial cells and their association with cell-cell and cell-matrix contacts (Gambaryan et al., 2001; Gertler et al., 1996; Lawrence et al., 2002; Reinhard et al., 1992). In future studies it would be interesting to investigate intestinal X-gal stainings of VASP$^{-/-}$ mice containing a *β-geo* gene trap.

X-gal stainings of spleen, thymus and liver tissue did not show β-galactosidase expression, apart from their vessels (Fig. 3-10). Slightly positive X-gal staining was detected in tubules of kidneys. Mena promoter activity here leads to the assumption that Mena either supports tight and adherens junctions or focal contacts of the tubular epithelial cells. But Mena could also play a role in the actin dynamics of the microvilli (cell extensions of the epithelial cells), which constitute the characteristic brush boarder of kidney tubules.

Interestingly, skeletal muscle tissue of Mena gene-trapped mice displayed no β-galactosidase activity, only the vessel walls were colored blue. This implicates that Mena activity is found in smooth and cardiac but not in skeletal muscle cells. The reason for this differential localization could be that Mena associates exclusively with α-cardiac-muscle-actin and α-smooth-muscle-actin but not with α-skeletal-muscle-actin.

To study Mena promoter activity in adolescent mice, we performed X-gal staining of full-length cryosections of neonatal Mena$^{-/-}$ mice (Fig. 3-11). Results showed Mena activity in almost every tissue. But blue staining was notably intense in the intestines, lung and heart, parts of the brain, eye and the tongue.

Mena promoter activity of neonatal intestines were investigated in more detail (Fig. 3-11, E-G) and was found in the muscularis but also in the mucosa (epithelial cells). This is in contrast to the results from intestine stainings of adult mice (see above), where the mucosa was not stained blue. This supports the hypothesis that expression of Ena/VASP proteins gradually decreases from embryonic and neonatal to adult mice, as described earlier (Gambaryan et al., 2001; Lanier et al., 1999). Moreover, Mena promoter activity in the intestinal mucosa is consistent with former studies, which state the importance of Ena/VASP in association with cell-cell junctions and focal contacts (Benz et al., 2008; Furman et al., 2007; Gertler et al., 1996; Reinhard et al., 1992).

4.2 Protein Expression of Ena/VASP Family Members

Whereas X-gal staining analysis revealed Mena promoter activity, Western blot analysis was performed to investigate the actual protein expression of Mena in wt mice (Fig. 3-12, 3-13)

Strongest Mena protein expression was detected in brain and testis, whereas Mena protein levels were also high in heart, lung, eye, stomach, large intestine, spleen and lymph nodes. In skeletal muscle, thrombocytes and salivary gland only trace amounts of Mena protein were observed and Mena expression in liver and kidney was not clearly detectable. This might be due to the degradation of Mena protein by local enzymes of these organs.

Surprisingly, Mena expression was also detected in spleen and thrombocytes. Former studies have claimed that VASP but not Mena is expressed in these tissues (Gambaryan et al., 2001). Hence, our investigations support the hypothesis that Mena could compensate for VASP. Low levels of Mena expression found in skeletal muscle probes are probably due to vessels of the skeletal muscle tissue.

As described above, there exist three different splice variants of Mena, which migrate at 80 kDa, 88 kDa and 140 kDa in SDS-PAGE. Neuronal Mena, the 140 kDa isoform, has been described to be expressed only in the brain (Gambaryan

et al., 2001; Lanier et al., 1999). Our Western blot investigations revealed the expression of neuronal Mena also in the eye, which is a part of the brain, but also in heart and stomach, slightly in the large intestine (Fig. 3-13). Reasons for this might be that the heart contains an autonomous nervous system and the intestines an enteric nervous system which is located in the submucosa and the muscularis (Auerbach´s and Meissner´s plexus).
We also detected an uncommon protein band at approximately 70 kDa in several kinds of wt tissues, such as lung, spleen and salivary gland. As the signals were reduced in the corresponding ko tissues, it is questionable whether there exists another uncommon Mena splice variant. This isoform could be identical to a Mena form described earlier by Tani et al. They also performed PCR and Western blotting and detected a Mena variant lacking 300-330 aminoacids. This short form they termed *mena(S)* (Tani et al., 2003).

The protein expression of VASP in wt and Mena mutated mice was also analysed by Western blotting (Fig. 3-14). The expression pattern differed much from the one investigating Mena expression. VASP was predominantly found in spleen and thrombocytes. Lower amounts were detected in lymph nodes, large intestine and lung. Previous studies have found stronger VASP protein expression in lung and stomach (Gambaryan et al., 2001; Hauser et al., 1999). VASP protein appeared as the doublet of 46 kDa and 50 kDa, showing the unphosphorylated and phosphorylated form of VASP. The phosphorylation of serine-157 of VASP is supposed to effect platelet inhibition (Halbrugge et al., 1990; Hauser et al., 1999; Horstrup et al., 1994). In our Western blot results, the 46 kDa protein band was much more intense than the 50 kDa band.
Overall, the tissue specific expressions of VASP and Mena are quite different. In literature, VASP and Mena functions are often simultaneously analysed in *in vitro* and *in vivo* assays (Eigenthaler et al., 2003; Furman et al., 2007; Sechi and Wehland, 2004). Thus it could be presumed that on cellular level, both proteins do promote similar cellular functions, such as actin proliferation and stabilisation of cell contacts. Our expression profiles, however, show divergent tissue distributions and therefore question overlapping cellular functions. By

performing Western blot analysis with wt and Mena ko mouse organs, using an anti-VASP antibody, we studied whether the lack of one protein would influence the expression of the other protein (Fig. 3-14). Increased VASP protein expression in Mena$^{-/-}$ mice would support the theory of functional compensation. However, VASP protein levels in wt and Mena ko mice did not differ substantially.

In a following step, we compared protein expression of Mena and VASP in double deficient mice and wt mice. Although previous studies have revealed that mice lacking both, Mena and VASP, are not viable and die during embryonic development (Eigenthaler et al., 2003; Furman et al., 2007; Lanier et al., 1999), we succeeded in generating double deficient mice (dko). The dko mice were generated by crossbreeding our Mena gene-trapped mice with the VASP ko mice from Hauser et al. However, compared to wt mice, dko mice were of smaller size and lower weight and died quite early postnatally. The reason for viability of the dko mice might be that the gene-trapped-based Mena-knockout was leaky, meaning the gene was not knocked out completely by the gene-trap insertion. This becomes evident by Western blot analysis and immunofluorescent stainings of Mena-mutant mice, which displayed some remaining Mena protein expression (Fig. 3-12, 3-13, 3-17, 3-20). A reason for this could be that in some cases splicing did not occur between exon 2 and the gene-trap construct, but between exon 2 and exon 3, thus yielding in the expression of a functional Mena protein (Fig. 4-1).

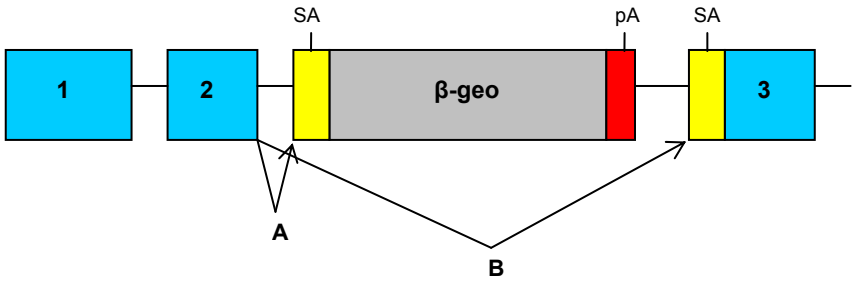

Fig. 4-1. Alternative Splicing of the Gene-trapped Mena Gene as Possible Explanation for Leakiness.
As our immunohistochemistry and Western blot results show, Mena was not knocked out completely by the gene-trap. A reason for this "leakiness" could be alternative splicing. (A) In an optimal way, splicing would occur between exon 2 and the splice acceptor (SA) of the gene-trap construct, thus yielding in a fusion transcript, which connects exons 1 and 2 to the *β-geo-cassette.* By this, expression of Mena protein is prevented. We propose that the gene-trap was sometimes "ignored" and splicing occurred between exon 2 and the splice acceptor of exon 3 (B), finally leading to the expression of a functional Mena protein.

Western blots that were performed with an anti-Mena antibody to detect Mena protein expression in wt and dko mice, showed that Mena expression was almost erased in heart, lung and spleen of dko mice. Wt probes implied Mena expression in heart, lung, brain and spleen. In brain and heart the 140 kDa form was also detectable.

The incubation of similar blots with an anti-VASP antibody showed expression of unphosphorylated and phosphorylated VASP predominantly in spleen but also in lung. Slight expression of VASP was also detected in heart probes. These Western blot analyses display again that the expression pattern of Mena in several tissues diverges from the expression of VASP.

By the incubation of those Western blots with an anti-EVL antibody we expected to support our hypothesis of compensation. Although our generated positive control (Sport6+EVL) was correctly detected by the antibody, the results were unsatisfying. In future, this experiment should be repeated, using other anti-EVL antibodies. By comparing EVL expression in wt and dko mice, one could receive information to support the theory of mutual compensation. For example, previous in vitro assays of Listeria have shown interchangeable roles of Ena, VASP and EVL (Ahern-Djamali et al., 1998; Laurent et al., 1999).

4.3 Detailed Mena Localisation in the Cardiovascular System

A principal aim of this study was to specify Mena localisation in the cardiovascular system to get an idea about physiological consequences associated with Mena gene defects or Mena protein dysfunction. Previous studies have proposed that the lack of Ena/VASP proteins cause common cardiovascular diseases, such as edema, haemorrhaging and dilated cardiomyopathy (Benz et al., 2008; Eigenthaler et al., 2003; Furman et al., 2007).

We used immunofluorescent microscopy of wt heart sections and labelled for Mena F-actin. The results in Fig. 3-16 indicate that Mena and F-actin colocalise at intercalated discs (IDs). But there was no colocalisation at the sarcomeric actin filaments. Mena located very strong at IDs and slightly at Z-discs. Previous studies that have shown colocalisation of Mena, VASP, connexin-43, and β-catenin have already proposed the importance of Ena/VASP family at IDs (Eigenthaler et al., 2003; Gambaryan et al., 2001; Markert et al., 1996). Defects at IDs may lead to dysfunctions in electrical and mechanical conduction between cardiomyocytes, resulting in weak heart contractility. *Eigenthaler et al.* suggested that the displacement of VASP and Mena from the IDs leads to dilated cardiomyopathy (Eigenthaler et al., 2003).

Main features of dilated cardiomyopathy (DCM) are impaired systolic pump function and diastolic dysfunction, cardiomegaly and reduced ejection fraction. These defects result in cardiac insufficiency and heart rhythm disturbances. Causes of DCM are idiopathic (40%), toxic, infectious and genetic defects (20%) (e.g. mutations of genes encoding for cytoskeletal proteins). Based on the present work, future functional analysis should investigate whether Mena and/or VASP mutated mice develop the stated dysfunctions.

Additional immunofluorescent labelling of heart sections was accomplished using antibodies to α-smooth-muscle-actin and VE-cadherin. The results shown in figures 3-17, 3-18, 3-21 demonstrate strong colocalisation of α-smooth-

muscle-actin and Mena in cardiac vessel walls. Colocalisation of VE-cadherin and Mena could not be verified. One reason for this could be that Mena is not expressed in endothelial cells. Another explanation could be that a low Mena expression in a single-layer epithelium, namely the endothelium, is outshone by the high expression of Mena in smooth muscle. Therefore, future studies should analyse isolated endothelial cells (ECs) by immunofluorescence microscopy. The analysis of isolated ECs by Western blotting has recently been performed, proving Mena expression in ECs (Benz et al., 2009). Our results also stand in contrast to other previous studies which suggest the importance of Ena/VASP in endothelial cells, especially at endothelial cell contacts (Benz et al., 2008; Furman et al., 2007; Markert et al., 1996). Another explanation to this discrepancy could be the fact that VASP and Mena are downregulated during postnatal development (Gambaryan et al., 2001). Our experiments were performed with adult mice.

Immunofluorescent stainings of lung sections were also performed with antibodies to Mena, α-smooth-muscle-actin and to VE-cadherin. The figures 3-19, 3-20, 3-22 confirm colocalisation of α-smooth-muscle-actin and Mena, not only in vascular walls but also in smooth muscle fibres of bronchioles (Fig. 3-20). However, Mena did not colocalise clearly with VE-cadherin (Fig. 3-22). As alveoles consist primarily of endothelial cells, anti-VE-cadherin antibody locates to alveolar tissue. Mena-immunoreactivity was absent at these spots. Mena signal was very strong at the respiratory epithelium which is a ciliated pseudostratified columnar epithelium. This finding affirms the importance of Mena at epithelial adherens junctions. But it could also suggest that Mena, via the regulation of actin dynamics, influences the movement or stability of the cilia which are epithelial cell extensions. From our results of immunofluorescent staining, demonstrating Mena localisation in bronchiole epithelium and smooth muscle, one could propose a great impact of Mena on pulmonary diseases, such as asthma and chronic obstructive pulmonary disease (COPD). However this issue has yet not been addressed experimentally. Studies of VASP have shown a decreased VASP phosphorylation in epithelial cells of asthmatics, leading to an inhibition of actin reorganization and thus preventing epithelial

repair (Hastie et al., 2006). Moreover, recent studies have identified VASP as a central protein in the control of the alveolar-capillary barrier properties during acute lung injury (ALI) (Henes et al., 2009). A similar mechanism could be supposed for Mena. For analysing Mena expression in asthmatic lung tissue, an appropriate mouse model could be used. For instance, previous studies have demonstrated mouse models for nonatopic asthma. For this purpose, hapten-induced pulmonary hypersensitivity reactions, which were induced by skin sensitization followed by an intra-airway application of dinitrofluorobenzene (DNFB) were performed (Kraneveld et al., 2002).

Finally, we performed immunohistochemistry analyses of heart sections with an anti-Mena antibody and with several antibodies for detecting αII-spectrin.

Spectrins are actin-binding proteins that assemble into dimers and tetramers, which are composed of alpha and beta subunits. The αIβI-combination is exclusive for the membrane skeleton of erythrocytes (Fig. 1-4). In contrast, the αII-spectrin subunit is found in most of human tissues and usually forms αIIβII-tetramers. These tetramers can build up meshworks underlying the plasma membranes. In general, spectrins are important for cell stability and elasticity, for cell dynamics and transmembrane signal transduction. In heart, αII-spectrin localises to Z-discs, lateral plasma membrane and to IDs (Baines and Pinder, 2005). Moreover, an alternatively spliced isoform of αII-spectrin, namely αII-SH3i, associates with connexin 43 (Ursitti et al., 2007). Earlier studies have revealed colocalisation of Mena, VASP and connexin 43. Finally, literature shows that non-phosphorylated VASP and spectrin create complexes that regulate the submembranous actin cytoskeleton assembly in endothelial cells. These assemblies are proposed to be important for endothelial barrier function (Benz et al., 2008). An impaired endothelial barrier leads to an increase of permeability which results in edema. In our experiments we tried to define whether Mena-spectrin complexes exist and investigated Mena/αII-spectrin colocalisation at the cell-cell-junctions in cardiomyocytes (IDs) using immunofluorescence microscopy.

However, most of the applied αII-spectrin-antibodies led to unspecific results and displayed red dots in most sections. Rather satisfying results were obtained

with the αII-spectrin antibody from Cell signaling (Fig. 3-23). Immunofluorescent images support the localisation of αII-spectrin at the lateral plasma membranes of cardiomyocytes and at the endothelium. But αII-spectrin was not found at the IDs. Therefore, we were not able to specify Mena-functioning at the IDs. On the other hand, Mena was (again) not detected in the endothelium. Thus, an endothelial barrier function as for VASP could not be ascribed for Mena.

4.4 Functional Analysis Revealed Cardiac Dysfunctions in Mutated Mice

We investigated the cardiac function of Mena$^{-/-}$, VASP$^{-/-}$ and Mena-VASP-double-ko (dko) mice compared to wt mice by generating electrocardiography (ECG) (Fig. 3-24). ECGs were performed at rest and at stress (isoprenaline injection). Striking differences between wt and dko mice could be detected at rest. The heart rate of dko mice was much higher (approximately 20%), which implicates that the heart contractility of the mutated mice is weaker as of wt mice. Heart rates of Mena$^{-/-}$ and VASP$^{-/-}$ mice did not differ much from wt mice suggesting that depletion of Mena or VASP does not interfere with normal heart function. Actually, at rest, heart rates of single knockout mice were even lower than of wt mice. After isoprenaline injection, the heart rate of double-deficient mice could not be increased to the same extend as of wt mice. In detail, the heart rate of dko mice was increased by only 7%, whereas heart rates of wt, VASP$^{-/-}$ and Mena$^{-/-}$ mice were elevated by approximately 20%. A reason for this could be that the physiological capacity of the heart of dko mice was nearly reached under resting conditions (650 bmp). Our results imply that Mena and VASP indeed mutually compensate for each other and that at least the expression of one of the proteins is required for normal heart function.

Additional experiments with Mena ko, dko and wt mice using a cardiac catheter were accomplished by Dr. Kai Hu. His results indicate that mutated mice develop a dilated cardiomyopathy. This is in good agreement with the ECG results because a dilated cardiomyopathy impairs contractility, which induces an

accelerate heart rate to maintain a sufficient cardiac output. Former studies have revealed that the disruption of Ena/VASP protein localisation at IDs causes dilated cardiomyopathy (Eigenthaler et al., 2003). However their mutated mice exhibited bradycardia, whereas our findings show rather a tachycardia.

4.5 Conclusions and Future Aspects

To sum up, our results have shown Mena localisation in several kinds of tissue. Mena was found in important areas of the brain, such as cortex and hippocampus, surely related to axonal pathways. In heart, Mena was especially located at IDs, implying its importance in force transduction and electrical conduction. Moreover, Mena was detected in all kinds of smooth muscle layers, for example of vessels, of bronchioles, of stomach and intestine. As Mena promoter activity was not detected in skeletal muscle tissue, we suppose that Mena interacts specifically with α-smooth-muscle-actin. Comparing the results of adult mice with images of neonatal mice, supports the thesis that Ena/VASP proteins are highly expressed during embryonic and neonatal development, but that the genes are down-regulated later-on (Gambaryan et al., 2001).

Immunofluorescent staining implicated colocalisation of Mena with filamentous and with α-smooth-muscle-actin. However, we could not detect any considerable colocalisation of Mena with VE-cadherin or with αII-spectrin, at least in part due to antibodies that were not well suited for immunofluorescent staining.

The question of mutual compensation is difficult to answer. On the one hand, Mena and VASP share a similar structural organisation. Besides, a single Mena ko or a VASP ko mouse is viable, whereas double-deficient mice usually die during embryonic development (Eigenthaler et al., 2003; Furman et al., 2007; Lanier et al., 1999). Both proteins are known to promote structural cell stability and organization. They locate to cell-matrix and cell-cell contacts and they regulate actin dynamics and stress fibre formation (Bear and Gertler, 2009; Benz et al., 2008; Furman et al., 2007; Vasioukhin et al., 2000). Both are found

in smooth muscle cells and at IDs of cardiomyocytes. But on the other side, there are differing aspects of Mena and VASP. VASP is associated with platelet inhibition and also with regulating endothelial barrier function in assembly with spectrin. Our studies provide no clear evidence that Mena fulfils similar functions. But Mena, in contrast to VASP, is expressed in neuronal tissue as neuronal Mena isoform. Furthermore, our Western blot analyses show a very differing expression pattern comparing both proteins. Mena seems to be broadly expressed in many organs, whereas VASP expression is rather limited to thrombocytes, spleen, lymph nodes and large intestine. From these findings, one could also presume the importance of VASP and to a lesser extent for Mena, in the regulation of the immune system. Previous studies have already presumed that Ena/VASP proteins play a key role in linking T-cell receptor signalling to the actin cytoskeleton (Krause et al., 2000). Moreover, other investigations have shown that Ena/VASP are important for the process of phagocytosis of macrophages and neutrophils (Coppolino et al., 2001).

One hypothesis to explain the mutual reaction of Ena/VASP proteins could be that on cellular level, both proteins regulate similar cellular functions, usually associated with actin dynamics, such as cellular contacts, cell protrusions, and stress fibre formation. But they fulfil these similar cellular functions in different kinds of tissues. For those tissues, in which they are known to colocalise, for example in smooth muscle and in cardiomyocytes at IDs, one could presume collective functioning of Mena and VASP.

All of the mentioned aspects let suppose that the lack or dysfunction of Ena/VASP proteins can lead to the development of cardiac and bronchiole abnormalities. To begin with, VASP is known to stabilize endothelial barrier function in assembly with spectrin. Its lack leads to endothelial barrier dysfunction, resulting in edema (Benz et al., 2008; Furman et al., 2007). Secondly, Mena and VASP are highly expressed in smooth muscle tissue (Gambaryan et al., 2001). The relaxation and contraction of vascular smooth muscle fibres have a great influence on the blood pressure. Furthermore, as described above, both proteins are localised at intercalated discs. It is obvious that a dysfunction of force transduction and electrical conduction between

adjacent cardiomyocytes interferes with cardiac pump function and may even lead to a dilated cardiomyopathy. Our functional analyses also give a hint to this assumption. Finally, Mena localisation at the respiratory epithelium of bronchioles suggests an important function of Mena for accurate lung function. This hypothesis is supported by the finding that in the case of pulmonary diseases, such as asthma, VASP phosphorylation is decreased (Hastie et al., 2006).

Future studies should try to elucidate the subcellular localisation of Mena and VASP in more detail, for example by using electron microscopy. Immunofluorescence analyses detecting αII-spectrin should be improved and staining using an antibody to EVL should also be accomplished. Analyses of Mena function in the heart have to be completed. Apart from cardiac catheter investigations of different mice genotypes, one could also apply echocardiography to answer the question of dilated cardiomyopathy in the case of dko mice. Moreover, we intend to analyse Mena and VASP expression in heart sections of wt mice that sustained a heart attack and compare them to control heart sections using immunofluorescence microscopy. Finally, we intend to perform aorta-banding with wt, Mena ko, VASP ko and dko mice. This should cause a dilated and hypertrophic heart muscle and would reveal a protective effect of Ena/VASP proteins for proper heart contraction. It would be interesting to find differences in Ena/VASP expression and functioning.

Summary

Proteins of the Ena/VASP protein family are important regulators of actin dynamics and participate in cell-cell and cell-matrix adhesions. To date, the physiological importance of Ena/VASP proteins for integrity of the cardiovascular system has remained unclear. To study cardiovascular functions of Mena and VASP, we used an established VASP knockout mouse in combination with a novel gene-trap-based model to ablate Mena function. In the mutated Mena mouse, the endogenous Mena gene is disrupted by the insertion of a β-galactosidase construct and β-galactosidase expression is under the control of the endogenous Mena promoter. X-gal staining of mouse organs revealed Mena promoter activity in smooth muscle layers of vessels, intestines and bronchioles, but also in cells of the brain, in cardiomyocytes and in the respiratory epithelium of bronchioles. In wild-type mice, Western blotting revealed differing protein expression patterns of VASP and Mena. Mena expression was observed in almost every tissue, predominantly in heart, lung, stomach, large intestine, testis, brain and eye. Additionally, the neuronal-specific Mena isoform was expressed in brain, eye, and slightly in heart and stomach. VASP protein, in contrast, was predominantly detected in spleen and thrombocytes. In gene-trapped mice, Mena expression was largely reduced in heart, lung and stomach but only slightly decreased in brain and testis. Immunofluorescence microscopy revealed colocalisation of Mena and F-actin at intercalated discs of cardiomyocytes and strong colocalisation of Mena and α-smooth-muscle-actin in vessels and bronchioles. Functional analysis of Mena/VASP-mutated and wild-type mice using electrocardiography suggested that the depletion of either Mena or VASP does not interfere with normal heart function. However, in double-deficient mice, the resting heart rate was significantly increased, probably reflecting a mechanism to compensate defects in ventricle contraction and to maintain a normal cardiac output. In agreement, cardiac catheter investigations suggested dilated cardiomyopathy in double-deficient mice. Thus, although Western blot analysis showed differing protein expression patterns of Mena and VASP, these findings suggest that Mena and VASP mutually compensate for each other. Concerning Mena, we propose an

important role of the protein in vessel walls, cardiomyocytes and bronchioles. Therefore, future studies should involve further functional analyses, for instance, echocardiography, aortic banding and a mouse model for pulmonal diseases.

Zusammenfassung

Proteine der Ena/VASP-Familie sind wichtige Regulatoren der Aktin-Dynamik und sind Bestandteile von Zell-Zell- und Zell-Matrix-Kontakten. Bis heute ist die physiologische Bedeutung der Ena/VASP-Proteine speziell im kardiovaskulären System noch nicht geklärt. Um die kardiovaskuläre Funktion von Mena (*mammalian* Ena) und VASP zu untersuchen, nutzten wir eine etablierte VASP-Knockout-Maus in Kombination mit einem neuen *Gene-trap*-Maus-Modell, welches die Mena-Funktion ausschaltet. In der mutierten Mena-Maus wird das endogene Mena-Gen durch die Insertion eines β-Galaktosidase-Konstrukts gespalten, sodass die Mena-Funktion ausfällt und die β-Galaktosidase-Expression unter der Kontrolle des endogenen Mena-Promoters steht. X-Gal-Färbungen von Mausorganen ließen Mena-Promoter-Aktivität in glatter Muskulatur von Gefäßen, Darm und Bronchiolen, aber auch in Zellen des Gehirns, in Kardiomyozyten und im respiratorischen Flimmerepithel der Bronchiolen erkennen. In Wildtyp-Mäusen, zeigten Western-Blot-Untersuchungen unterschiedliche Protein-Expressionsmuster für VASP und Mena. Mena-Expression wurde in fast allen Geweben entdeckt, hauptsächlich in Herz, Lunge, Magen, Dickdarm, Hoden, Gehirn und in den Augen. Zusätzlich wurde die neuronale Mena-Isoform im Gehirn, in den Augen und ein wenig auch in Herz und im Magen exprimiert. Im Gegensatz dazu, wurde VASP hauptsächlich in Thrombozyten und in Milzgewebe gefunden. In den auf dem *Gene*-trap basierenden Mäusen war die Expression von Mena im Herz, in der Lunge und im Magen deutlich reduziert, während nur eine leichte Verringerung im Gehirn und im Hodengewebe festzustellen war. Immunfluoreszenz-Mikroskopie legten Kolokalisation von Mena und F-Aktin an Glanzstreifen von Kardiomyozyten und deutliche Kolokalisation von Mena und glattmuskulärem Aktin in Gefäßen und Bronchien dar. Funktionsanalysen von Mena/VASP-mutierten und Wildtyp-Mäusen anhand von EKG-Aufzeichnungen, ließen vermuten, dass ein Verlust von entweder Mena oder VASP die normale Herzfunktion nicht negativ beeinträchtigt. Wohingegen die Ruheherzrate von doppeldefizienten Mäusen deutlich erhöht war, was möglicherweise auf einen

Mechanismus zur Kompensation der defizienten Ventrikelkontraktion zurückzuführen ist, um ein normales Herz-Zeit-Volumen aufrecht zu erhalten. Dies stimmt mit Herzkatheter-Untersuchungen überein, die auf eine Dilatative Kardiomyopathie bei doppeldefizienten Mäusen hindeuteten. Folglich ist davon auszugehen, dass Mena- und VASP-Proteine füreinander kompensieren können, obwohl Western-Blot-analysen unterschiedliche Expressionsmuster gezeigt haben. Mena betreffend, vermuten wir eine wichtige Rolle des Proteins in Gefäßwänden, in Kardiomyozyten und in Bronchien. aus diesem Grund sollten zukünftige Studien weitere Funktionsanalysen beinhalten, wie zum Beispiel Echokardiographie und Maus-Modelle für Aortenligatur und Lungenerkrankungen.

References

Ahern-Djamali, S.M., Comer, A.R., Bachmann, C., Kastenmeier, A.S., Reddy, S.K., Beckerle, M.C., Walter, U., and Hoffmann, F.M. (1998). Mutations in Drosophila enabled and rescue by human vasodilator-stimulated phosphoprotein (VASP) indicate important functional roles for Ena/VASP homology domain 1 (EVH1) and EVH2 domains. Mol Biol Cell *9*, 2157-2171.

Applewhite, D.A., Barzik, M., Kojima, S., Svitkina, T.M., Gertler, F.B., and Borisy, G.G. (2007). Ena/VASP proteins have an anti-capping independent function in filopodia formation. Mol Biol Cell *18*, 2579-2591.

Aszodi, A., Pfeifer, A., Ahmad, M., Glauner, M., Zhou, X.H., Ny, L., Andersson, K.E., Kehrel, B., Offermanns, S., and Fassler, R. (1999). The vasodilator-stimulated phosphoprotein (VASP) is involved in cGMP- and cAMP-mediated inhibition of agonist-induced platelet aggregation, but is dispensable for smooth muscle function. EMBO J *18*, 37-48.

Bachmann, C., Fischer, L., Walter, U., and Reinhard, M. (1999). The EVH2 domain of the vasodilator-stimulated phosphoprotein mediates tetramerization, F-actin binding, and actin bundle formation. J Biol Chem *274*, 23549-23557.
Baines, A.J., and Pinder, J.C. (2005). The spectrin-associated cytoskeleton in mammalian heart. Front Biosci *10*, 3020-3033.

Ball, L.J., Jarchau, T., Oschkinat, H., and Walter, U. (2002). EVH1 domains: structure, function and interactions. FEBS Lett *513*, 45-52.

Barzik, M., Kotova, T.I., Higgs, H.N., Hazelwood, L., Hanein, D., Gertler, F.B., and Schafer, D.A. (2005). Ena/VASP proteins enhance actin polymerization in the presence of barbed end capping proteins. J Biol Chem *280*, 28653-28662.
Bear, J.E., and Gertler, F.B. (2009). Ena/VASP: towards resolving a pointed controversy at the barbed end. J Cell Sci *122*, 1947-1953.

Bear, J.E., Svitkina, T.M., Krause, M., Schafer, D.A., Loureiro, J.J., Strasser, G.A., Maly, I.V., Chaga, O.Y., Cooper, J.A., Borisy, G.G.*, et al.* (2002). Antagonism between Ena/VASP proteins and actin filament capping regulates fibroblast motility. Cell *109*, 509-521.

Bennett, P.M., Baines, A.J., Lecomte, M.C., Maggs, A.M., and Pinder, J.C. (2004). Not just a plasma membrane protein: in cardiac muscle cells alpha-II spectrin also shows a close association with myofibrils. J Muscle Res Cell Motil *25*, 119-126.

Bennett, V., and Baines, A.J. (2001). Spectrin and ankyrin-based pathways: metazoan inventions for integrating cells into tissues. Physiol Rev *81*, 1353-1392.

Benz, P.M., Blume, C., Moebius, J., Oschatz, C., Schuh, K., Sickmann, A., Walter, U., Feller, S.M., and Renne, T. (2008). Cytoskeleton assembly at endothelial cell-cell contacts is regulated by alphaII-spectrin-VASP complexes. J Cell Biol *180*, 205-219.

Benz, P.M., Blume, C., Seifert, S., Wilhelm, S., Waschke, J., Schuh, K., Gertler, F., Munzel, T., and Renne, T. (2009). Differential VASP phosphorylation controls remodeling of the actin cytoskeleton. J Cell Sci *122*, 3954-3965.

Bignone, P.A., and Baines, A.J. (2003). Spectrin alpha II and beta II isoforms interact with high affinity at the tetramerization site. Biochem J *374*, 613-624.

Chakraborty, T., Ebel, F., Domann, E., Niebuhr, K., Gerstel, B., Pistor, S., Temm-Grove, C.J., Jockusch, B.M., Reinhard, M., Walter, U*., et al.* (1995). A focal adhesion factor directly linking intracellularly motile Listeria monocytogenes and Listeria ivanovii to the actin-based cytoskeleton of mammalian cells. EMBO J *14*, 1314-1321.

Cohen-Tannoudji, M., and Babinet, C. (1998). Beyond 'knock-out' mice: new perspectives for the programmed modification of the mammalian genome. Mol Hum Reprod *4*, 929-938.

Coppolino, M.G., Krause, M., Hagendorff, P., Monner, D.A., Trimble, W., Grinstein, S., Wehland, J., and Sechi, A.S. (2001). Evidence for a molecular complex consisting of Fyb/SLAP, SLP-76, Nck, VASP and WASP that links the actin cytoskeleton to Fcgamma receptor signalling during phagocytosis. J Cell Sci *114*, 4307-4318.

Drees, B., Friederich, E., Fradelizi, J., Louvard, D., Beckerle, M.C., and Golsteyn, R.M. (2000). Characterization of the interaction between zyxin and members of the Ena/vasodilator-stimulated phosphoprotein family of proteins. J Biol Chem *275*, 22503-22511.

Drenckhahn (2003). Bennninghoff-Drenckhahn Anatomie - Makroskopische Anatomie, Histologie, Embryologie, Zellbiologie, Vol 16 (München, Jena, Urban & Fischer).

Eigenthaler, M., Engelhardt, S., Schinke, B., Kobsar, A., Schmitteckert, E., Gambaryan, S., Engelhardt, C.M., Krenn, V., Eliava, M., Jarchau, T*., et al.* (2003). Disruption of cardiac Ena-VASP protein localization in intercalated disks causes dilated cardiomyopathy. Am J Physiol Heart Circ Physiol *285*, H2471-2481.

Friedel, R.H., Plump, A., Lu, X., Spilker, K., Jolicoeur, C., Wong, K., Venkatesh, T.R., Yaron, A., Hynes, M., Chen, B*., et al.* (2005). Gene targeting using a promoterless gene trap vector ("targeted trapping") is an efficient method to mutate a large fraction of genes. Proc Natl Acad Sci U S A *102*, 13188-13193.

Furman, C., Sieminski, A.L., Kwiatkowski, A.V., Rubinson, D.A., Vasile, E., Bronson, R.T., Fassler, R., and Gertler, F.B. (2007). Ena/VASP is required for endothelial barrier function in vivo. J Cell Biol *179*, 761-775.

Gambaryan, S., Hauser, W., Kobsar, A., Glazova, M., and Walter, U. (2001). Distribution, cellular localization, and postnatal development of VASP and Mena expression in mouse tissues. Histochem Cell Biol *116*, 535-543.

Gertler, F.B., Comer, A.R., Juang, J.L., Ahern, S.M., Clark, M.J., Liebl, E.C., and Hoffmann, F.M. (1995). enabled, a dosage-sensitive suppressor of mutations in the Drosophila Abl tyrosine kinase, encodes an Abl substrate with SH3 domain-binding properties. Genes Dev *9*, 521-533.

Gertler, F.B., Niebuhr, K., Reinhard, M., Wehland, J., and Soriano, P. (1996). Mena, a relative of VASP and Drosophila Enabled, is implicated in the control of microfilament dynamics. Cell *87*, 227-239.

Grimm, H.P., Verkhovsky, A.B., Mogilner, A., and Meister, J.J. (2003). Analysis of actin dynamics at the leading edge of crawling cells: implications for the shape of keratocyte lamellipodia. Eur Biophys J *32*, 563-577.

Halbrugge, M., Friedrich, C., Eigenthaler, M., Schanzenbacher, P., and Walter, U. (1990). Stoichiometric and reversible phosphorylation of a 46-kDa protein in human platelets in response to cGMP- and cAMP-elevating vasodilators. J Biol Chem *265*, 3088-3093.

Halbrugge, M., and Walter, U. (1989). Purification of a vasodilator-regulated phosphoprotein from human platelets. Eur J Biochem *185*, 41-50.

Halbrugge, M., and Walter, U. (1990). Analysis, purification and properties of a 50,000-dalton membrane-associated phosphoprotein from human platelets. J Chromatogr *521*, 335-343.

Han, Y.H., Chung, C.Y., Wessels, D., Stephens, S., Titus, M.A., Soll, D.R., and Firtel, R.A. (2002). Requirement of a vasodilator-stimulated phosphoprotein family member for cell adhesion, the formation of filopodia, and chemotaxis in dictyostelium. J Biol Chem *277*, 49877-49887.

Harbeck, B., Huttelmaier, S., Schluter, K., Jockusch, B.M., and Illenberger, S. (2000). Phosphorylation of the vasodilator-stimulated phosphoprotein regulates its interaction with actin. J Biol Chem *275*, 30817-30825.

Hastie, A.T., Wu, M., Foster, G.C., Hawkins, G.A., Batra, V., Rybinski, K.A., Cirelli, R., Zangrilli, J.G., and Peters, S.P. (2006). Alterations in vasodilator-stimulated phosphoprotein (VASP) phosphorylation: associations with asthmatic phenotype, airway inflammation and beta2-agonist use. Respir Res *7*, 25.

Hauser, W., Knobeloch, K.P., Eigenthaler, M., Gambaryan, S., Krenn, V., Geiger, J., Glazova, M., Rohde, E., Horak, I., Walter, U*., et al.* (1999). Megakaryocyte hyperplasia and enhanced agonist-induced platelet activation in vasodilator-stimulated phosphoprotein knockout mice. Proc Natl Acad Sci U S A *96*, 8120-8125.

Henes, J., Schmit, M.A., Morote-Garcia, J.C., Mirakaj, V., Kohler, D., Glover, L., Eldh, T., Walter, U., Karhausen, J., Colgan, S.P*., et al.* (2009). Inflammation-associated repression of vasodilator-stimulated phosphoprotein (VASP) reduces alveolar-capillary barrier function during acute lung injury. FASEB J *23*, 4244-4255.

Hoffman, L.M., Jensen, C.C., Kloeker, S., Wang, C.L., Yoshigi, M., and Beckerle, M.C. (2006). Genetic ablation of zyxin causes Mena/VASP mislocalization, increased motility, and deficits in actin remodeling. J Cell Biol *172*, 771-782.

Horstrup, K., Jablonka, B., Honig-Liedl, P., Just, M., Kochsiek, K., and Walter, U. (1994). Phosphorylation of focal adhesion vasodilator-stimulated phosphoprotein at Ser157 in intact human platelets correlates with fibrinogen receptor inhibition. Eur J Biochem *225*, 21-27.

Huang, S.F., Liu, D.B., Zeng, J.M., Yuan, Y., Xiao, Q., Sun, C.M., Li, C.L., Tao, K., Wen, J.P., Huang, Z.G*., et al.* (2009). Cloning, expression, purification, distribution and kinetics characterization of the bacterial beta-galactosidase fused to the cytoplasmic transduction peptide in vitro and in vivo. Protein Expr Purif *68*, 167-176.

Kraneveld, A.D., van der Kleij, H.P., Kool, M., van Houwelingen, A.H., Weitenberg, A.C., Redegeld, F.A., and Nijkamp, F.P. (2002). Key role for mast cells in nonatopic asthma. J Immunol *169*, 2044-2053.

Krause, M., Sechi, A.S., Konradt, M., Monner, D., Gertler, F.B., and Wehland, J. (2000). Fyn-binding protein (Fyb)/SLP-76-associated protein (SLAP), Ena/vasodilator-stimulated phosphoprotein (VASP) proteins and the Arp2/3 complex link T cell receptor (TCR) signaling to the actin cytoskeleton. J Cell Biol *149*, 181-194.

Krugmann, S., Jordens, I., Gevaert, K., Driessens, M., Vandekerckhove, J., and Hall, A. (2001). Cdc42 induces filopodia by promoting the formation of an IRSp53:Mena complex. Curr Biol *11*, 1645-1655.

Kwiatkowski, A.V., Gertler, F.B., and Loureiro, J.J. (2003). Function and regulation of Ena/VASP proteins. Trends Cell Biol *13*, 386-392.

Kwiatkowski, A.V., Rubinson, D.A., Dent, E.W., Edward van Veen, J., Leslie, J.D., Zhang, J., Mebane, L.M., Philippar, U., Pinheiro, E.M., Burds, A.A*., et al.*

(2007). Ena/VASP Is Required for neuritogenesis in the developing cortex. Neuron *56*, 441-455.

Lambrechts, A., Kwiatkowski, A.V., Lanier, L.M., Bear, J.E., Vandekerckhove, J., Ampe, C., and Gertler, F.B. (2000). cAMP-dependent protein kinase phosphorylation of EVL, a Mena/VASP relative, regulates its interaction with actin and SH3 domains. J Biol Chem *275*, 36143-36151.

Lanier, L.M., Gates, M.A., Witke, W., Menzies, A.S., Wehman, A.M., Macklis, J.D., Kwiatkowski, D., Soriano, P., and Gertler, F.B. (1999). Mena is required for neurulation and commissure formation. Neuron *22*, 313-325.

Laurent, V., Loisel, T.P., Harbeck, B., Wehman, A., Grobe, L., Jockusch, B.M., Wehland, J., Gertler, F.B., and Carlier, M.F. (1999). Role of proteins of the Ena/VASP family in actin-based motility of Listeria monocytogenes. J Cell Biol *144*, 1245-1258.

Lawrence, D.W., Comerford, K.M., and Colgan, S.P. (2002). Role of VASP in reestablishment of epithelial tight junction assembly after Ca2+ switch. Am J Physiol Cell Physiol *282*, C1235-1245.

Layne, E. (1957). Spectrophotometric and turbidimetric methods for measuring proteins. In Methods Enzymology pp. 447-454.

Lottspeich, F., and Zorbas, H. (1998). Gezielte Genmodifikation. In Bioanalytik, F. Lottspeich, and H. Zorbas, eds. (Heidelberg, Berlin, Spektrum Akademischer Verlag GmbH), pp. 921 - 939.

Markert, T., Krenn, V., Leebmann, J., and Walter, U. (1996). High expression of the focal adhesion- and microfilament-associated protein VASP in vascular smooth muscle and endothelial cells of the intact human vessel wall. Basic Res Cardiol *91*, 337-343.

Mehta, D., and Malik, A.B. (2006). Signaling mechanisms regulating endothelial permeability. Physiol Rev *86*, 279-367.

Melton, D.W. (1994). Gene targeting in the mouse. Bioessays *16*, 633-638.

Menzies, A.S., Aszodi, A., Williams, S.E., Pfeifer, A., Wehman, A.M., Goh, K.L., Mason, C.A., Fassler, R., and Gertler, F.B. (2004). Mena and vasodilator-stimulated phosphoprotein are required for multiple actin-dependent processes that shape the vertebrate nervous system. J Neurosci *24*, 8029-8038.

Niebuhr, K., Ebel, F., Frank, R., Reinhard, M., Domann, E., Carl, U.D., Walter, U., Gertler, F.B., Wehland, J., and Chakraborty, T. (1997). A novel proline-rich motif present in ActA of Listeria monocytogenes and cytoskeletal proteins is the ligand for the EVH1 domain, a protein module present in the Ena/VASP family. EMBO J *16*, 5433-5444.

Pula, G., and Krause, M. (2008). Role of Ena/VASP proteins in homeostasis and disease. Handb Exp Pharmacol, 39-65.

Reinhard, M., Giehl, K., Abel, K., Haffner, C., Jarchau, T., Hoppe, V., Jockusch, B.M., and Walter, U. (1995). The proline-rich focal adhesion and microfilament protein VASP is a ligand for profilins. EMBO J *14*, 1583-1589.

Reinhard, M., Halbrugge, M., Scheer, U., Wiegand, C., Jockusch, B.M., and Walter, U. (1992). The 46/50 kDa phosphoprotein VASP purified from human platelets is a novel protein associated with actin filaments and focal contacts. EMBO J *11*, 2063-2070.

Revenu, C., Athman, R., Robine, S., and Louvard, D. (2004). The co-workers of actin filaments: from cell structures to signals. Nat Rev Mol Cell Biol *5*, 635-646.

Samarin, S., Romero, S., Kocks, C., Didry, D., Pantaloni, D., and Carlier, M.F. (2003). How VASP enhances actin-based motility. J Cell Biol *163*, 131-142.

Schirenbeck, A., Arasada, R., Bretschneider, T., Stradal, T.E., Schleicher, M., and Faix, J. (2006). The bundling activity of vasodilator-stimulated phosphoprotein is required for filopodium formation. Proc Natl Acad Sci U S A *103*, 7694-7699.

Scott, J.A., Shewan, A.M., den Elzen, N.R., Loureiro, J.J., Gertler, F.B., and Yap, A.S. (2006). Ena/VASP proteins can regulate distinct modes of actin organization at cadherin-adhesive contacts. Mol Biol Cell *17*, 1085-1095.

Sechi, A.S., and Wehland, J. (2004). ENA/VASP proteins: multifunctional regulators of actin cytoskeleton dynamics. Front Biosci *9*, 1294-1310.

Sheldon, H., Andre, M., Legg, J.A., Heal, P., Herbert, J.M., Sainson, R., Sharma, A.S., Kitajewski, J.K., Heath, V.L., and Bicknell, R. (2009). Active involvement of Robo1 and Robo4 in filopodia formation and endothelial cell motility mediated via WASP and other actin nucleation-promoting factors. FASEB J *23*, 513-522.

Simmer, J.P., Hu, Y., Lertlam, R., Yamakoshi, Y., and Hu, J.C. (2009). Hypomaturation enamel defects in Klk4 knockout/LacZ knockin mice. J Biol Chem *284*, 19110-19121.

Skarnes, W.C. (2005). Two ways to trap a gene in mice. Proc Natl Acad Sci U S A *102*, 13001-13002.

Smith, G.A., Theriot, J.A., and Portnoy, D.A. (1996). The tandem repeat domain in the Listeria monocytogenes ActA protein controls the rate of actin-based motility, the percentage of moving bacteria, and the localization of vasodilator-stimulated phosphoprotein and profilin. J Cell Biol *135*, 647-660.

Stanford, W.L., Cohn, J.B., and Cordes, S.P. (2001). Gene-trap mutagenesis: past, present and beyond. Nat Rev Genet *2*, 756-768.

Tani, K., Sato, S., Sukezane, T., Kojima, H., Hirose, H., Hanafusa, H., and Shishido, T. (2003). Abl interactor 1 promotes tyrosine 296 phosphorylation of mammalian enabled (Mena) by c-Abl kinase. J Biol Chem *278*, 21685-21692.

Thornell, L.E., Johansson, B., Eriksson, A., Lehto, V.P., and Virtanen, I. (1984). Intermediate filament and associated proteins in the human heart: an immunofluorescence study of normal and pathological hearts. Eur Heart J *5 Suppl F*, 231-241.

Tondeleir, D., Vandamme, D., Vandekerckhove, J., Ampe, C., and Lambrechts, A. (2009). Actin isoform expression patterns during mammalian development and in pathology: Insights from mouse models. Cell Motil Cytoskeleton.

Toyofuku, T., Yabuki, M., Otsu, K., Kuzuya, T., Hori, M., and Tada, M. (1998). Direct association of the gap junction protein connexin-43 with ZO-1 in cardiac myocytes. J Biol Chem *273*, 12725-12731.

Tse, W.T., and Lux, S.E. (1999). Red blood cell membrane disorders. Br J Haematol *104*, 2-13.

Ulrich, M., Schuh, K. (2009). Gene trap: knockout on the fast lane. Methods Mol Biol. *561*, 145-159.

Ursitti, J.A., Petrich, B.G., Lee, P.C., Resneck, W.G., Ye, X., Yang, J., Randall, W.R., Bloch, R.J., and Wang, Y. (2007). Role of an alternatively spliced form of alphaII-spectrin in localization of connexin 43 in cardiomyocytes and regulation by stress-activated protein kinase. J Mol Cell Cardiol *42*, 572-581.

Vasioukhin, V., Bauer, C., Yin, M., and Fuchs, E. (2000). Directed actin polymerization is the driving force for epithelial cell-cell adhesion. Cell *100*, 209-219.

Waldmann, R., Nieberding, M., and Walter, U. (1987). Vasodilator-stimulated protein phosphorylation in platelets is mediated by cAMP- and cGMP-dependent protein kinases. Eur J Biochem *167*, 441-448.

Winder, S.J., and Ayscough, K.R. (2005). Actin-binding proteins. J Cell Sci *118*, 651-654.

Acknowledgements

I would like to thank…

Prof. Dr. Kai Schuh for giving me the possibility to do my dissertation in his institute, for his interest in my work, his constant support and for answering to all my questions at any time.

Dr. Peter Benz for his continuous support, for excellent explanations, for his advice and really helpful critics, for the accurate and time consuming reading of my manuscript and for excellent working conditions.

All members of AG Schuh who all contributed to the pleasant working atmosphere. In particular, I would like to thank Melanie Ullrich for her help in retroorbital blood collection of mice, Tobias Fischer for providing wt controls whenever needed, Marco Abeißer for recording ECGs of Mena/VASP mutated and wt mice.

Dr. Kai Hu for accomplishing cardiac catheter analysis of mutated and wt mice.

My parents for their encouragement, advice and for their financial support during my studies in Würzburg and abroad.

My brother for his help and advice in every situation and for always supporting me.

My grandfather for his interest in my work and my studies.

All my friends, who contributed in improving every day. In particular I would like to thank Karin for a long friendship for such a long time, my friends in Würzburg who not only improved my time during lectures but also during my spare time.

…and especially I would like to thank my boyfriend Martin for being there for me when I needed him, for continuously strengthening my self-confidence, for his support, encouragement and his love.